Identification of Glutathione *S*-Transferase Inhibiting Natural Products from *Caesalpinia bonduc, Nauclea latifolia* and *Ambrosia psilostachya*

By

CHIBUIKE CHINEDU UDENIGWE

A Thesis submitted to the Faculty of Graduate Studies
The University of Manitoba
in partial fulfillment of the requirements of the degree of

MASTER OF SCIENCE

Department of Chemistry
The University of Manitoba
Winnipeg, Manitoba
Canada

THE UNIVERSITY OF MANITOBA

FACULTY OF GRADUATE STUDIES

*****

COPYRIGHT PERMISSION

Identification of Glutathione *S*-Transferase Inhibiting Natural Products from *Caesalpinia bonduc*, *Nauclea latifolia* and *Ambrosia psilostachya*

BY

CHIBUIKE CHINEDU UDENIGWE

A Thesis/Practicum submitted to the Faculty of Graduate Studies of The University of Manitoba in partial fulfillment of the requirement of the degree

MASTER OF SCIENCE

Abstract

For this thesis, phytochemical studies on three medicinally important plants, *Caesalpinia bonduc*, *Nauclea latifolia* and *Ambrosia psilostachya*, were carried out in a bid to isolate glutathione *S*-transferase inhibitors. A summary of this research work is described below.

1. Phytochemical studies on the crude extract of *Caesalpinia bonduc* resulted in the isolation of neocaesalpin O (**40**), 17-hydroxy-campesta-4,6-dien-3-one (**41**), caesaldekarin J (**42**), apigenin (**43**), pipataline (**44**), betulinic acid (**45**), 13,14-*seco*-stigmasta-5,14-dien-3α-ol (**46**) and 13,14-*seco*-stigmasta-9(11),14-dien-3α-ol (**47**). These compounds showed weak to moderate or no inhibitory activities against GST, an enzyme that has been implicated in resistances of cancer cells and parasitic organisms towards chemotherapeutic agents. An attempt to study the structure-activity relationships of compounds **43**, **44**, **46** and **47** resulted in the synthesis of compounds **57-61**. These compounds were also assayed, and some showed weak but enhanced GST inhibition.
2. The chemical constituents of the crude ethanolic extract of *Nauclea latifolia* were also investigated. This resulted in the isolation of strictosamide (**70**), quinovic acid-3-O-α-quinovosylpyranoside (**95**), quinovic acid-3-O-β-rhamnosylpyranoside (**96**), quinovic acid-3-O-α-rhamnosylpyranoside (**97**) and quinovic acid-3-O-β-fucosylpyranoside (**98**). These compounds also showed varying extents of GST inhibitory activities with strictosamide (**70**) showing the best activity. Bioactivity data of the triterpenoidal glycosides (**95-98**) indicated that the nature of the sugar molecules attached to the quinovic acid aglycone may have an effect in their GST-inhibiting potentials.

3. Similarly, phytochemical studies on *Ambrosia psilostachya* have resulted in the isolation of coronopilin (**100**), a pseudoguaianolide sesquiterpene lactone. Coronopilin (**100**) showed a concentration-dependent weak inhibition of the activity of GST and no activity in an antifungal assay against two strains of *Candida albicans*. The structures of these compounds were deciphered by spectroscopic studies. The structure of compound **100** was also confirmed by X-ray crystallographic studies.

Acknowledgements

I give all the glory to Almighty God, the author and finisher of my faith, who made all things possible. I thank my thesis supervisor, Dr. Athar Ata, for accepting me in his lab as a graduate student and for his guidance and outstanding contributions towards the successful completion of this thesis. I also thank the examining committee members who made out time to read and evaluate this thesis. I thank my parents and siblings for their spiritual, moral and financial support; my Dad for teaching me perseverance and patience, and my Mum for teaching me bravery and love. I would like to appreciate the parental roles of Dr. Michael Eze and his family, who have been my source of inspiration during these two years of stay in Canada. I appreciate the technical support I received from Gunders Reinsfield of University of Winnipeg and Dr. Kirk Marat of the NMR Facility, University of Manitoba. I thank Dr. Kathy Gough and Richard Wiens of the University of Manitoba for their help with FT-IR spectroscopy. I thank Dr. Pete Uzoegwu of the University of Nigeria and Dr. Radhika Samaresekera of Industrial Technology Institute, Sri Lanka for supplying the plant extracts used in this study. I also appreciate the company of every member of Dr. Ata's lab, past and present, during my stay. The graduate scholarships received from the Faculty of Science and Faculty of Graduate Studies, The University of Manitoba is gratefully acknowledged. Thanks to my friend, Ogo Ogidi, for her love and care and to everybody who asked me "how is your thesis going?" I am indebted to all my past and present teachers who have made positive contributions to my academic pursuit.

This thesis is dedicated to all men of goodwill, lovers of excellence and my family

TABLE OF CONTENTS

LIST OF TABLES

LIST OF FIGURES

LIST OF SCHEMES

CHAPTER 1

General Introduction

1.1 Natural Products

Natural products are secondary metabolites derived from plants, microorganisms, higher animals and marine organisms. They are not directly utilized in primary metabolism of plants in growth and development, but they may serve defensive roles against invading organisms and also play reproductive roles as attractants of pollinators and seed dispersers.[1] In general, most natural products are classified as terpenoids, alkaloids and phenolic compounds based on their biosynthetic origins and structural features.[1,2] Despite their minor roles in plant metabolism, natural products have been shown to possess medicinal value in the treatment of diseases in man and other animals.

1.1.1 Natural Products as Drug Candidates

Natural products have played leading roles in the drug discovery program.[3,4] It has been estimated that approximately 49% of 877 small molecules introduced between 1981 and 2002 by New Chemical Entities were either natural products, their semisynthetic analogues or synthetic products based on natural product models.[4] Prior to this report, natural products have been placed on the forefront of drug discovery programs as over 60% of approved drugs between 1989 and 1995 were based on natural products.[3] It has also been reported that 45% of the 20 best-selling non-protein drugs in 1999 were natural products based, and these accounted for a combined annual sales of over US$16 billion.[5] Moreover, 23 new drugs introduced to the market during 2000 and 2005 were natural products.[6] The leading position of natural products in drug discovery as against their synthetic counterparts is mainly in the area of infectious diseases and

cancer chemotherapy.[7] This could be observed in the new approved antibacterial drugs between 1983 and 1994; natural products accounted for 78% of the drugs whereas 61% of 31 anticancer drugs were modeled on natural products.[7]

The numerous emerging infectious diseases and the continuous development of drug resistance by many pathogens to currently used drugs are some of the primary reasons for a need of new sources of structurally diverse drug leads in antimicrobial chemotherapy.[7] Koehn and Carter[7] reported that the rather lengthy period (approximately 10 years) needed to develop a drug resulted in a shift of emphasis from natural products. This drift, they reported, has been attributed to a number of factors which include 1) introduction of high-thoroughput screening (HTS) for synthetic compounds, 2) introduction of combinatorial chemistry for screening of libraries of wide chemical diversity, 3) advances in molecular biology which increased the number of molecular targets and prompted shorter drug discovery timeline, and 4) reduced interest of pharmaceutical companies in infectious disease therapy, an area where natural products play a leading role.[6-8] Koehn and Carter also suggested that this decline in interest is commercial rather than scientific as natural products offer such a structurally diverse library of compounds than the recent innovative strategies.[7] The trend is presently moving back towards natural products since the new strategies were not successful in producing significant results. For example, some large library of chemical compounds from combinatorial chemistry were synthesized in a drug discovery program, and it was later observed that there was little or no hit for the pharmaceutical activity of the comounds.[9] It was suggested that this could be due to the fact that these compounds were designed based on chemical accessibility and without any biologically relevant chemical

diversity.[5,7,10] Moreover, the structural complexity of some natural product-based prospective drug leads would require multisteps cost-ineffective synthetic procedures that may not produce enough yield for commercial production. The structural diversity offered by natural products is an advantage in drug discovery, and this makes them distinct from synthetic and combinatorial compounds.[7] Natural products are selected by evolutionary processes to associate with a wide array of biological molecules for specific purposes, a property that qualifies them as prospective chemotherapeutic agents.[7] This can be exemplified in many natural product derived drugs which can bind the active sites of enzymes and proteins, and as such produce the desired chemotherapeutic activity. For example, lovastatin (mevinolin, **1**) originally isolated from *Aspergillus terreus* and subsequently identified in other fungi including a mushroom *Pleurotus ostreatus*,[11] is a HMG-CoA reductase inhibitor.[7] HMG-CoA reductase is an enzyme that catalyzes the rate limiting step in cholesterol biosynthesis, and therefore, lovastatin has been applied as a cholesterol-lowering agent based upon the inhibition of this enzyme.[7] Simvastatin (**2**), a synthetic analogue of lovastatin, has also been used as a more potent hypolipidemic drug based on inhibition of HMG-CoA reductase.[12] Artemisinin (**3**), a sesquiterpene lactone isolated from a Chinese tree *Artemisia annua*, binds hemin and inhibits hemeozoin formation induced by the activity of malarial parasites. The presence of a peroxide bridge in the compound is responsible for this bioactivity.[13]

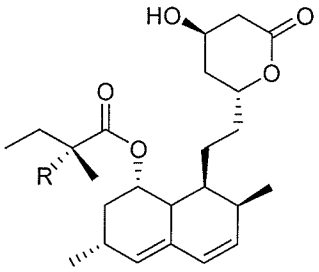

(**1**) R = H
(**2**) R = CH_3

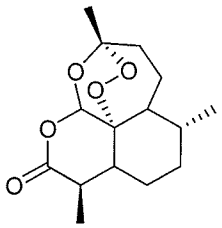

(**3**)

Micafungin (**4**), an echinocandin lipopeptide modelled on a fermentation product of *Coleophoma empetri*, inhibits β-(1→3)-glucan synthase in fungi and, based on this activity, has been used as fungicidal agent against *Candida* sp.[7,14] Physostigmine (eserine, **5**), a compound isolated from Calabar bean *Physostigma venenosum*, reversibly inhibits acetylcholinesterase (AChE) and has been used in the treatment of glaucoma.[15] An AChE inhibiting synthetic analogue of physostigmine (**5**), eptastigmine (heptyl-physostigmine tartarate, **6**),[16] is currently under clinical trials in the treatment of Alzheimer's disease.[17]

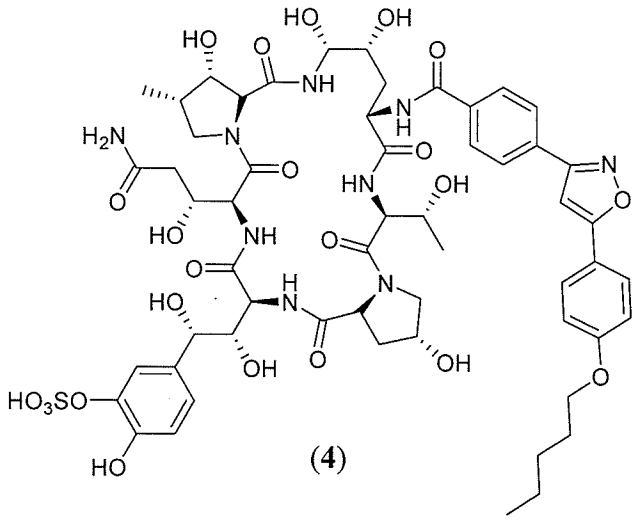

(**4**)

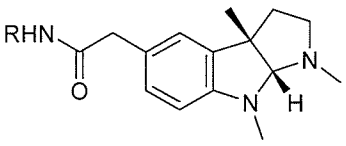

(**5**) R = CH_3
(**6**) R = $(CH_2)_6CH_3$

In addition, natural products may also disrupt protein-protein interactions, and this property has been applied in chemotherapy. For example, rapamycin (sirolimus, **7**),[18] FK506 (tacrolimus or fujimycin, **8**)[19] and ascomycin (**9**)[20] are macrolides derived from soil actinomycetes that are presently in clinical use in organ transplantation (**7**, **8**) and in the treatment of atopic dermatitis or eczema (**9**). These macrolides function by binding the FK-binding protein and modulating protein-protein interactions in the signal transduction pathway of T-cell activation.[7] Compounds **7-9** have polyketide biosynthetic origin.

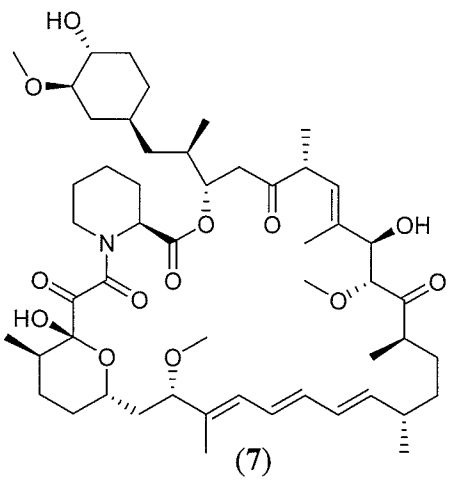

(7)

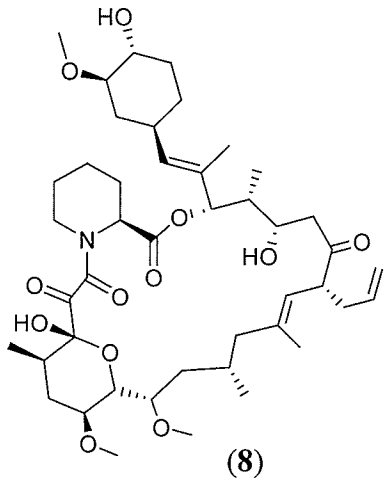

(8)

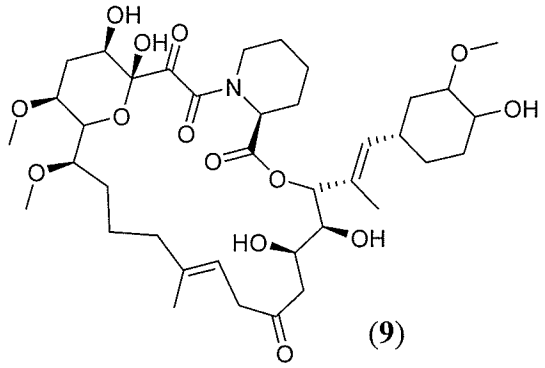

(9)

Natural products have provided a number of pharmaceuticals that include paclitaxel (**10**), ciprofloxacin (**11**), etoposide (**12**), amoxicillin (**13**), enalapril (**14**), captopril (**15**), camptothecin (**16**) and reserpine (**17**). The vinca alkaloids, vincristine (**18**) and vinblastine (**19**), have been applied in cancer chemotherapy against various cancers whereas the epipodophyllotoxins, etoposide (**12**) and teniposide (**20**), are well known for their cytotoxicity against leukemia, testicular tumor and lymphomas especially Hodgkin's disease.[21] Camptothecin (**16**), an alkaloid isolated from *Camptotheca acuminata*, has been used as an anticancer agent. This compound has also shown activity in the inhibition of the growth of *Trypanosoma brucei* and *Leishmania donovani*, parasites which cause sleeping sickness and leishmaniasis, respectively.[22] These activities of camptothecin are due to its inhibitory activity on DNA topoisomerase 1.[22] In addition to these agents, a

number of biomedical agents including marine-derived compounds are presently at different phases of clinical trials as cytotoxic agents against various human cancer cells.[23]

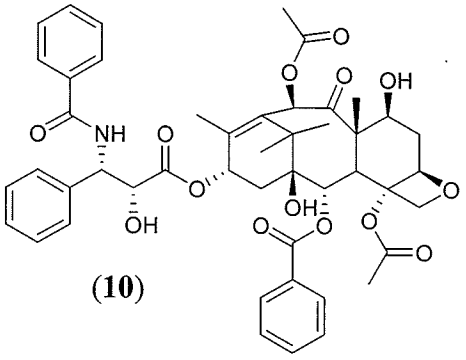

(**10**)

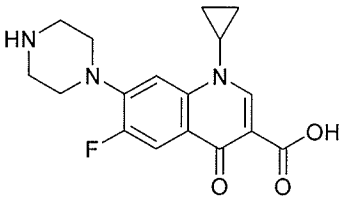

(**11**)

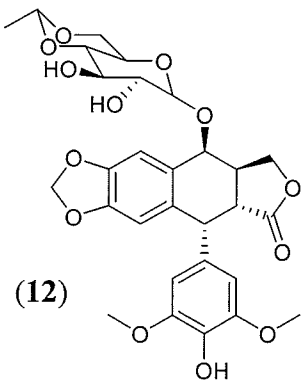

(**12**)

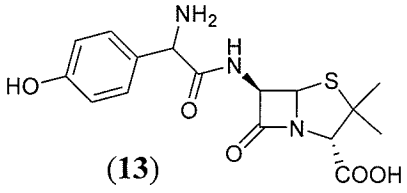

(**13**)

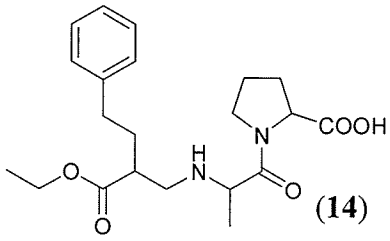

(**14**)

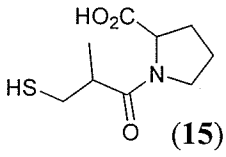

(**15**)

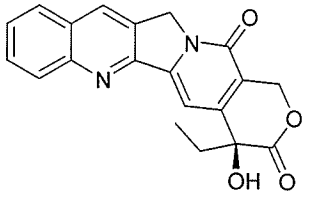

(**16**)

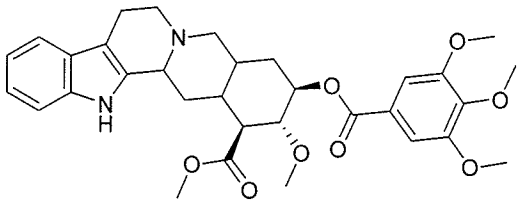

(**17**)

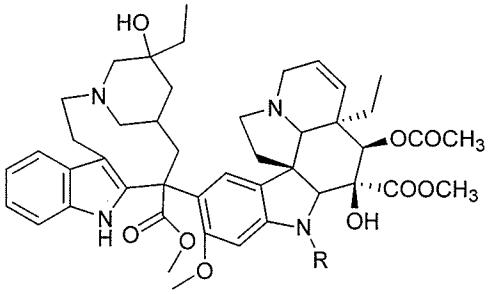

(**18**) R = CHO
(**19**) R = CH_3

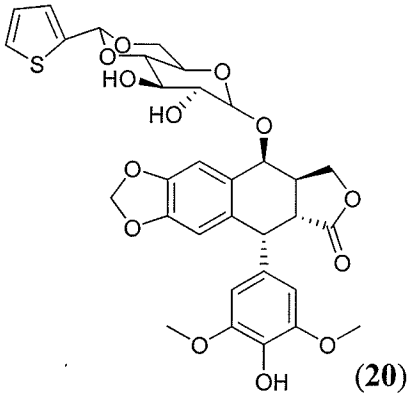

(**20**)

A natural product chemistry drug discovery program is based on bioassay-directed fractionations in order to isolate biomedical agents.[24] This strategy involves screening various plant extracts to identify the active extracts, and subsequent fractionation of the extracts based on the bioassay until the pure compounds responsible for the activity are isolated. This procedure is represented in Figure 1.1.

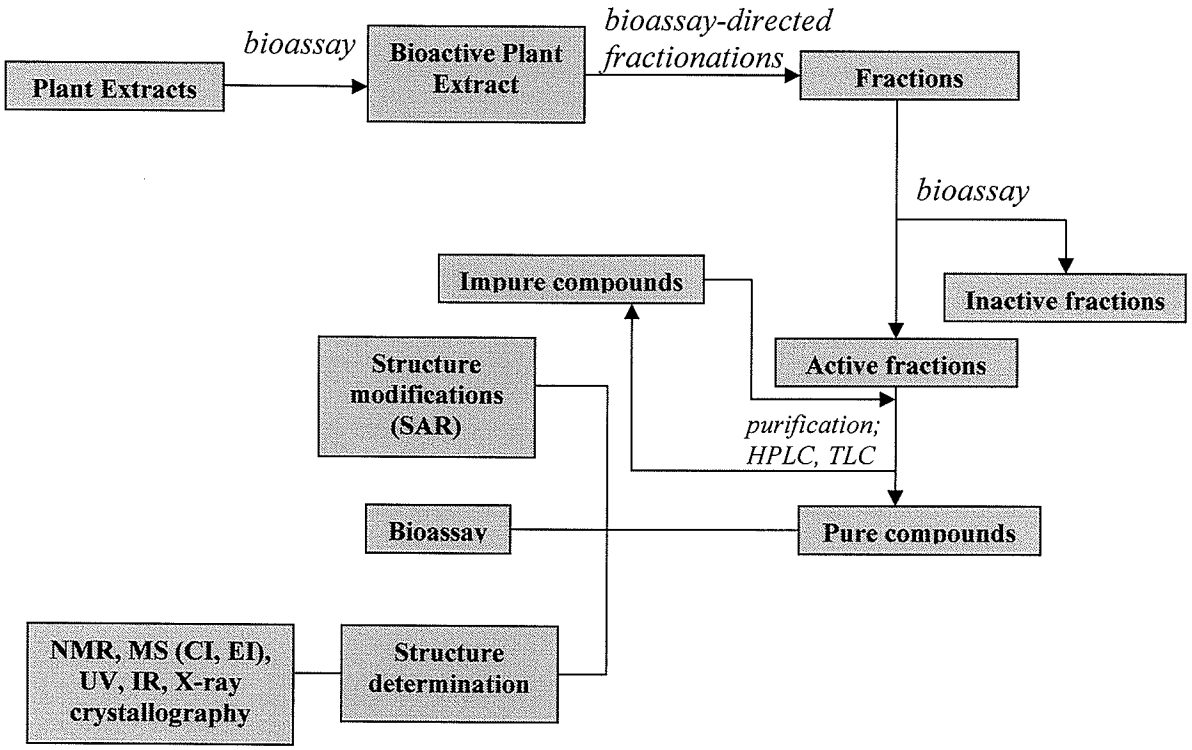

Fig. 1.1 Procedure for bioassay-directed isolation of natural products in drug discovery

Nature has adopted its own form of diversity in that some natural products occur as a series of structurally related analogues. These compounds, when isolated, could be employed in the study of structure-activity relationships (SAR). Previously, the inability to purify such complexes led to the use of a consortium of compounds as chemotherapeutic agents.[7] For instance, ivermectin from the class avermectins, isolated

from *Streptomyces* sp[25], was developed and marketed as a complex of natural products and was used as antiparasitic agent.[26] However, the advent of sophisticated techniques such as liquid chromatography (LC) coupled to nuclear magnectic resonance (NMR) spectrometer has enabled the purification and structure elucidation of the constituents of natural product complexes even at nanogram scale.[24] This has enabled the exploitation of the structurally diverse analogues of natural products provided by nature in SAR studies during drug discovery. This principle has been applied in the mannopeptimycin antibiotics.[27] Moreover, chemical transformations can also be carried out on natural products to produce analogues for SAR studies. The chemical derivatives sometimes produce better activity than their parent compounds. This has been observed in a SAR study using artemisinin (**3**) where an ether derivative, artemeter (**21**), showed better antimalarial activity than the parent natural product,[28] and this derivative shows prospects in the eradication of malaria in major parts of the world.[29]

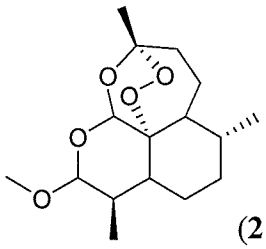

(21)

1.2 Glutathione *S*-Transferase Isoenzymes as Potential Targets in Chemotherapy

The concept of anticancer drug resistance has raised a lot of consciousness in the present day chemotherapist. Several research investigations have been conducted in the past in a bid to explain the mechanisms of acquired drug resistance in the treatment of cancer and parasitic diseases. Interestingly, amidst several possible factors responsible for such resistances, a ubiquitous predominantly cytosolic detoxification enzyme, glutathione

S-transferase (GST; E.C. 2.1.5.18), has been implicated to play an active role.[30] GSTs are phase II detoxification isozymes that function in the conjugation of a wide variety of exogenous and endogenous electrophilic substances to glutathione (GSH; γ-glutamyl-cysteinyl-glycine) producing a less toxic water-soluble conjugate that can easily be excreted from the body.[31] A typical reaction catalyzed by GST is shown in scheme 1.1.

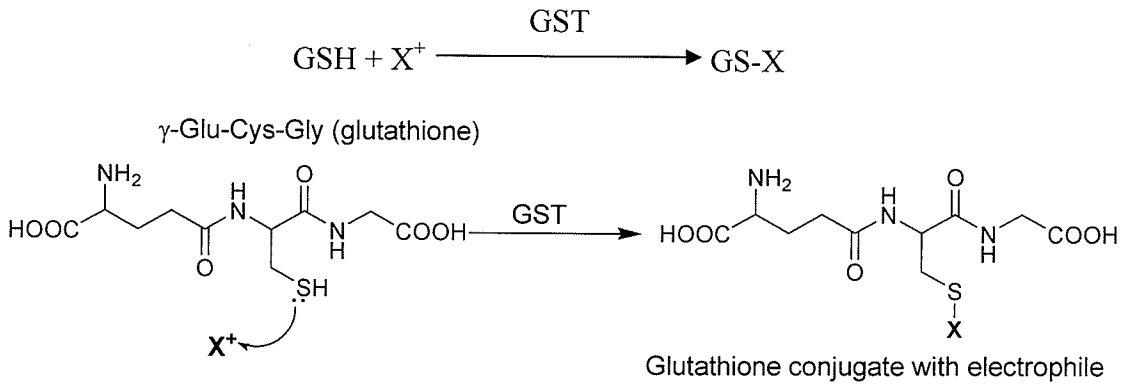

Scheme 1.1 General reaction catalyzed by GST; X^+ = electrophilic substance

GSTs are divided into two groups: the membrane-bound microsomal and the cytosolic GSTs.[30] Microsomal GSTs exist in homo- and hetero-trimerized forms with a single active site, and function in the endogenous metabolism of leucotrienes and prostaglandins.[30] In humans, cytosolic GSTs exist in the form of various dimerized isoenzyme classes: α (A), μ (M), ω, π (P), θ (T), ζ (Z) and σ classes.[30,32] Their existence in different forms has provided broad substrate specificities promoting detoxification of many toxic substances. Some GSTs from disease-causing parasites have also been characterized and reported. Ov GST2 has been reported for *Onchocerca volvulus*, a parasite that causes Onchocerciasis, and was proposed to be unique but with a little resemblance to human GST-P.[33] Several other GST classes have been characterized from

other parasitic organisms.[34-36] Recently, the X-ray crystal structure of GST of the malaria-causing parasite, *Plasmodium falciparum*, was elucidated.[37] These GST isoenzymes are related in their amino acid constituents and very little in their conformation except at specific regions, two of which are needed for the coupling activity. This distinguishing uniqueness is attributed to the catalytic hydrophobic site (H-site) and a glutathione-binding site (G-site),[32,38-40] which offer diversity in specificities of the different isoenzymes for different substrates. In addition to their xenobiotic detoxification roles, human and parasitic GSTs have been implicated as lead actors in cellular drug resistances,[30] which is a major factor in the failure of chemotherapy. Electrophilic alkylating anticancer and antiparasitic drugs have been reported to be either substrates or ligands for the different GST isoenzymes, and this forms the basis of cellular drug resistances.[30,41]

1.2.1 Role of GST in anticancer drug resistance

Many tumor cells have shown over-expression of GST isoenzymes especially GST-P and GST-M.[42] Both catalytic and non-catalytic ligand-binding activities of these isoenzymes have been implicated in the development of resistance by these cells towards chemotherapeutic agents;[30] several electrophilic alkylating drugs have been effectively metabolized by cancer cells. For example, anticancer agents, chlorambucil (Scheme 1.2), mechloroethamine, aldophosphamine and melphalan, have been reported to be substrates for GST and, as a result, can be directly conjugated to GSH through thioester bond formation.[30] In this case, the enzyme utilizes its detoxification mechanisms in the

biotransformation of these cytotoxic agents into harmless metabolites leading to failure of chemotherapy.

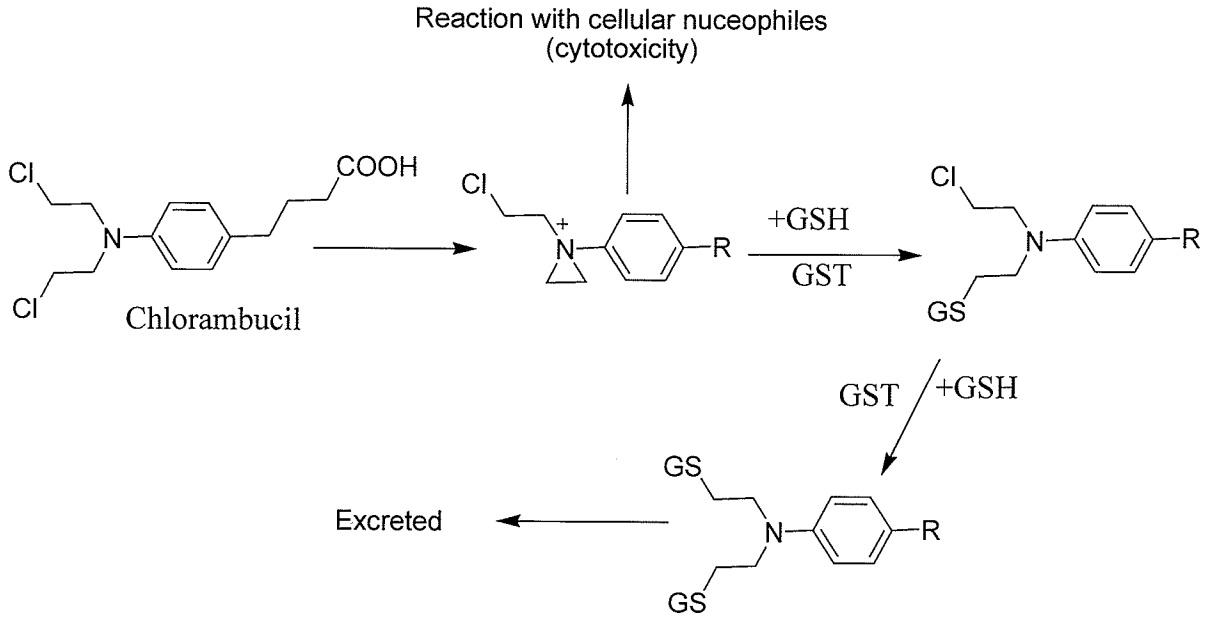

Scheme 1.2 The role of GST and GSH in the detoxification of anticancer drug, chlorambucil[30]

However, cancer cells have also shown resistance to some other drugs that were neither characterized as substrates for GST nor subject to conjugation with GSH.[30] This phenomenon spurred vigorous research activities that later discovered that non-enzymatic, ligand-binding activity of GST interferes with cellular functions.[43,44] Most anticancer drugs function by activation of apoptosis through the mitogen activation protein (MAP) kinase signal transduction pathway (Table 1.1).[30] GST-P and GST-M have been reported to play significant roles in regulating MAP kinase pathway through protein-protein interaction with cJun N-terminal kinase (JNK) and apoptosis signal-regulating kinase (ASK-1).[43-46] Activated JNK is involved in induction of apoptosis,

stress response and cellular proliferation via phosphorylation of transcription factors cJun, ATF2, p53 and ELK-1, which are involved in cell kinetics and survival.[44,47] ASK-1 activates JNK and p38 pathways leading to cytokine- and stress-induced apoptosis.[43]

In non-stressed cells, the monomeric forms of GST-P and GST-M covalently bind JNK and ASK-1, respectively[43] thus decreasing the activity of the kinases in transmission of death signals and in response to cellular stress. This non-thiol-mediated role of GST has contributed immensely to the resistance of cancer cells towards apoptosis-dependent anticancer drugs, and has added a new dimension to the prospects and significance of GST as a drug target in anticancer chemotherapy.

Table 1.1 Non-GST substrate anticancer drugs that require JNK activation for their cytotoxic activities

Anticancer drugs that require JNK activation
Antimicrotuble drugs
Mitomycin A
Adriamycin A
Cisplatin
Topoisomerase I & II inhibitors
Antimetabolites

1.2.2 Role of GST in antiparasitic drug resistance

GST has been described as the parasitic helminthes' tool that provides their major phase II detoxification mechanism in resistance towards the host defense mechanism.[41] In

general, nematode cestodes and digenean GSTs have significant activity in either conjugation of GSH with lipid peroxidation derived carbonyl derivatives or effective neutralization of their precursors.[35] Helminthes GST isoenzymes also have the potential to neutralize exogenously derived toxic substances such as anti-helminthes agents[36] as does *Fasciola hepatica* GST, which possesses considerable GSH-dependent catalytic activity with secondary lipid peroxidation products.[48] These activities are primarily linked to the resistance of these parasites to the host immune system, since its cytotoxic activity depends in part on cellular oxidation products.[41] Moreover, GST may not only conjugate toxic substances with GSH but could also passively interact with hydrophobic ligands including phenolic anti-helminthes compounds.[36,48] This obviously interferes with chemotherapeutic strategies employed towards the treatment of infections due to these parasites.

Recently, GST activity was reported for all the intraerythrocytic stages of existence of rodent (*Plasmodium berghei, Plasmodium yoelii*), simian (*Plasmodium knowlesi*) and human (*Plasmodium falciparum*) malarial parasites.[49] This was thought to exhibit significant metabolism of xenobiotics and endobiotics, and as a result, plays an important role in conferment of resistance to the parasites against chloroquine, a known antimalarial drug.[49] Additionally, GSTs from *Schistosoma japonica*[50] and *S. hematobium*[51] have been characterized and have also been speculated to act as a primary defense tool against electrophilic and oxidative damage.[33,50,51] The ability of these parasite GSTs to effectively neutralize known cytotoxic products, including those arising from oxidative attacks on cell membranes, and to bind exogenous toxic substances

provides evidence that GST protects parasites against the host immune response and antiparasitic drugs.

1.2.3 GST as a target for therapeutic agents

A number of investigations have been conducted in the past two decades to improve the understanding of the therapeutic prospects of targeting GST. The involvement of GST in drug resistances has created an alternative target in the enhancement of potency of therapeutic agents. A rationale has been established to utilize agents that selectively inhibit the various classes of GST as adjuvant in anticancer chemotherapy as well as anti-parasitic drugs.[32,52] This concept was formulated in a bid to discover compounds that can inactivate GST for enhanced activity of the desired drug. These agents could act by either inhibiting the catalytic activity of GST in metabolism of electrophilic drugs or in disruption of the complex formed between GST and stress signal kinases[30] as discussed in a previous section.

Several classes of naturally occurring and synthetic compounds have been reported to exhibit *in vivo* and *in vitro* inhibitory activities against different GST isoenzymes. These compounds could be classified as α,β-unsaturated carbonyl derivatives (e.g. ethacrynic acid, **22**),[53] steroids (e.g. quinone derivative of 2-hydroxy-17-β-estradiol, **23**),[54] peptidomimetic glutathione analogues (e.g. TLK117, **24**),[30] nitrobenzoxadiazole derivatives (e.g. 6-(7-nitro-2,1,3-benzoxadiazole-4-ylthio) hexanol, **25**),[55] flavonoids (e.g. quercetin, **26**)[56] and others.[57-59] These representative compounds displayed the most potent activities in GST inhibition; some of these compounds have

been extensively studied for their applicability as adjuvant in anticancer chemotherapy, and in the treatment of parasitic infections.

The discovery of GST inhibitors from natural sources has not been extensively investigated. Taking into consideration the structural diversity observed in natural products, this thesis discusses the results of the phytochemical analyses of plant materials in a bid to discover GST inhibiting compounds. Chapters 2, 3 and 4 contain results of investigations of the phytochemistry of *Caesalpinia bonduc*, *Nauclea latifolia* and *Ambrosia psilostachya*, respectively.

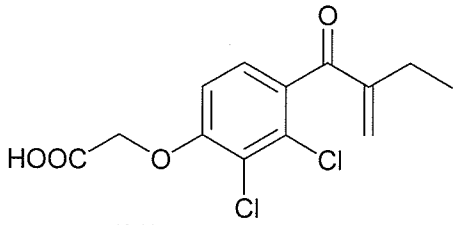

(22)

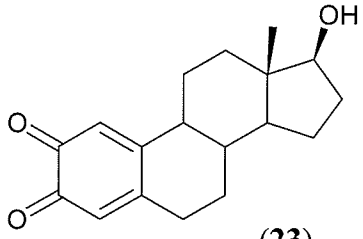

(23)

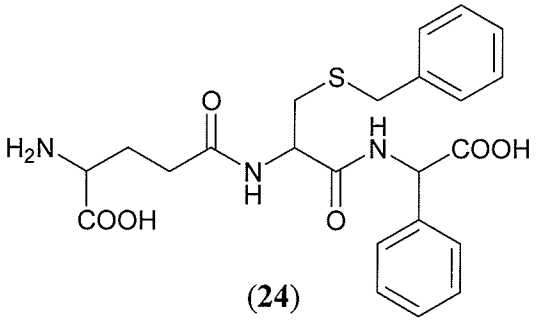

(24)

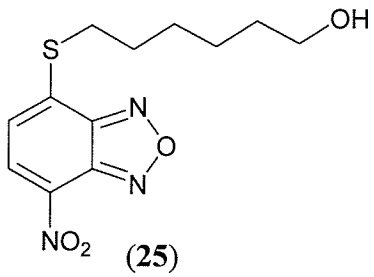

(25)

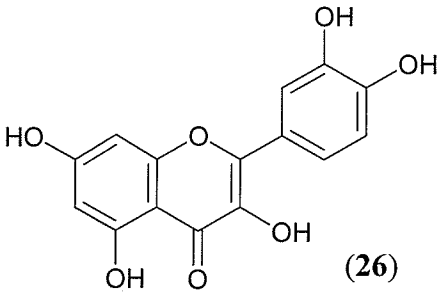

(26)

1.3 REFERENCES

1. Croteau, R., Kutchan, T. M. and Lewis, N. G. Natural products (secondary metabolites). In: "Biochemistry & Molecular Biology of Plants", Ed.(s): Buchanan, B. B., Gruissem, W. and Jones, R. L., American Society of Plant Physiologists, Rockville, MD, U.S.A., **2000**, 1250-1318.
2. Dewick, P. M. "Medicinal Natural Products: A biosynthetic approach", *2nd ed.*, John Wiley & Sons, **2001**.
3. Newman, D. J., Cragg, G. M. and Snader, K. M. Natural products in drug discovery and development. *J. Nat. Prod.*, **1997**, *60*, 52-60.
4. Newman, D. J., Cragg, G. M. and Snader, K. M. Natural products as sources of new drugs over the period 1981-2002. *J. Nat. Prod.*, **2003**, *66*, 1022-1037.
5. Harvey, A. Strategies for discovering drugs from previously unexplored natural products. *Drug Discovery Today*, **2000**, *5*, 294-300.
6. Chin, Y-. W., Balunas, M. J., Chai, H. B. and Kinghorn, D. Drug discovery from natural sources. *AAPS J.*, **2006**, *8*, E239-E253.
7. Koehn, F. E. and Carter, G. T. The evolving role of natural products in drug discovery. *Nat. Rev. Drug Discov.*, **2005**, *4*, 206-220.
8. Overbye, K. M. and Barrett, J. F. Antibiotics: where did we go wrong? *Drug Discovery Today*, **2005**, *10*, 45-52.
9. Martin, Y. C. and Critchlow, R. E. Beyond mere diversity: tailoring combinatorial libraries for drug discovery. *J. Comb. Chem.*, **1999**, *1*, 32-45.
10. Myers, P. L. Will combinatorial chemistry deliver real medicines? *Curr. Opin. Biotechnol.*, **1997**, *8*, 701-707.

11. Bobek, P., Ozdín, L. and Galbavý, S. Dose- and time-dependent hypocholesterolemic effect of oyster mushroom (*Pleurothus ostreatus*) in rats. *Nutrition*, **1998**, *14*, 282-286.

12. Hoffman, W. F., Alberts, A. W., Anderson, P. S., Chen, J. S., Smith, R. L. and Willard, A. K. 3-Hydroxy-3-methylglutaryl-coenzyme A reductase inhbitors. Side chain ester derivatives of mevinolin. *J. Med. Chem.*, **1986**, *29*, 849-852.

13. Dhingra, V., Rao, K. V. and Narasu, L. Current status of artemisinin and its derivatives as antimalarial drugs. *Life Sci.*, **1999**, *66*, 279-300.

14. Denning, D. W. Echinocandin antifungal drugs. *Lancet*, **2003**, *362*, 1142-1151.

15. Sneader, W. From ordeal poison to Alzeihmer's therapy. *Drug News Perspect.*, **1999**, *12*, 433-437.

16. Unni, L. K., Hutt, V., Imbimbo, B. P. and Becker, R. E. Kinetics of cholinesterase inhibition by eptastigmine in man. *Eur. J. Clin. Pharmacol.*, **1991**, *41*, 83-84.

17. Braida, D. and Sala, M. Eptastigmine: ten years of pharmacology, toxicology, pharmacokinetics and clinical studies. *CNS Drug Rev.*, **2001**, *7*, 369-386.

18. Abraham, R. T. and Wiederrecht, G. J. Immunopharmacology of rapamycin. *Ann. Rev. Immunol.*, **1996**, *14*, 483-510.

19. Dumont, F. J. FK506, An immunosuppressant targeting calcineurin function. *Curr. Med. Chem.*, **2000**, *7*, 731-748.

20. Hersperger, R. and Keller, T. H. Ascomycin derivatives and their use as immunosuppressive agents. *Drugs Future*, **2000**, *25*, 269-277.

21. Pung, T. Isolation of natural products from plant extracts. M. Sc. Thesis. Department of Chemistry, Virginia Polytechnic Institute and State University, U.S.A., **2000**.

22. Sriram, D., Yogeeswari, P., Thirumurugan, R. and Bal, T. R. Camptothecin and its analogues: a review on their chemotherapeutic potential. *Nat. Prod. Res.*, **2005**, *19*, 393-412.

23. Jimeno, J., Faircloth, G., Fernández Sousa-Faro, J. M., Scheuer, P. and Rinehart, K. New marine derived anticancer therapeutics – a journey from the sea to clinical trials. *Mar. Drugs*, **2004**, *2*, 14-29.

24. Hostettmann, K. and Wolfender, J-. L. Strategy in the search for new lead compounds and drugs from plants. *Chimica*, **2005**, *59*, 291-295.

25. Davies, H. G. and Green, R, H. Avermectins and Milbemycins. *Nat. Prod. Rep.*, **1986**, *3*, 87-121.

26. Chabala, J. C., Mrozik, H., Tolman, R. L., Eskola, P., Lusi, A., Peterson, L. H., Woods, M. F. And Fischer, M. H. Ivermectin, a new broad-spectrum antiparasitic agent. *J. Med. Chem.*, **1980**, *23*, 1134-1136.

27. He, H., Williamson, R. T., Shen, B., Graziani, E. I., Yang, H. Y., Sakya, S. M., Petersen, P. J and Carter, G. T. Mannopeptimycins, novel antibacterial glycopeptides from *Streptomyces hygroscopicus*. *J. Am. Chem. Soc.*, **2002**, *124*, 9729-9736.

28. Brossi, A., Venugopalan, B., Dominguez, Gerpe, L., Yeh, H. J. C., Flippen-Anderson, J. L., Buchs, P., Luo, X. D., Milhous, W. and Peters, W. Arteeter, a

new antimalarial drug: synthesis and antimalarial properties. *J. Med. Chem.*, **1988**, *31*, 645-650.

29. Klayman, D. L. Qinghaosu (artemisinin): an antimalarial drug from China. *Science*, **1985**, *228*, 1049-1055.
30. Townsend, D. M. and Tew, K. D. The role of glutathione *S*-transferase in anti-cancer drug resistance. *Oncogene*, **2003**, *22*, 7369-7375.
31. Chasseaud, L. F. Role of glutathione and glutathione *S*-transferases in the metabolism of chemical carcinogens and other electrophilic agents. *Adv. Cancer Res.*, **1979**, *29*, 175-274.
32. Mahajan, S. and Atkins, W. M. The chemistry and biology of inhibitors and pro-drugs targeted to glutathione *S*-transferase. *Cell. Mol. Life Sci.*, **2005**, *62*, 1221-1233.
33. Perbandt, M., Höppner, J., Betzel, C., Walter, R. D. and Liebau, E. Structure of the major cytosolic glutathione *S*-transferase from the parasitic nematode *Onchocerca volvulus*. *J. Biol. Chem.*, **2005**, *280*, 12630-12636.
34. Rossjohn, J., Feil, S. C., Wilce, M. C. J., Sexton, J. L., Spithill, T. W. and Parker, M. W. Crystallization, structural determination and analysis of a novel parasite vaccine candidate: *Fasciola hepatica* glutathione *S*-transferase. *J. Mol. Biol.*, **1997**, *273*, 857-872.
35. Brophy, P. M., Southan, C. and Barrett, J. Glutathione *S*-transferases in the tapeworm *Monieza expansa*. *Biochem. J.*, **1989**, *262*, 939-946.
36. Brophy, P. M., Papadopoulos, A., Touraki, M., Coles, B., Körting, W. and Barrett, J. Purification of cytosolic glutathione transferases from *Schistocephalus*

solidus (plerocercoid): interaction with antihelmintics and products of lipid peroxidation. *Mol. Biochem. Parasitol.*, **1989**, *36*, 187-196.

37. Hiller, N., Fritz-Wolf, K., Deponte, M., Wende, W., Zimmerman, H. and Becker, K. *Plasmodium falciparum* glutathione *S*-transferase – structural and mechanistic studies on ligand binding and enzyme inhibition. *Protein Sci.*, **2006**, *15*, 281-289.
38. Mannervik, B. and Danielson, U. H. Glutathione *S*-transferases – structure and catalytic activity. *CRC Crit. Rev. Biochem.*, **1988**, *23*, 283-337.
39. Rushmore, T. H. and Pickett, C. B. Glutathione *S*-transferases, structure, regulation, and therapeutic implications. *J. Biol. Chem.*, **1993**, *268*, 11475-11478.
40. Sato, K. Glutathione transferases as markers of preneoplasia and neoplasia. *Adv. Cancer Res.*, **1989**, *52*, 205-255.
41. Brophy, P. M. and Pritchard, D. I. Parasitic helminth glutathione *S*-transferases: an update on their potential as target for immuno- and chemotherapy. *Exptl. Parasitol.*, **1994**, *79*, 89-96.
42. Tew, K. D. Glutathione-associated enzymes in anticancer drug resistance. *Cancer Res.*, **1994**, *54*, 4313-4320.
43. Adler, V., Yin, Z., Fuchs, S. Y., Benezra, M., Rosario, L., Tew, K. D., Pincus M. R., Sardana, M., Henderson, C. J., Wolf, C. R., Davis, R. J. and Ronai, Z. Regulation of JNK signaling by GSTp. *EMBO J.*, **1999**, *18*, 1321-1334.
44. Wang, T., Arifoglu, P., Ronai, Z. and Tew, K. D. Glutathione *S*-transferase P1-1 (GSTP1-1) inhibits cJun N-terminal kinase (JNK) signaling through interaction with the C-terminus. *J. Biol. Chem.*, **2001**, *276*, 20999-21003.

45. Cho, S. G., Lee, Y. H., Park, H. S., Ryoo, K., Kang, K. W., Park, J., Eom, S. J., Kim, M. J., Chang, T. S., Choi, S. Y., Shim, J., Kim, Y., Dong, M. S., Lee, M. J., Kim, S. G., Ichijo, H. and Choi, E. J. Glutathione *S*-transferase mu modulates the stress-activated signals by suppressing apoptosis signal-regulating kinase 1. *J. Biol. Chem.*, **2001**, *276*, 12749-12755.

46. Elsby, R., Kitteringham, N. R., Goldring, C. E., Lovatt, C. A., Chamberlain, M., Henderson, C. J., Wolf, C. R. and Park, B. K. Increased constitutive c-Jun N-terminal kinase signaling in mice lacking glutathione *S*-transferase Pi. *J. Biol. Chem.*, **2003**, *278*, 22243-22249.

47. Davis, R. J. Signal transduction by the JNK group of MAP kinases. *Cell*, **2000**, *103*, 239-252.

48. Brophy, P. M., Crowley, P. and Barrett, J. Detoxification reactions of *Fasciola hepatica* cytosolic glutathione transferases. *Mol. Biochem. Parasitol.*, **1990**, *39*, 155-161.

49. Srivastava, P., Puri, S. K., Kamboj, K. K. and Pandey, V. C. Glutathione *S*-transferase activity in malarial parasites. *Trop. Med. Int. Health*, **1999**, *4*, 251-254.

50. McTigue, M. A., Williams, D. R. and Tainer, J. A. Crystal structures of a Schistosomal drug and vaccine target: glutathione *S*-transferase from *Schistosoma japonica* and its complex with leading antischistosomal drug praziquantel. *J. Mol. Biol.*, **1995**, *246*, 21-27.

51. Johnson, K. A., Angelucci, F., Belleli, A., Herve, M., Fountaine, J., Tsernoglou, D., Capron, A., Trottein, F. and Brunori, M. Cystal structure of the 28 kDa glutathione *S*-transferase from *Schistosoma haematobium*. *Biochemistry*, **2003**, *42*, 10084-10094.

52. Schultz, M., Dutta, S. and Tew, K. D. Inhibitors of glutathione *S*-transferases as therapeutic agents. *Adv. Drug Delv. Rev.*, **1997**, *26*, 91-104.

53. Zhao, G., Yu, T., Wang, R., Wang, X. and Jing, Y. Synthesis and structure–activity relationship of ethacrynic acid analogues on glutathione *S*-transferase P1-1 activity inhibition. *Bioorg. Med. Chem.*, **2005**, *13*, 4056-4062.

54. Abel, E., Lyon, R. P., Bammler, T. K., Verlinde, C. L. M. J., Lau, S. S., Monks, T. J. and Eaton, D. L. Estradiol metabolites as isoform-specific inhibitors of human glutathione *S*-transferases. *Chem. Biol. Interact.*, **2004**, 151, 21-32.

55. Turella, P., Cerella, C., Filomeni, G., Bullo, A., De Maria, F., Ghibelli, L., Ciriolo, M. R., Cianfriglia, M., Mattei, M., Federici, G., Ricci, G., Caccuri, M. Proapoptotic activity of new glutathione *S*-transferase inhibitors. *Cancer Res.*, **2005**, *65*, 3751-3761.

56. Zanden van, J. J., Hamman, O. B., Iersel van, M. L. P. S., Boeren, S., Cnubben, N. H. P., Lo Bello, M., Vervoort, J., Bladeren van, P. J. and Rietgens, I. M. C. M. Inhibition of human glutathione *S*-transferase P1-1 by the flavonoid quercetin. *Chem. Biol. Interact.*, **2003**, *145*, 139-148.

57. Zheng, J., Mitchell, A. E., Jones, A. D. and Hammock, B. D. Haloenol lactone is a new isozyme-selective and site-directed inactivator of glutathione *S*-transferase. *J. Biol. Chem.*, **1996**, *271*, 20421-20425.

58. Haneshi, R., Mukanganyama, S., Hazra, B., Abegaz, B. and Hasler, J. The interaction of selected natural products with human glutathione *S*-transferases. *Phytother. Res.*, **2004**, *18*, 877-883.

59. Haaften van, R. I. M., Haenen, G. R. M. M., Bladeren van, P. J., Bogaards, J. J. P., Evelo, C. T. A. and Bast, A. Inhibition of various glutathione *S*-transferase isoenzymes by *RRR*-α-tocopherol. *Toxicol. In Vitro*, **2003**, *17*, 245-251.

CHAPTER 2

Chemical Studies on *Caesalpinia bonduc*

2.1 INTRODUCTION

Caesalpinia bonduc L. (Fabaceae) is a medicinally important plant predominantly distributed in the tropical and subtropical regions of Asia and the Caribbean. It is locally known as Nata Karanja (Hindi) in India and Kuburu in Sri Lanka, and has been applied in folk medicine for the treatment of several diseases and disorders. For instance, the aqueous and ethanolic extracts of its seeds have been reported to possess *in vivo* hyperglycemic effect in alloxan and streptozitocin induced type 2 diabetes in rat models at a dose of 250 mg/kg body weight.[1] The methanol, ethyl acetate and water fractions of the methanolic extract of this plant have exhibited *in vitro* activity against the growth of an array of pathogenic bacteria and fungi.[2] Antibacterial activities have also been reported for several plants belonging to the family Caesalpinaceae, and these plants have been previously utilized traditionally in the treatment of headache, dyspepsia, skin diseases, rheumatism and malaria.[3] In addition, the methanolic extract of the leaves of *C. bonduc* has been reported to possess anti-tumor and antioxidant activities in Swiss albino mice with Ehrlich ascites carcinoma.[4] The anti-tumor activity of this plant extract was observed at a minimum concentration 50 mg/kg body weight, and its antioxidant activity was actualized by the restoration of glutathione and antioxidant enzymes, superoxide dismutase (SOD) and catalase, with toxicity at concentration 300 mg/kg body weight and above.[4] Furthermore, the latter extract of *C. bonduc* was reported to exhibit anti-inflammatory activity in acute phase carrageenan, dextran and histamine induced pedal edema with a 50% maximum inhibition at 200 mg/kg body weight using an experimental

animal model.[5] It was further reported in the same paper that the same extract possesses *in vivo* analgesic and anti-pyretic activities.[5] These physiological activities of *C. bonduc* increase the possibility of exploring the constituents of these plant extracts for therapeutic purposes.

Previous phytochemical investigations on *C. bonduc* have resulted in the isolation of several compounds most of which belong to the cassane furanoditerpene class of compounds. Cassane furanoditerpenoids (**27**)[6] are characterized by a 4-ring isoprene-derived structure with the furan positioned as the D ring and, in most cases, the presence of a hydroxylated C-5 and a methyl group attached to C-14.

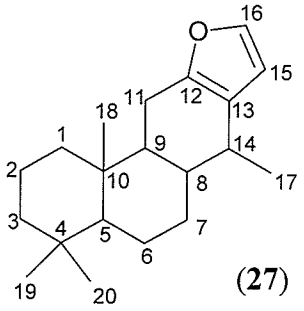

(**27**)

Amongst the initial compounds isolated from *C. bonduc* are caesalpin F (**28**)[7] and its analogues.[8] The first compound in the cassane diterpenoid series has also been isolated from *C. bonduc*.[8] Several other compounds belonging to the series bonducellpins[9] and caesaldekarins[10,11] have been isolated from this plant. In addition to these compounds, lactone-containing cassane diterpenes have also been isolated from *C. bonduc*. These compounds belong to the neocaesalpin series and include, neocaesalpin A (**29**) and its analogues.[10,12] Their structural features are similar to the cassane furanoditerpnes except the replacement of the D ring furan moiety by an α,β-unsaturated γ-lactone moiety. Structurally distinct compounds, caesaldekarin G (**30**)[11] and L (**31**),[10] which possess an opened D ring system, and caesalpinin B (**32**), which possess a rearranged A ring, have

also been isolated from this plant.[13] Caesaldekarin L (**31**) was the first reported cassane diterpene from *C. bonduc* with the absence of a C-5 hydroxyl group.[10] Several other cassane diterpenoids have been isolated from other members of the genus *Caesalpinia*, for example *C. pulcherrima*,[14,15] *C. minax*[16] and *C. crista*[17-20] as well as from other members of the family Fabaceae, for example, *Vouacapoua americana*.[21]

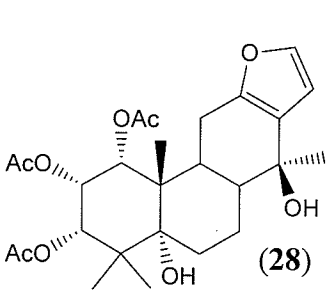

(**28**)

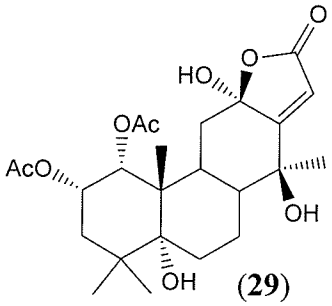

(**29**)

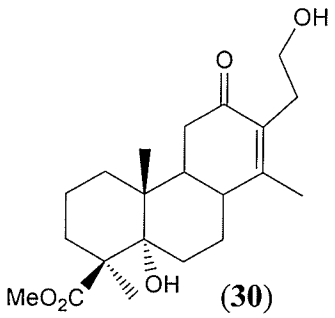

(**30**)

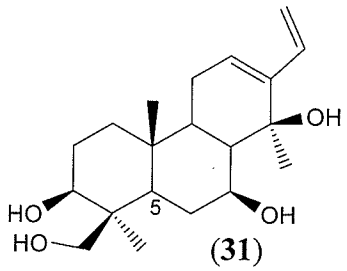

(**31**)

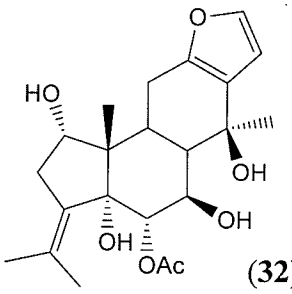

(**32**)

Some of these compounds isolated from *C. bonduc* have displayed *in vitro* biological activities. Recently, phytochemical studies on *in vivo* anti-plasmodial CH_2Cl_2 extract of *C. bonduc* resulted in the isolation of several compounds belonging to the caesalpinin, norcaesalpinin and norcaesalpin series of cassane furanoditerpene.[22] These

compounds exhibited significant dose-dependent *in vitro* activity against the growth of *Plasmodium falciparum* FCR-3/A2 with IC_{50} values ranging from 90 nM to 6.5 μM.[22] Norcaesalpinin E (**33**) and 2-acetoxy-3-deacetoxycaesaldekarin E (**34**) showed the most potent inhibitory activities with IC_{50} values 90 and 98 nM, respectively.[22] Norcaesalpinin E (**33**) represents another structural type of cassane diterpenoids with an oxidized C-14 and the absence of the methyl group at the same position. The activities of these compounds show that they have prospects in application towards the treatment of malaria, a parasitic disease affecting over 200 million people in the tropical and subtropical regions of the world.[23] In addition, bondenolide,[24] another cassane diterpene of distinct structural features, has displayed antibacterial activity against Gram-negative bacteria, *Pseudomonas aeruginosa*, *Klebsiella pneumoniae*, *Escherischia coli* and Gram-positive *Staphylococcus aureus*.[2]

Cassane fuanditerpene isolated from *C. minax* have shown moderate antiviral activities against Para3 virus with inhibitory activity highest for caesalmin B (**35**) and bonducellpin D (**36**), which had IC_{50} values of 55 and 48 μM, respectively.[16] These compounds (**35**, **36**) represent another structurally different cassane diterpene with a 5-membered γ-lactone ring on the B/C ring system. Another member of the latter type of cassane diterpene, macrocaesalmin (**37**), containing a 10-membered macrocyclic 1,5-diketone and a *cis* B/D ring system, has also been reported to possess antiviral activity against respiratory syncytial virus (RSV) with IC_{50} = 24.2 μg/mL.[25] In addition, a cassane diterpenoid has been reported to possess inhibitory activity against mitogen responses of mouse spleen cells and the production of interleukin-1.[26]

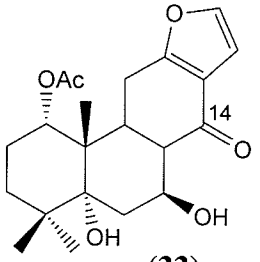

(33)

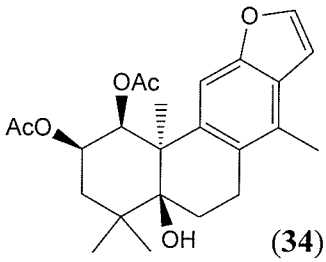

(34)

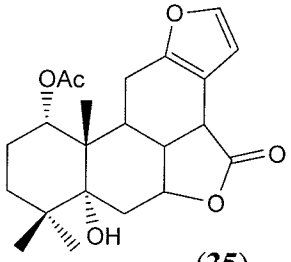

(35)

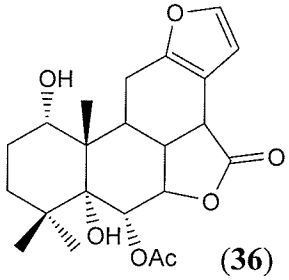

(36)

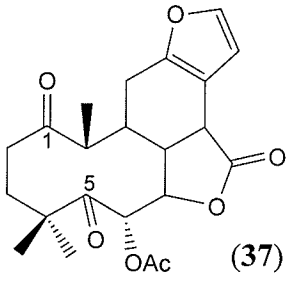

(37)

Apart from cassane diterpenods, flavonoids have also been reported from the members of genus *Casesalpinia*. Bonducellin (**38**) and isobonducellin (**39**), isolated from *C. pulcherrima*, have shown the most potent anti-inflammatory activities, amongst some other isolated flavonoids, in an assay that involves inhibition of inflammatory mediators, nitric oxide (NO) and cytokines – Tumour Necrosis Factor alpha (TNF-α) and Interleukin-12 (IL-12).[27] This result could support the application of *C. pulcherrima* extracts in folk medicine in the treatment of inflammatory diseases.[27]

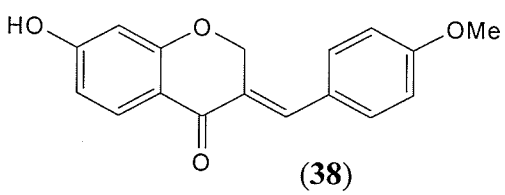

(**38**)

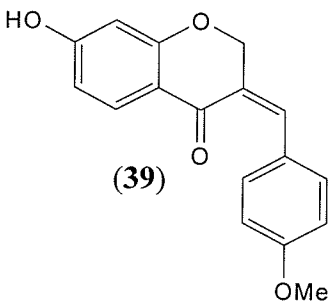

(**39**)

The crude ethanolic extract of *C. bonduc* exhibited moderate concentration-dependent GST inhibitory activity with an inhibitory concentration-50 (IC_{50}) value of 83μg/mL. This is the concentration of the extract that inhibited 50% of the activity of the enzyme. Based on this bio-activity, we performed fractionations on this crude extract to isolate natural products that exhibit GST inhibitory activity. Some of the non-polar column chromatographic fractions of *C. bonduc* exhibited moderate *in vitro* GST inhibition. Consequently, a number of compounds were isolated from these fractions and these include neocaesalpin O (**40**), 17-hydroxy-campesta-4,6-dien-3-one (**41**), caesaldekarin J (**42**), apigenin (**43**), pipataline (**44**), betulinic acid (**45**), 13,14-*seco*-stigmasta-5,14-dien-3α-ol (**46**) and 13,14-*seco*-stigmasta-9(11),14-dien-3α-ol (**47**). Spectroscopic methods were used to establish the structures of these compounds. In an effort to study the structure-activity relationships of **43**, **44**, **46** and **47**, different synthetic chemical analogues of these compounds were prepared. This section of the thesis describes the isolation and structure elucidation of these compounds as well as their GST inhibitory activity data, where applicable. Nearly half a dozen 13,14-*seco*-steroids have been reported in the literature, and no comments on their biosynthetic origin have been published. We have also proposed a plausible biogenetic pathway that could lead to the formation of the C/D *seco* ring of the 13,14-*seco*-steroids.

2.2 RESULTS AND DISCUSSION

The bark of the stem of *C. bonduc* collected from Sri Lanka was dried and ground into small pieces. The ground stem was extracted with 98% aqueous ethanol at room temperature. The solvent was evaporated under reduced pressure to yield a brownish gummy material (85 g). The gummy extract was subjected to chromatographic techniques including column chromatography and thin-layer chromatography (TLC) to isolate eight compounds (**40-47**). Compounds **40** and **41** were new natural products while **42-47** were known natural products.

2.2.1 Neocaesalpin O (40)

The first compound (**40**) was isolated as colorless oil in a low yield from a column chromatography fraction. Its UV spectrum showed maximum absorption at 286 nm indicating the presence of an α,β-unsaturated system of a cyclopentenone with a double bond extended conjugation.[28] The EI mass spectrum showed a molecular ion peak at *m/z* 360. A combination of EI MS, ^{1}H and ^{13}C NMR data provided a molecular formula, $C_{21}H_{28}O_5$, for **40**.

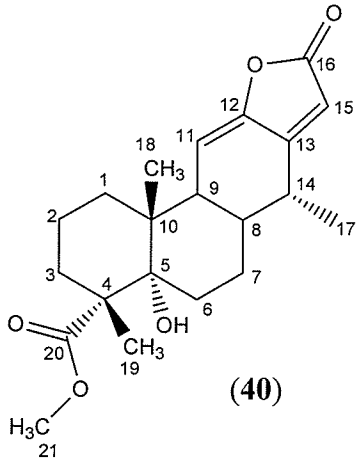

(40)

The ^{1}H NMR ($CDCl_3$, 300 MHz) of compound **40** displayed two three-proton singlets at δ 0.78 and 1.15, and these were assigned to the C-19 and C-18 methyl protons, respectively. A three-proton doublet was observed at δ 1.07 (J = 7.2 Hz) and this was due to the C-17 methyl protons. A downfield CH_3 signal was observed at δ 3.62 (*s*) and was assigned to the C-21 acetoxy methyl protons. The two-proton signals at δ 5.74 (*d*, J = 1.6 Hz) and 5.73 (*br s*) were due to the C-15 and C-11 olefinic protons, respectively. The small J value observed for H-15 was as a result of allylic coupling of this proton with the C-14 proton. The COSY-45° spectrum provided important information about ^{1}H-^{1}H spin correlation that helped in establishing the structure of this compound. H-14 (δ 2.85) showed interactions with H-17 (δ 1.07) while the signal at δ 1.56 (H-8) exhibited cross peaks with the H-9 signal at δ 1.92 in the spectrum. The ^{13}C-NMR spectrum (acetone-d_6, 50 MHz) showed resonances for all 19 carbon atoms, and their multiplicities were determined by attached proton test (APT). The APT spectrum ($CDCl_3$, 50 MHz) showed the presence of 4 CH_3, 5 CH_2, 5 CH and 5 quaternary carbon atoms in compound **40**. This showed the presence of signals at δ 76.8 and 178.0, which were due to quaternary C-5 and C-18, respectively. Negative phase CH_3 signals at δ 14.6, 15.9, 24.0 and 51.6 were assigned to C-17, C-19, C-18 and C-21, respectively. Olefinic carbon signals were also observed at δ 110.3, 112.9 and 162.8, and were due to C-15, C-11 and C-13, respectively. The other two quaternary carbon atoms did not show conspicuous peaks in neither the ^{13}C NMR nor the APT spectra.

The heteronuclear single quantum coherence (HSQC) spectrum of compound **40** aided the assignment of the proton signals to their respective carbon atoms. The ^{1}H, ^{13}C NMR and HSQC data of **40** are shown in Table 2.1. In addition, the heteronuclear

multiple bond connectivity (HMBC) spectrum was applied in the unambiguous determination of the position of the methoxy group and in establishing the structure of compound **40**. H_3-21 (δ 3.62) showed $^1H/^{13}C$ long range connectivity with C-20 (δ 178.4) while H_3-19 (δ 0.78) and H_3-18 (δ 1.15) showed interactions with C-5 (δ 76.8). H_3-18 also showed HMBC interactions with C-1 (δ 32.5), C-4 (δ 49.8) and C-20 (δ 178.4). The long range connectivities of H_3-17 (δ 1.07) with C-8 (δ 38.8), C-14 (δ 34.2) and C-13 (δ 162.8) as well as interactions of H-11 (δ 5.73) and H-15 (δ 5.74) with C-16 (δ 170.2) were also observed in the spectrum. The observed HMBC interactions in compound **40** are shown in **40a**.

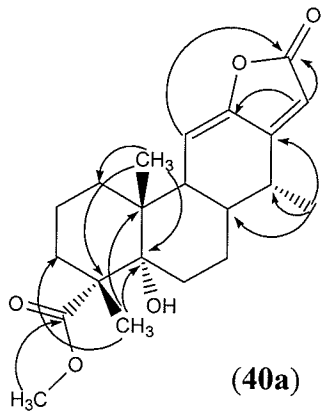

(**40a**)

The ^{13}C NMR data of **40** were similar to that of neocaesalpin I (**52**)[18] except for the presence of a signal at δ 76.8 due to the hydroxylated C-5, and this resulted in a slight shift in the δ values of some of the carbon signals in the ^{13}C NMR of **40** relative to that of neocaesalpin I. Some neocaesalpins are peculiar because of the absence of C-5 hydroxyl group in their structures. Neocaesalpins H and I were both reported as the first neocaesalpins having α,β-butenolide (α,β-unsaturated-γ-lactone) D ring system with oxidized C-20 and the absence of C-5 hydroxyl group.[18] This is the first report of cassane diterpene having α,β-butenolide system with both C-5 hydroxyl group and oxidized C-20.

Based on these spectral data, structure **40** was proposed for this new natural product. The possible biosynthetic origin of compound **40** is shown in scheme 2.1. Neocaesalpins H (**51**) and I (**52**) have been reported as part of the chemical constituents of different *Caesalpinia* species.[15,18]

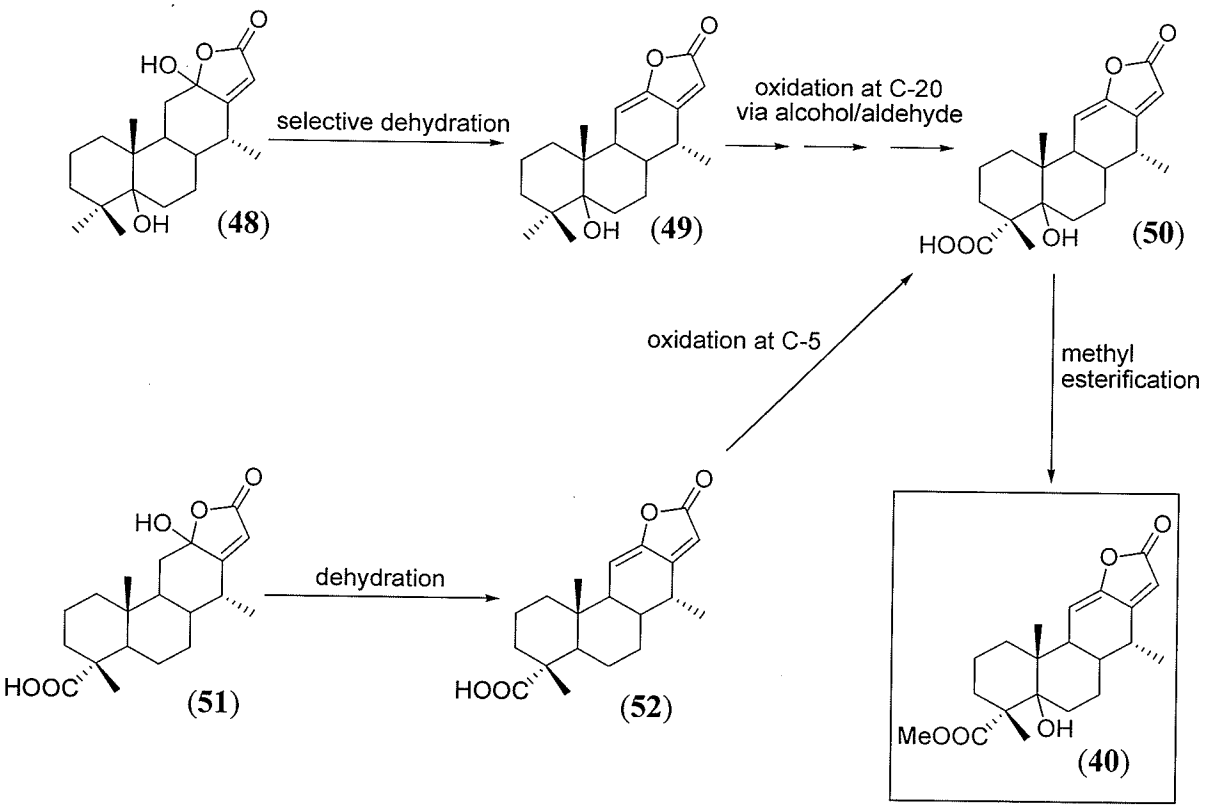

Scheme 2.1 Possible pathways towards the biosynthesis of compound **40**

Table 2.1 ^{1}H and ^{13}C NMR Spectroscopic Data (300 and 50 MHz, respectively) in $CDCl_3$ and acetone-d_6, respectively for compound **40**

	(40)	
Position	**δ_C**	**δ_H (*J* in Hz)**
1	32.5	
2	19.4	
3	31.3	
4	49.8	-
5	76.8	-
6	28.3[a,b]	
7	24.9	
8	38.8	1.56, *m*
9	41.8	1.92
10	41.6[b]	-
11	112.9	5.73, *br s*
12	150.4[c]	-
13	162.8	-
14	34.2	2.85, *m*
15	110.3	5.74, *d* (1.6)
16	170.2[c]	-
17	14.6	1.07, *d* (7.2)
18	24.0	1.15, *s*
19	15.9	0.78, *s*
20	178.4[c]	-
21	51.6	3.62, *s*

[a)]signal overlapped with d_6-acetone
[b)]signals observed in spectrum obtained in $CDCl_3$
[c)]signals observed in the HMBC spectrum

2.2.2 17-Hydroxy-campesta-4,6-dien-3-one (41)

The column chromatographic fraction, Fr-F, was loaded onto a silica gel column. The column on gradient elution with 0-50% hexane-ethylacetate yielded a fraction (FFQ9) which was subjected to preparative TLC using hexane-diethylether (1:4) as the mobile phase (see Experimental) to yield the second compound (**41**) as colorless oil.

The UV spectrum showed an absorption maximum at 284 nm indicating the presence of a six-membered enone with a double bond extended conjugation.[28] The IR spectrum displayed intense absorption bands at 3420 (OH), 2926 (CH), 1762 (C=O), 1384 (C=C) cm^{-1}. EI mass spectrum of **41** showed a molecular ion peak at *m/z* 412. HREIMS showed a molecular ion peak at *m/z* 412.3138, corresponding to the molecular formula $C_{28}H_{44}O_2$ (calc. 412.3141). This indicated the presence of seven double bond equivalents in compound **41**. Six degrees of unsaturation were due to the steroidal skeleton with two double bonds incorporated in the rings. The seventh double bond equivalent was due to the presence of carbonyl functionality in this compound.

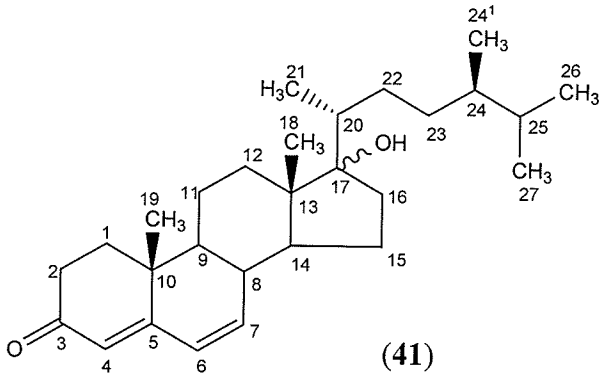

(41)

The ^1H NMR spectrum ($CDCl_3$, 300 MHz) of compound **41** showed the presence of two three-proton singlets at δ 0.72 and 1.16 due to the C-18 and C-19 methyl protons bonded to quaternary C-13 and C-10, respectively. Four three-proton doublets observed at δ 0.71 (J = 6.6 Hz), 0.80 (J = 6.5 Hz), 0.82 (J = 6.5 Hz) and 1.17 (J = 6.6 Hz) were

assigned to secondary C-24[1] (C-28), C-26, C-27 and C-21 methyl protons, respectively. Downfield resonances were observed at δ 5.76 (*dd*, J = 7.4, 10.2 Hz), 5.72 (*br s*) and 4.92 (*dd*, J = 1.3, 3.9 Hz), and these were assigned to the sp^2 hybridized C-6, C-4 and C-7 methine protons, respectively. The ^1H-^1H correlation spectroscopy (COSY-45°) spectrum of **41** displayed the presence of three spin systems "**41a-c**" in the compound. The molecular formula suggested the presence of two oxygen atoms in compound **41**. The presence of a hydroxyl group was confirmed by IR spectrum, which showed an absorption band at 3420 cm^{-1}. The ^{13}C NMR spectrum showed two resonances of two signals at δ 82.5 and 199.6, indicating the presence of oxygen functionalities at these carbon atoms. The ^{13}C NMR chemical shift values of the C-17 side chain was found to be similar to values for synthetic campestane steroid of similar structure.[29] Complete ^{13}C NMR chemical shift assignments of **41** and $^1H/^{13}C$ one-bond shift correlations of all protonated carbon atoms, as determined from HSQC spectrum, are presented in Table 2.2.

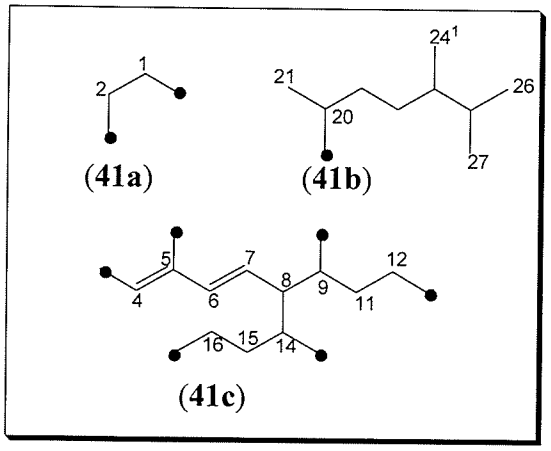

Table 2.2 ^{1}H and ^{13}C NMR Spectroscopic Data (300 and 50 MHz, respectively in $CDCl_3$) for compound **41**

	(41)	
Position	δ_C	δ_H (*J* in Hz)
1	35.7	2.10, 1.65, *m*
2	32.0	2.58, 2.38, *m*
3	199.6	-
4	110.0	5.72, *br s*
5	171.6	-
6	123.7	5.76, *dd* (7.4, 1.2)
7	123.7	4.92, *dd* (7.4, 5.6)
8	35.3	2.28, *m*
9	50.6	1.53, *m*
10	38.8	-
11	24.2	1.55, 1.33, *m*
12	39.6	2.02, 1.10, *m*
13	51.2	-
14	55.8	1.18, *m*
15	27.4	1.61, 1.20, *m*
16	33.9	2.09, 1.52, *m*
17	82.5	-
18	11.9	0.72, *s*
19	15.2	1.16, *s*
20	53.8	1.78, *m*
21	18.7	1.17, *d* (6.6)
22	32.9	1.28, 1.01, *m*
23	35.6	1.30, 1.22, *m*
24	55.8	1.12, *m*
25	56.0	1.64, *m*
26	17.3	0.80, *d* (6.5)
27	18.7	0.82, *d* (6.5)
28 (24^1)	21.0	0.71, *d* (6.6)

The heteronuclear multiple bond connectivity (HMBC) spectrum of **41** was useful in the unambiguous determination of the position of the oxygenated quaternary carbon atom, and in connecting the partial structures of **41** as obtained from the COSY-45° spectrum. The HMBC spectrum showed $^{1}H/^{13}C$ long-range couplings of H-18 (δ 0.72) with C-12 (δ 39.6) and C-14 (δ 55.8). The observed long-range interactions of H-18 with

the oxygenated quaternary C-17 (δ 82.5) and the methine C-20 (δ 53.8) resulted in the connection of the COSY-derived **41b** and **41c** partial structures. Other HMBC interactions observed in the HMBC spectrum of compound **41** are shown in structure **41d**. This shows that the C-19 methyl protons (δ 1.16) exhibited HMBC interactions with C-1 (δ 35.7), C-5 (δ 171.6), C-8 (δ 35.3), C-9 (δ 50.6) and C-10 (δ 38.8). These latter long-range couplings enabled the connection of the **41a** and **41b** partial structures of the compound. A combination of ^{1}H, ^{13}C NMR and mass spectral data suggested that compound **41** has a campestane skeleton. The presence of steroidal skeleton was also confirmed by a positive Liebermann-Burchard test (see Experimental for details).

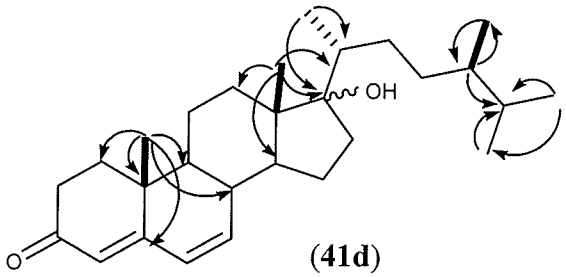

(41d)

After establishing a structure for compound **41**, the relative configuration of the chiral centers was established using the nuclear Overhauser effect spectroscopy (NOESY) spectrum. It has been established that H-9 and H-14 exist in the α-orientation while H-8, H_3-18 and H_3-19 have β-stereochemistry in steroidal compounds. The other stereogenic centers have the same orientations as those of reported compounds in this class of steroids.[30] The stereochemistry at C-17 of **41** was not established. Based on these spectroscopic data and comparison with literature data[29,30], structure **41** was proposed for this natural product characterized as 17-hydroxy-campesta-4,6-dien-3-one.

2.2.3 Caesaldekarin J (42)

The secondary column chromatographic fraction (FFQ9) of *C. bonduc* that resulted from the column chromatography of fraction F, on preparative TLC using hexane-diethylether (1:4) as the mobile phase (see Experimental), yielded caesaldekarin J (**42**) as a white solid.

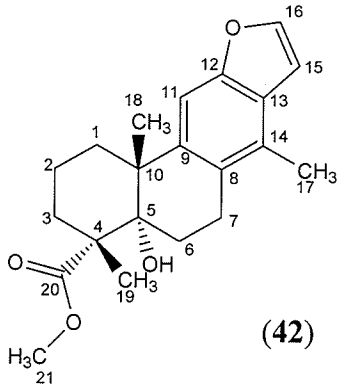

(**42**)

The IR spectrum of compound **42** showed absorption bands at 3439 (OH), 2933 (CH), 1713 (C=O), 1460 (C=C) and 1460 (C-O) cm^{-1}. The absorption band at 774 cm^{-1} showed the presence of a furan moiety in compound **42**.[10] The EI mass spectra of **42** showed molecular ion peaks at *m/z* 342. This was further confirmed by the CIMS which showed the $[M-H]^+$ peak at *m/z* 343. An ion at *m/z* 324 was due to the loss of a water molecule from the M^+. This indicated the presence of a hydroxyl group in the compound. The ^1H NMR spectrum ($CDCl_3$, 300 MHz) of **42** displayed four three proton singlets at δ 1.12, 1.29, 2.39 and 3.69 due to the C-19, C-18, C-17 and C-21 methyl protons, respectively. Downfield doublets, integrating for one proton each, were also observed at δ 6.78 (J = 2.2 Hz) and 7.59 (J = 2.2 Hz), and these were due to the two CH of the 1,2-disubstituted furan ring. A signal observed at δ 7.30 was assigned to the aromatic H-11 of the penta-substituted benzene C ring. The ^{13}C NMR spectrum of **42** showed the signals for all of the 21 carbon atoms in this compound. Distortionless enhancement by

polarization transfer (DEPT) spectrum was used in determining the multiplicities of these carbon atoms. This showed the presence of 4 CH_3, 5 CH_2 and 3 CH in compound **42**. Subtraction of the DEPT spectrum from the broadband ^{13}C NMR spectrum of **42** showed the presence of 9 quaternary carbon atoms in the compound. Two-dimensional NMR spectra (COSY, HSQC and HMBC) of **42** were also obtained and used in the elucidation of the structure of the compound. The ^{1}H, ^{13}C NMR, 2D NMR, IR and mass spectral data of **42** were identical to those of caesaldekarin J as reported in the literature.[10] Based on these data, compound **42** was identified as a known diterpene, caesaldekarin J. This compound (**42**) was previously isolated from *C. bonduc* by Reynold and co-workers.[10]

2.2.4 Apigenin (43)

Compound **43** was isolated as a yellow precipitate from the solution of fraction FQ11 (see Experimental) in hexane-ethylacetate (2:3) at room temperature. EI mass spectrum of **43** showed the presence of a molecular ion peak at *m/z* 270.

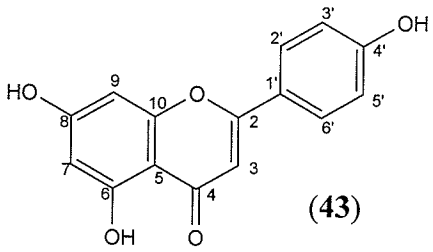

(43)

The ^{1}H NMR spectrum (C_5D_5N, 300 MHz) of **43** displayed downfield signals at δ 6.94, 6.86 and 6.79 which were assigned to H-3, H-9 and H-7, respectively. The two doublets observed at δ 7.94 (J = 8.6 Hz) and 7.25 (J = 8.6 Hz), each integrating for two protons, were due to the four methine protons of the di-substituted benzene ring of the compound. The ^{13}C NMR spectrum (pyridine-d_5, 75 MHz) of **43** showed signals for all 15 carbon atoms (see Experimental for complete ^{1}H and ^{13}C NMR δ assignments). The

HSQC spectrum was used in assigning the protons to their respective carbon atoms whereas HMBC spectrum was obtained to aid the complete connection of the various proton signals. The ^{1}H, ^{13}C NMR and mass spectral data of **43** were identical to those of apigenin as reported in the literature.[31,32] Based on these data, compound **43** was identified as a known flavonoid, apigenin.

2.2.5 Pipataline (44)

The column chromatographic fraction F, on gradient elution with 0-50% hexane-ethylacetate, yielded another fraction (FFQ1) which was subjected to preparative TLC to afford pipataline (**44**) as white solid. The IR spectrum of **44** showed intense absorption bands at 1602 (C=C) cm^{-1} whereas the EI-MS showed the molecular ion peak at *m/z* 288.

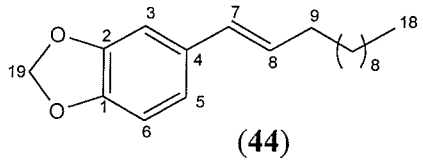

(**44**)

The ^{1}H NMR spectrum ($CDCl_3$, 300 MHz) of **44** showed the presence of two olefinic proton signals at δ 6.32 (*d*, *J* = 16.0 Hz) and 6.08 (*dt*, *J* = 16.0, 6.8, 3.0 Hz) due to the C-7 and C-8 methine protons, respectively. The singlet at δ 6.91 was assigned to the C-3 methine proton whereas the double-doublet observed at δ 6.72 (*J* = 8.0, 1.7 Hz), integrating for two protons, was due to H-5 and H-6. The signal for the methylene group of the dioxane ring was observed at δ 5.91. The ^{13}C NMR spectrum of **44** showed resonances for all the 19 carbon atoms in this compound (see Experimental for complete ^{1}H and ^{13}C NMR δ assignments). Two dimensional NMR spectra (COSY and HSQC) of **44** were also obtained and used in assigning the ^{1}H and ^{13}C NMR spectral data. Based on

these data, compound **44** was identified as pipataline (5-(1-dodeceneyl)-b 1,3-benzodioxol) previously isolated from *Piper peepuloides* by Atal *et al.*[33]

2.2.6 Betulinic acid (45)

Column chromatography of fraction F (0-50% hexane-ethylacetate) afforded fraction FQ14. Compound **45** precipitated as a white solid from a solution of fraction FQ14 in hexane-ethylacetate (1:1) at room temperature. The EI MS of **45** showed a molecular ion peak at *m/z* 456. This was further confirmed by CI mass spectrum which showed the $[M-H]^+$ peak at *m/z* 457. An ion observed at *m/z* 438 was due to the loss of a water molecule from the M^+. This indicated the presence of a hydroxyl group in this compound.

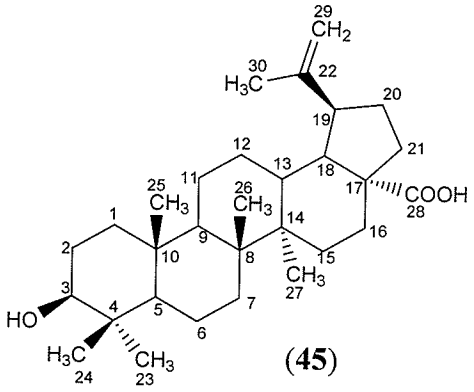

(45)

The ^1H NMR spectrum ($CDCl_3$, 300 MHz) of **45** showed the presence of two downfield broad singlets at δ 4.71 and 4.57, each integrating for one proton, due to the C-29 olefinic methylene protons. The double-doublet at δ 3.13 (J = 11.5, 5.0 Hz) was assigned to H-3 whereas the double-triplet at δ 3.02 was due to the C-19 methine proton. The four three-proton singlets observed at δ 0.74, 0.84, 1.04 and 1.68 were due to the C-25, C-24, C-23 and C-30 methyl protons, respectively whereas the six-proton singlet at δ 0.95 was due to H_3-26 and H_3-27. The ^{13}C NMR spectrum of **45** showed the resonances

for all of the 30 carbon atoms in this compound (see Experimental for ^{1}H and ^{13}C NMR δ assignments). Two dimensional NMR spectra (COSY, NOESY, HSQC and HMBC) of **45** were used to characterize this compound. The ^{1}H and ^{13}C NMR spectral data of **45** were identical to the spectral data of betulinic acid.[34] These helped to identify compound **45** as 3α-hydroxylup-20(29)-en-28-oic acid (betulinic acid).[34]

2.2.7 13,14-*seco*-stigmasta-5,14-dien-3α-ol (46)

The column chromatographic fraction G was loaded onto a silica gel column. The column on gradient elution with 0-100% hexane-ethylacetate yielded compound **46** as a white solid after crystallization in methanol at room temperature. The IR spectrum of **46** displayed intense absorption bands at 3419 (OH), 2965 (CH), 1598 (C=C) cm^{-1}. EI MS of **46** showed the molecular ion peaks at *m/z* 414. This was also confirmed by the CI MS which showed the $[M-H]^{+}$ peak at *m/z* 415.

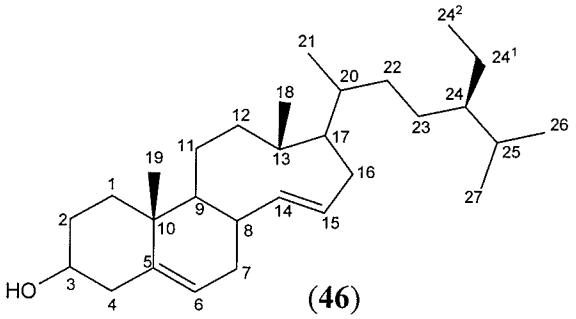

(46)

The ^{1}H NMR spectrum ($CDCl_3$, 300 MHz) of **46** showed three olefinic signals at δ 5.40 (*d*, *J* = 5.4 Hz), δ 5.12 (*dd*, *J* = 8.5, 8.8 Hz) and 5.00 (*dd*, *J* = 8.5, 8.8 Hz) due to H-6, H-14 and H-15, respectively. The C-18 methyl protons signal was observed at δ 0.68 (*J* = 6.6 Hz) as a doublet and this suggested the existence of a C/D *seco* ring system in the compound. The C-3 oxymethine proton resonated as a multiplet at δ 3.52. The ^{13}C NMR spectrum ($CDCl_3$, 300MHz) of **46** showed signals for all 29 carbon atoms. DEPT

spectrum indicated the presence of 6 CH_3, 10 CH_2 and 11 CH. Subtraction of DEPT from ^{13}C NMR signals showed the existence of 2 quaternary carbons in **46**. The COSY-45° and HSQC spectra of **46** were used to correctly assign all of the protons to their respective carbons and also completely elucidate the structure. The 2D NMR spectral data of **46** suggested that the C-14 and C-15 olefinic methine protons of compound **46** resonated at δ 5.12 and 5.00, respectively. In the HSQC spectrum, H-14 (δ 5.12) and H-15 (δ 5.00) showed $^{1}H/^{13}C$ one-bond shift correlations with C-14 (δ 138.3) and C-15 (δ 129.3), respectively. Previous reports interchanged these ^{1}H and ^{13}C NMR chemical shift assignments at C-14 and C-15.[35,36] These spectral data were found to be identical to those of 13,14-*seco*-stigmasta-5,14-dien-3α-ol reported in the literature.[35,36] These helped to characterize compound **46** as 13,14-*seco*-stigmasta-5,14-dien-3α-ol.

2.2.8 13,14-*seco*-stigmasta-9(11),14-dien-3α-ol (47)

In addition to compound **46**, preparative TLC on fraction FFQ11 using 75%Hex – 25%EtOAc yielded another *seco*-steroid (**47**) as a white amorphous solid. Its IR and EI mass spectra data were similar to those of **46**, suggesting that **47** may be an isomer of **46**.

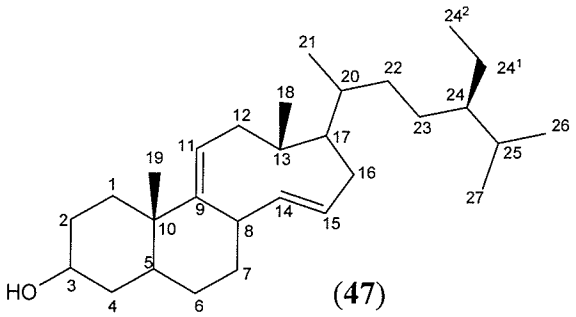

(**47**)

The ^{1}H NMR spectrum ($CDCl_3$, 300 MHz) of **47** showed three olefinic signals at δ 5.32 (*d*, *J* = 5.4 Hz), δ 5.20 (*dd*, *J* = 8.5, 8.8 Hz) and 5.06 (*dd*, *J* = 8.5, 8.8 Hz) due to H-11, H-14 and H-15, respectively, and a three-proton doublet at δ 0.68 (*J* = 6.6 Hz) due to

H_3-18. The multiplet at δ 3.38 was assigned to the C-3 oxymethine proton. The ^{13}C NMR spectrum ($CDCl_3$, 75MHz) of **47** also showed signals for 29 carbon atoms. DEPT spectrum of **47** was also used to establish multiplicity of these carbon atoms (see Experimental for complete ^{13}C NMR δ assignments). The positions of the double bonds in the compound were determined using information derived from HMBC spectrum of **47**. The ^{1}H-, ^{13}C-NMR and mass spectral data of compounds **46** and **47** were identical to the spectral data of *seco*-steroids previously reported in the literature.[35,36] Based on these data, compound **47** was identified as 13,14-*seco*-stigmasta-9(11),14-dien-3α-ol (**47**).[35,36] Compounds **46** and **47** were previously isolated from *Phyllanthus amarus*.[36] Compounds **43**, **44**, **46** and **47** were isolated for the first time from *C. bonduc*. Compounds **46** and **47** have not been previously isolated from any member of genus *Caesalpinia*.

2.2.9 Biogenesis of 13,14-*seco*-steroids

About half a dozen natural products have been previously reported in the class of 13,14-*seco*-steroids.[35-37] To the best of my knowledge, their biogenesis has not been previously reported in the literature. We hereby propose a plausible route that could lead to the production of the steroids. Biogenetically, the C/D *seco* ring may be produced in nature as illustrated in scheme 2.2 starting from a widely produced plant secondary metabolite, stigmast-5-en-3α-ol (**53**). Compound **53** is a plant sterol that is produced in nature from the mevalonate biosynthetic pathway. We propose that selective dehydration of **56**, produced from the reduction of the 14-keto-*seco*-steroid (**55**), could lead to the production of the 13,14-*seco*-steroid (**46**). However, there is no reported evidence of the existence of compounds **54-56** in nature.

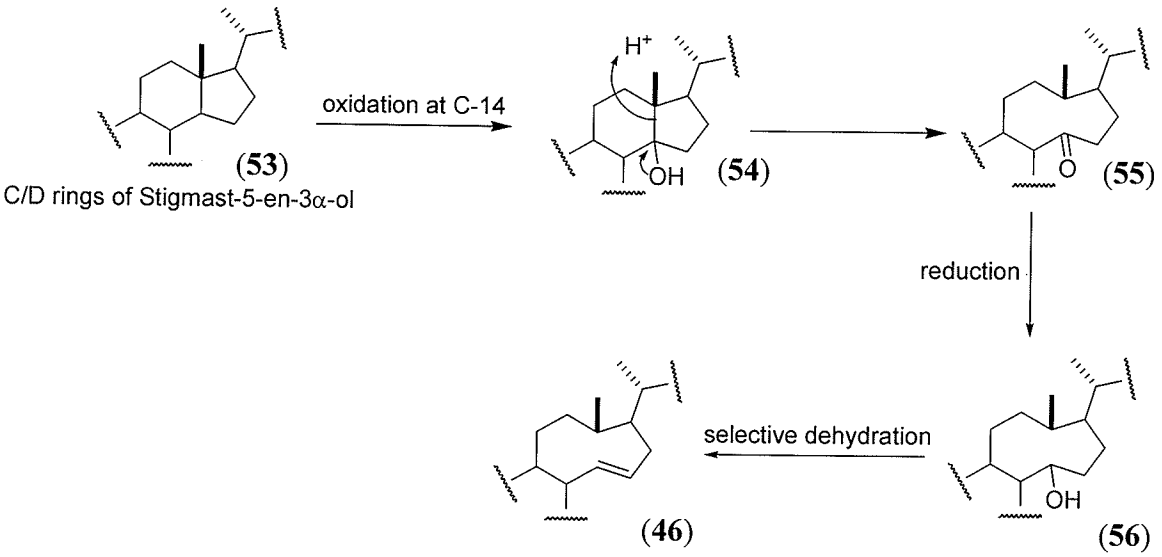

Scheme 2.2 Possible pathway towards the biosynthesis of the C/D *seco* ring of compound **46** starting from stigmast-5-en-3α-ol

2.2.10 Structure Activity Relationships (SAR)

Chemical derivatives of compounds **43**, **44**, **46** and **47** were synthesized to investigate the effects of changes in structural features on bioactivity. Compound **43** was transformed to its triacetate derivative (**57**) using acetic anhydride in pyridine. Compound **46** was oxidized to its monooxirane derivative (**59**) by reacting **46** with *m*-chloroperbenzoic acid using CH_2Cl_2 as solvent. The structure of **59** was confirmed by MS and ^{1}H-NMR. Pipataline (**44**) was also derivatized into its epoxide (**58**) under the same condition as above. Compound **47** was oxidized to its C-3 keto derivative (**60**) by treatment with PCC for 3 hours at room temperature. An acetyl derivative (**61**) of **47** was also prepared by reacting **47** with acetic anhydride using pyridine as a solvent. Details about these reactions and the spectroscopic data of the products are found in Experimental.

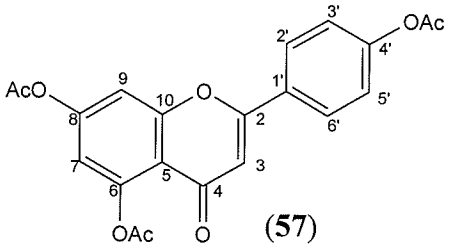

(**57**)

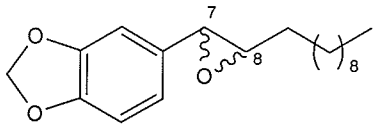

(**58**)

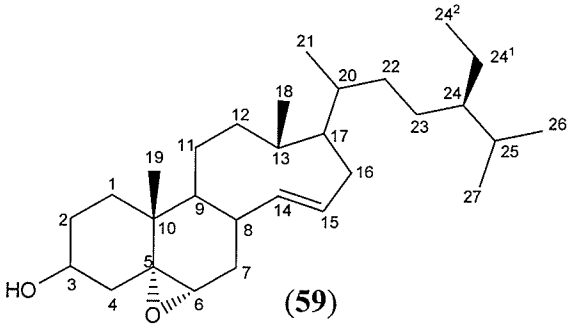

(**59**)

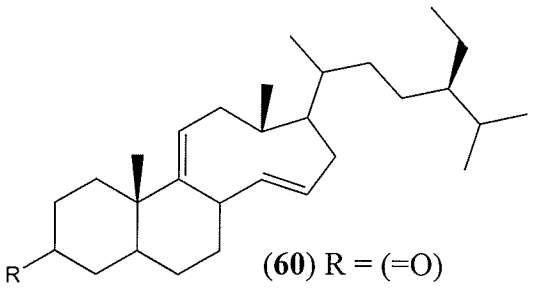

(**60**) R = (=O)
(**61**) R = OAc

2.2.11 Results of Enzyme Inhibition Assay

Table 2.3 shows the data for GST inhibition assay carried out on compounds **40-47**, **57-61**. Some of these compounds showed weak to moderate *in vitro* inhibitory activity against equine liver GST.

Table 2.3 Results of GST inhibition assay for compounds isolated from *C. bonduc* (**40-47**) and their derivatives (**57-61**). Activities are represented as IC_{50} (μM).

Compound	IC_{50} (μM)	Compound	IC_{50} (μM)
40	162.8	**47**	248.0
41	380.0	**57**	NA
42	250.0	**58**	86.9
43	NA	**59**	118.0
44	57.0	**60**	158.0
45	NA	**61**	153.0
46	230.0	-	-

NA = No Activity at 66.6 μg/mL

Amongst all the compounds assayed, pipataline (**44**) showed the best GST inhibitory activity with an IC_{50} value of 57 μM. In an attempt to study structure-activity relationship of this compound, epoxidation reaction was carried out on the C-7/C-8 double bond using *m*-CPBA in CH_2Cl_2. The resulting epoxide (**58**) displayed a lower GST inhibitory activity (IC_{50} = 86.9 μM) than the parent compound. This observation indicated that the C-7/C-8 double bond of pipataline may be an important structural feature required for its activity in GST inhibition. The cassane diterpenoids (**40**, **42**) both

showed insignificant activities in GST inhibition with IC_{50} values of 162 and 250 μM, respectively. Apigenin (**43**) was inactive in this assay. Acetylation of the three hydroxyl groups in apigenin yielded the triacetate (**57**) which was also found to be inactive in the GST inhibition assay at a maximum concentration of 66.6μg/mL. At this concentration, betulinic acid (**45**) showed no inhibition against the activity of GST. The *seco*-steroids (**46**, **47**) were weakly active in this assay. However, chemical modifications of their structures meagerly enhanced their GST inhibitory activity. The epoxide derivative (**59**) of **46** showed a significantly increased GST inhibition (IC_{50} = 118 μM) compared to its parent compound. These activities were compared to the activity of a steroidal non-substrate GST inhibitor, sodium taurocholate, which inhibited half of the activity of the enzyme at 398 μM under similar assay conditions.

2.3 EXPERIMENTAL

2.3.1 General

UV spectra were recorded on *Shimadzu UV-250 1 PC* spectrophotometer whereas IR spectra were recorded on *Bomem Hartmann and Braun (MB Series)* spectrometer. Optical rotation data were measured on a *Hitachi Polatronic-D* polarimeter. The ^{1}H-, ^{13}C-NMR, ^{1}H-^{1}H COSY, HSQC, HMBC and NOESY spectra were recorded on a *Bruker Avance 300* and *Varian Inova 200* spectrometers; chemical shifts are in ppm (δ) relative to tetramethylsilane (TMS) and coupling constants (*J*) are in Hz. EI/CI and HREI MS were measured on *Hewlett Packard 5989B* and *INCOSSO FINNIGA-MAT* mass spectrometers, respectively. Column chromatography was carried out on silica gel (200-400 mesh). Thin-layer chromatography was performed on *Merck* silica gel GF_{245} pre-coated plates. GST activity was measured on a *HP 8452* Diode Array spectrophotometer. Equine liver GST was purchased from *Sigma-Aldrich*. Glutathione (GSH) and 1-chloro-2,4-dinitrobenzene (CDNB) were purchased from *MP Biomedicals*.

2.3.2 Plant Material

The bark of *C. bonduc* was collected from Chalaw, Sri Lanka in December 2004 and identified by Dr. Radhika Samarasekera. The voucher specimen was deposited in the herbarium of the Industrial Technology Institute, Colombo, Sri Lanka.

2.3.3 Extraction and Isolation

The bark of *C. bonduc* (2 kg) was extracted with 98% ethanol at room temperature and the solvent evaporated under reduced pressure to yield a brownish gum.

The crude extract (85 g) was loaded onto a silica gel column and eluted using 0-100% Hex-EtOAc and 0-100% EtOAc -MeOH, to afford several fractions. These fractions were analyzed by analytical TLC, and fractions of same R_f were pooled together to afford fractions A-S. GST inhibition assay was carried out on these fractions, and this provided fractions F to H as the most active fractions with about 44-60% GST inhibition at 41.66 µg/mL. Column chromatography (0-50% hexane-EtOAc) on fraction F yielded 23 fractions FFQ1-23. Compound **40** (2.5 mg) was isolated from FFQ17 as a colorless oil. Preparative TLC of FFQ9 (20%hexane – 80%Et_2O) yielded compound **41** (7.8 mg) as a colorless oil and compound **42** (21 mg) as a white solid. Compound **43** (18.2 mg, light yellow solid) precipitated out of solution of FQ11 in 40%hexane – 60%EtOAc. Compound **44** (23.74 mg) was isolated by performing the preparative TLC (75%hexane – 25%EtOAc) of fraction FFQ1. Compound **45** (12.8 mg, white solid) precipitated out of solution of FQ14 in 50%hexane – 50%EtOAc. Column chromatography on fraction G (0-100% hexane-EtOAc) provided compound **46** as a white amorphous solid (28.3 mg) after crystallization in methanol. Preparative TLC on FFQ11 (75%hexane – 25%EtOAc) yielded compound **47** (9.6mg) as a white amorphous solid. Purity of these compounds was confirmed by the observation of homogenous spots on TLC using various solvent systems.

Compound **40**; Colorless oil, 2.5 mg, 0.002% yield, R_f 0.82 in 100% EtOAc; UV λ_{max} (CH_3OH): = 286 nm; ^{1}H-NMR ($CDCl_3$, 300 MHz) δ = see Table 2.1. ^{13}C-NMR ($CDCl_3$, 50 MHz) δ = see Table 2.1; CI MS = 361 (M^++1); EI MS *m/z* = 360 (M^+), 342, 334, 310, 282, 229, 214, 161, 105, 91, 69, 43.

17-Hydroxy-campesta-4,6-dien-3-one (**41**); Colorless oil, 7.8 mg, 0.009% yield, R_f 0.678 in 20%hexane – 80%Et_2O; $[\alpha]^{25}_D$ = +18 (*c* = 0.14, $CHCl_3$). UV λ_{max} ($CHCl_3$) = 284 nm; IR ν_{max} (KBr) = 3332 (OH), 2918 (CH), 1662 (C=C), 1082 (C-O) cm^{-1}. ^{1}H-NMR ($CDCl_3$, 300 MHz) δ = see Table 2.2. ^{13}C-NMR ($CDCl_3$, 75 MHz) δ = see Table 2.2. HREI MS *m/z* = 412.3138 (M^+, $C_{28}H_{44}O_2$, calcd 412.6478). CI MS = 413 (M^++1). EI MS *m/z* = 412, 394, 386, 370, 288, 271, 229, 147, 124, 43.

Caesaldekarin J (**42**); White solid, 21 mg, 0.0247% yield, R_f 0.76 in 1:4 hexane-Et_2O; IR ν_{max} (KBr) = 3439 (OH), 2933 (CH), 1713 (C=O), 1460 (C=C), 1150 (C-O), 774 (furan) cm^{-1}; ^{1}H NMR ($CDCl_3$, 300 MHz) δ = 7.59 (1H, *d*, *J* = 2.2 Hz, H-16), 7.30 (1H, *s*, H-11), 6.78 (1H, *d*, *J* = 2.2 Hz, H-15), 3.69 (1H, *s*, OMe-21), 2.84 (2H, *ddd*, *J* = 17.8, 8.1, 4.1 Hz, H_2-7), 2.64 (1H, *ddd*, *J* = 13.7, 8.1, 2.7 Hz, H-6), 2.39 (3H, *s*, H_3-17), 2.22 (1H, *ddd*, *J* = 13.7, 7.8, 4.1 Hz, H-6), 2.08 (1H, *m*, H-1), 2.02 (1H, *m*, H-3), 1.98 (1H, *m*, H-2), 1.82 (1H, *m*, H-1), 1.65 (1H, *m*, H-2), 1.62 (1H, *ddd*, *J* = 12.6, 5.0 Hz, H-3), 1.29 (3H, *s*, H_3-19), 1.12 (3H, *s*, H_3-18); ^{13}C NMR ($CDCl_3$, 75 MHz) δ = 179.1 (C-20), 155.3 (C-12), 145.5 (C-9), 145.3 (C-16), 128.6 (C-14), 128.3 (C-13), 126.4 (C-8), 106.2 (C-11), 105.8 (C-15), 76.9 (C-5), 52.1 (C-21), 49.5 (C-4), 44.8 (C-10), 33.6 (C-1), 33.0 (C-3), 28.3 (C-19), 26.9 (C-6), 24.9 (C-7), 24.6 (C-18), 20.7 (C-2), 16.0 (C-17); CI MS *m/z* = 343 (M^++1); EI MS *m/z* = 342 (M^+), 324, 265, 249, 209, 198, 185, 169, 146, 142, 115, 69, 55, 41.

Apigenin (**43**); Light yellow solid, 18.2 mg, 0.021% yield, R_f 0.14 in hexane-EtOAc (1:1); ^{1}H NMR (pyridine-d_5, 300 MHz) δ = 14.10 (1H, *s*, 6-OH), 13.32 (1H, *br s*, 8-OH), 7.94 (2H, *d*, *J* = 8.6 Hz, H-3′ and H-5′), 7.25 (2H, *d*, *J* = 8.6 Hz, H-2′ and H-6′), 6.94 (1H, *s*, H-3), 6.86 (1H, *d*, *J* = 2.0 Hz, H-9), 6.79 (1H, *d*, *J* = 2.2 Hz, H-7), 5.17 (1H, *br s*, 4′-OH); ^{13}C NMR (pyridine-d_5, 75 MHz) δ = 184.7 (C-4), 167.8 (C-10), 166.5 (C-2), 165.1 (C-4′), 164.6 (C-8), 160.4 (C-6), 130.9 (C-3′, C-5′), 124.2 (C-5), 118.8 (C-2′, C-6′), 106.9 (C-1′), 105.8 (C-3), 102.0 (C-9), 96.8 (C-7); EI MS *m/z* = 270 (M^+), 242, 213, 171, 153, 121, 84, 55, 44.

Acetylation of Apigenin (43):

5 mg of apigenin (**43**) was dissolved in equal parts of pyridine and acetic anhydride. The mixture was stirred at room temperature for 6 h. The reaction progress was monitored on TLC after every 2 h until all the starting material has been converted to the product. On completion of reaction, the mixture was evaporated to dryness and reconstituted using CH_2Cl_2. The organic extract was washed using 2N HCl and aq. $NaHCO_3$, and dried over anhydrous $MgSO_4$. The resultant slightly impure product (based on ^{1}H-NMR) was subsequently purified using column chromatography (40%hexane – 60%EtOAc) to yield 3.6 mg of pure apigenin triacetate (**57**).

Apigenin triacetate (**57**); White amorphous solid, 72% yield, R_f 0.60 in hexane-EtOAc (4:6); ^{1}H NMR ($CDCl_3$, 300 MHz) δ = 7.98 (2H, *d*, *J* = 8.6 Hz, H-3′ and H-5′), 7.35 (1H, *d*, *J* = 8.6 Hz, H-9), 7.28 (2H, *d*, H-2′ and H-6′), 6.85 (1H, *d*, *J* = 2.0 Hz, H-7), 6.62 (1H, *s*, H-3), 2.44 (3H, *s*, -$COCH_3$), 2.35 (3H, *s*, -$COCH_3$), 2.34 (3H, *s*, -$COCH_3$).

Pipataline, 5-(1-dodecenyl)-b 1,3-benzodioxol (**44**); White solid, 23.74 mg, 0.029% yield, R_f 0.76 in 80:20:0.1 hexane-Et_2O-AcOH; UV ($CHCl_3$): λ_{max} = 260 nm; IR (KBr) υ_{max} = 1602 (C=C) cm^{-1}; ^1H NMR ($CDCl_3$, 300 MHz) δ = 6.91 (1H, *s*, H-3), 6.72 (2H, *dd*, *J* = 8.0, 1.7 Hz, H-5 and H-6), 6.32 (1H, *d*, *J* = 16.0 Hz, H-7), 6.08 (1H, *dt*, *J*= 16.0, 6.8, 3.0 Hz, H-8), 5.91 (2H, *s*, H_2-19), 2.17 (2H, *m*, H_2-9), 1.34 (14H, *s*, H_2-10 to H_2-16), 0.82 (3H, *t*, *J* = 5.7 Hz, H-18); ^{13}C NMR ($CDCl_3$, 50 MHz) δ = 148.5 (C-1), 148.0 (C-2), 105.3 (C-6), 129.6 (C-7), 129.2 (C-8) 128.5 (C-4), 120.2 (C-5), 100.5 (C-19), 33.1 (C-9), 32.9 (C-10), 31.9 (C-11), 29.1 (C-12), 29.5 (C-13), 29.5 (C-14), 29.3 (C-15), 29.2 (C-16), 22.7 (C-17), 14.2 (C-18); EI MS *m/z* = 288, 131, 161, 135.

Epoxidation of pipataline (44):

3 mg pipataline (**44**) dissolved in 10 mL of CH_2Cl_2 was mixed with an equal amount of water containing 1g of $NaHCO_3$, followed by the cautious addition of 3.58 mg of *m*-chloroperbenzoic acid. The reaction mixture was stirred at room temperature for 18 h. Thereafter, 10 mL of Na_2SO_3 was added to the reaction mixture, which was later extracted twice with 10 mL of CH_2Cl_2. The organic phase was washed twice with 25 mL $NaHCO_3$ and dried over anhydrous $MgSO_4$ to give 2.76 mg (92% yield) of 7,8-epoxepipataline (**58**) as a white solid.

7,8-Epoxypipataline (**58**); White powder; ^{1}H NMR ($CDCl_3$, 200 MHz) δ = 6.91 (1H, *s*, H-3), 6.72 (2H, *dd*, *J* = 8.00, 1.5 Hz, H-5 and H-6), 3.37 (1H, *d*, *J* = 2.0 Hz, H-7), 2,8 (1H, *ddd*, *J* = 7.3, 2.4, 2.0 Hz, H-8), 5.91 (2H, *s*, H-15), 2.17 (2H, *m*, H-9), 1.34 (14H, *s*, H-10 to H-16), 0.82 (3H, *t*, *J* = 6.0 Hz, H-18); ^{13}C NMR ($CDCl_3$, 50 MHz) δ = 147.8 (C-1), 147.9 (C-2) 105.3 (C-6), 62.9 (C-7), 58.6 (C-8) 128.5 (C-4) , 120.2 (C-5), 100.5 (C-19), 33.1 (C-9), 32.9 (C-10), 31.9 (C-11), 29.1 (C-12), 29.5 (C-13), 29.5 (C-14), 29.3 (C-15), 29.2 (C-16), 22.7 (C-17), 14.2 (C-18); EI MS *m/z* = 304, 150, 135, 63, 177.

Betulinic acid, 3α-hydroxylup-20(29)-en-28-oic acid (**45**); White solid, 12.8 mg, 0.015% yield, R_f 0.41 in 1:1 hexane-EtOAc; ^{1}H NMR ($CDCl_3$, 300 MHz) δ = 4.71 (1H, *br s*, H_a-29), 4.57 (1H, *br s*, H_b-29), 3.13 (1H, *dd*, *J* = 11.5, 5.0 Hz, H-3), 3.02 (1H, *dt*, *J* = 11.5, 5.0 Hz, H-19), 2.35 (1H, *m*, H-13), 2.24 (1H, *m*, H_β-16), 1.68 (3H, *s*, H_3-30), 1.52 (1H, *m*, H_α-16), 1.04 (3H, *s*, H_3-23), 0.95 (3H, *s*, H_3-27), 0.95 (3H, *s*, H_3-26), 0.84 (3H, *s*, H_3-24), , 0.74 (3H, *s*, H_3-25); ^{13}C NMR ($CDCl_3$, 50 MHz) δ = 178.6 (C-28), 151.8 (C-20), 108.4 (C-29), 76.9 (C-3), 56.2 (C-5), 56.1 (C-17), 51.3 (C-9), 49.7 (C-18), 47.9 (C-19), 43.1 (C-14), 41.4 (C-8), 39.5 (C-4), 39.4 (C-1), 38.9 (C-13), 37.9 (C-22), 37.7 (C-10), 35.1 (C-7), 32.8 (C-16), 31.3 (C-21), 30.0 (C-15), 28.5 (C-23), 28.2 (C-2), 26.3 (C-12), 21.6 (C-11), 19.4 (C-30), 19.0 (C-6), 16.6 (C-26), 16.4 (C-24), 16.0 (C-27), 14.9 (C-25). CI MS = *m/z* 457 (M^++1); EI MS = *m/z* 456 (M^+), 438, 423, 410, 395, 377, 369, 302, 296, 248, 204, 189, 175, 148, 136, 121, 118, 107, 80, 67, 55, 43.

13,14-*Seco*-stigmasta-5,14-diene-3α-ol (**46**); White amorphous solid, 28.3 mg, 0.033% yield, R_f 0.31 in 20%hexane – 80%Et_2O; IR (KBr) ν_{max} = 3419 (OH), 2965 (C-H), 1598 (C=C) cm^{-1}; ^1H NMR ($CDCl_3$, 300 MHz) δ = 5.40 (1H, *d*, *J* = 5.4 Hz, H-6), 5.12 (1H, *dd*, *J* = 8.8, 8.5 Hz, H-14), 5.00 (1H, *dd*, *J* = 8.8, 8.5 Hz, H-15), 3.52 (1H, *m*, H-3), 2.27 (1H, *m*, $H_α$-4), 2.26 (1H, *m*, $H_β$-1), 2.17 (1H, *m*, $H_β$-4), 2.01 (1H, *m*, $H_α$-7), 1.81 (1H, *m*, $H_α$-1), 1.55 (1H, *m*, H-17), 1.50 (1H, *m*, H-13), 1.00 (3H, *s*, H_3-19), 0.91 (3H, *d*, *J* = 6.6 Hz, H_3-21), 0.85 (3H, *d*, *J* = 6.6 Hz, H_3-26), 0.83 (3H, *d*, *J* = 6.5 Hz, H_3-27), 0.80 (3H, *t*, *J* = 4.4 Hz, H_3-29), 0.68 (3H, *d*, *J* = 6.6 Hz, H_3-18); ^{13}C-NMR ($CDCl_3$, 75 MHz) δ = 140.7 (C-5), 138.3 (C-14), 129.3 (C-15), 121.7 (C-6), 71.7 (C-3), 56.7 (C-17), 51.2 (C-8), 50.1 (C-9), 45.8 (C-24), 42.2 (C-4), 40.5 (C-13), 39.6 (C-22), 37.2 (C-1), 36.5 (C-10), 36.1 (C-20), 34.0 (C-7), 31.8 (C-28), 31.6 (C-2), 29.1 (C-25), 28.2 (C-16), 25.8 (C-23), 24.3 (C-11), 21.1 (C-12), 19.8 (C-19), 19.4 (C-22), 19.0 (C-26), 18.8 (C-21), 12.0 (C-18), 11.9 (C-29); CI MS *m/z* = 415 (M^++1); EI MS *m/z* = 414, 396, 382, 368, 351, 329, 303, 273, 255, 213, 199, 159, 145, 91, 57, 43.

Epoxidation of 13,14-*seco*-stigmasta-5,14-dien-3α-ol (46):

Compound **46** (5 mg) was dissolved in 4 mL of CH_2Cl_2 and 0.64 mM *m*-chloroperbenzoic acid. The mixture was stirred for 3 h at room temperature and the progress of the reaction monitored using TLC after every 1 h. On completion of reaction, the mixture was air dried, reconstituted using CH_2Cl_2, and the resulting organic component purified using column chromatography (0-50% Hex-$CHCl_3$) to obtain 3.6 mg of the monooxirane (**59**) derivative of the sterol in 72% yield.

5α,6α-Epoxy-13,14-*seco*-stigmast-14-en-3α-ol (**59**); White solid, R_f 0.34 in 1:1 hexane-EtOAc; ^{1}H-NMR ($CDCl_3$, 300 MHz) δ = 3.96 (1H, *m*, H-3), 2.95 (1H, *dd*, H_α-6); 1D-NOE ($CDCl_3$, 300 MHz) δ = 1.95 (1H, *dd*, H_α-4), 1.25 (1H, *dd*, H_α-7), 1.45 (1H, *dd*, H-8); CI MS *m/z* = 431 (M^++1); EI MS *m/z* = 430 (M^+), 412, 398, 289, 253.

13,14-*Seco*-stigmasta-9(11),14-diene-3α-ol (**47**); White amorphous solid, 9.6 mg, 0.0113% yield, R_f 0.396 in 20%hexane – 80%Et_2O; IR (KBr) ν = 3410 (OH), 2962 (C-H), 1586 (C=C) cm^{-1}; ^1H NMR ($CDCl_3$, 300 MHz) δ = 5.32 (1H, *d*, *J* = 5.4 Hz, H-11), 5.20 (1H, *dd*, *J* = 8.8, 8.5 Hz, H-14), 5.06 (1H, *dd*, *J* = 8.8, 8.5 Hz, H-15), 3.38 (1H, *m*, H-3), 2.20 (1H, *m*, $H_α$-4), 2.20 (1H, *m*, $H_β$-1), 2.01 (1H, *m*, $H_α$-2), 1.84 (1H, *m*, $H_β$-4), 1.57 (1H, *m*, H-5), 1.55 (1H, *m*, H-13), 1.45 (1H, *m*, H-17), 1.42 (1H, m, $H_β$-2), 1.21 (1H, m, $H_α$-1), 1.01 (3H, *s*, H_3-19), 0.97 (3H, *d*, *J* = 6.6 Hz, H_3-21), 0.86 (3H, *d*, *J* = 6.6 Hz, H_3-26), 0.85 (3H, *d*, *J* = 6.5 Hz, H_3-27), 0.83 (3H, *t*, *J* = 4.3 Hz, H_3-29), 0.68 (3H, *d*, *J* = 6.6 Hz, H_3-18); ^{13}C-NMR ($CDCl_3$, 75 MHz): *δ*= 142.3 (C-9), 139.3 (C-14), 130.0 (C-15), 121.5 (C-11), 71.6 (C-3), 57.7 (C-17), 52.1 (C-8), 51.2 (C-5), 46.6 (C-24), 41.4 (C-4), 40.6 (C-13), 40.5 (C-22), 38.2 (C-1), 37.3 (C-20), 36.9 (C-10), 34.6 (C-12), 32.7 (C-28), 32.3 (C-2), 29.9 (C-25), 26.7 (C-16), 26.6 (C-23), 24.9 (C-6), 21.7 (C-7), 20.1 (C-27), 19.8 (C-19), 19.3 (C-26), 19.2 (C-21), 12.4 (C-18), 12.2 (C-29); CI MS *m/z* = 415 (M^++1); EI MS *m/z* = 414, 396, 382, 368, 351, 273, 255, 213, 145, 57, 43.

Oxidation of 13,14-*seco*-stigmasta-9(11),14-diene-3α-ol (47):

Compound **47** (3 mg; 10 mM) was dissolved in CH_2Cl_2 and 15 mM pyridinium chlorochromate (PCC) solution in CH_2Cl_2. The reaction mixture was stirred at room temperature for 3 h and reaction progress monitored using TLC after every 1 h. On completion of reaction, the mixture was evaporated to dryness and the organic component extracted with CH_2Cl_2. The extract was washed twice using 2N HCl and subsequently with equal volume of aqueous $NaHCO_3$. The organic layer was separated and dried over anhydrous $MgSO_4$ to afford 1.9 mg (63.3% yield) of the oxidized derivative (**60**) of the sterol.

3-Oxo-13,14-*seco*-stigmasta-9(11),14-diene (**60**); R_f 0.89 in 1:1 hexane-EtOAc; ^{1}H-NMR ($CDCl_3$, 300 MHz) δ = 5.32 (1H, *d*, *J* = 5.4 Hz, H-11), 5.20 (1H, *dd*, *J* = 8.8, 8.5 Hz, H-14), 5.05 (1H, *dd*, *J* = 8.8, 8.5 Hz, H-15), 3.32 (1H, *ddd*, H-4), 3.24 (1H, *ddd*, H-4), 2.47 (1H, *dd*, H-2), 2.40 (1H, *dd*, H-2), 2.33 (1H, *m*, H-5), 1.19 (3H, *s*, H_3-19), 0.70 (3H, *d*, H_3-18); CI MS *m/z* = 413 (M^++1). EI MS *m/z* = 412 (M^+), 271.

Acetylation of 13,14-*seco*-stigmasta-9(11),14-diene-3α-ol (47):

Compound **47** (3 mg; 3.62 mM) was dissolved in equal parts of pyridine and acetic anhydride. The mixture (5 mL) was stirred at room temperature for 3 h. On completion of reaction, the mixture was evaporated to dryness and reconstituted using CH_2Cl_2. The organic extract was washed using 2N HCl and aq. $NaHCO_3$, and dried over anhydrous $MgSO_4$ to afford 2.5 mg (83.3% yield) of the acetyl derivative (**61**) of the sterol.

3α-Acetoxy-13,14-*seco*-stigmasta-9(11),14-diene (**61**); White solid, R_f 0.91 in 1:1 hexane-EtOAc; ^{1}H-NMR ($CDCl_3$, 300 MHz) δ = 5.30 (1H, *d*, *J* = 5.4 Hz, H-11), 5.22 (1H, *dd*, *J* = 8.8, 8.5 Hz, H-14), 5.04 (1H, *dd*, *J* = 8.8, 8.5 Hz, H-15), 4.62 (1H, *m*, H-3), 2.05 (3H, *s*, acetyl CH_3), 1.02 (3H, *s*, H_3-19), 0.97 (3H, *d*, *J* = 6.6 Hz, H_3-21), 0.86 (3H, *d*, *J* = 6.6 Hz, H_3-26), 0.85 (3H, *d*, *J* = 6.5 Hz, H_3-27), 0.83 (3H, *t*, *J* = 4.3 Hz, H_3-29), 0.66 (3H, *d*, *J* = 6.6 Hz, H_3-18). CI MS *m/z* = 457 (M^+-H). EI MS *m/z* = 456 (M^+).

Liebermann-Burchard test

The presence of steroidal skeleton in compounds **41**, **46** and **48** was confirmed by conducting Liebermann-Burchard test on these compounds. One drop of H_2SO_4 and 3 drops acetic anhydride were added to a test tube containing the compound. The mixture was allowed to stand for a period of 10 min at room temperature. A resulting green-blue color indicates the presence of a steroidal skeleton in the compound. Compounds **41**, **46** and **48** tested positive in this test.

2.3.4 Assay for Glutathione *S*-Transferase Inhibition

The inhibitory activity of the fractions and isolated compounds against GST was assayed according to the spectrophotometric method of Habig *et al.*[38] This assay measures the activity of the enzyme in conjugation of 1-chloro-2,4-dinitrobenzene (CDNB) with glutathione (GSH), and the resulting conjugate (GS-DNB) measured at 340 nm. Various concentrations of the compounds were incubated with the enzyme at 22 °C for 30 min after which the assay was performed. The assay mixture contains final concentrations of 5 mM GSH, 1 mM CDNB, 100 mM phosphate buffer (*p*H 6.5) and GST in a 3 mL total assay volume. The rate of release of GS-DNB adduct was measured at 340 nm after 40 sec using a UV/Vis *HP 8452 Diode Array* spectrophotometer. Basal coupling between the substrates was analyzed and observed to be insignificant under these assay conditions. Substrate limitation was also taken into consideration, and was observed not to occur during the initial 60 sec of the assay under the same assay conditions. The effects of the compounds against the activity of the enzyme were calculated as IC_{50}, which are concentrations of the inhibitors at which the enzyme losses 50% of its activity. The IC_{50} values of the fractions and isolated compounds were calculated relative to a control assay. Sodium taurocholate, a steroidal GST inhibitor, was used as a positive control in this assay.

2.4 REFERENCES

1. Chakrabarti, S., Biswas, T. K., Rokeya, B., Ali, L., Mosihuzzaman, M., Nahar, N., Khan-Azad, A. K. and Mukherjee, B. Advanced studies on the hypoglycemic effect of *Caesalpinia bonducella* F. in type 1 and 2 diabetes in Long Evans rats. *J. Ethnopharmacol.*, **2003**, *84*, 41-46.
2. Simin, K., Khaliq-uz-Zaman, S. M. and Ahmad, V. U. Antimicrobial activity of seed extracts and bondenolide from *Caesalpinia bonduc* (L.) Roxb. *Phytother. Res.*, **2001**, *15*, 437-440.
3. Ali, M. S., Azhar, I., Amtul, Z., Ahmad, K. and Usmanghani, K. Antimicrobial screening of some Caesalpiniaceae. *Fitoterapia*, **1999**, *70*, 299-304.
4. Gupta, M., Mazumder, U. K., Kumar, R S., Sivakumar, T. and Vamsi, M. L. M. Antitumor activity and antioxidant status of *Caesalpinia bonducella* against Ehrlich ascites carcinoma in Swiss albino mice. *J. Pharmacol. Sci.*, **2004**, *94*, 177-184.
5. Gupta, M., Mazumder, U. K., Kumar, R S. and Kumar, T. S. Studies on anti-inflammatory, analgesic and antipyretic properties of methanol extracts of *Caesalpinia bonducella* leaves in experimental animal models. *Iran. J. Pharmacol. Ther.*, **2003**, *2*, 30-34.
6. Godoy, R. L. de O., Lima, P. D. de D. B., Pinto, A. C. and DeAquino Neto, F. R. Diterpenoids from *Dypterix odorata*. *Phytochemistry*, **1989**, *28*, 642-644.
7. Pascoe, K. O., Burke, B. A. and Chan, W. R. Caesalpin F: a new furanoditerpene from Caesalpinia bonducella. *J. Nat. Prod.*, **1986**, *49*, 913-915.

8. Peter, S. R., Tinto, W. F., McLean, S., Reynolds, W. F., Tay, L-. L., Yu, M. and Chan, W. R. Complete 1H and 13C NMR assignments of four caesalpin furanoditerpenes of *Caesalpinia bonducella*. *Magn. Reson. Chem.*, **1998**, *36*, 124-127.

9. Peter, S. R. and Tinto, W. F. Bonducellpins A-D, new cassane furanoditerpene of *Caesalpinia bonduc*. *J. Nat. Prod.*, **1997**, *60*, 1219-1221.

10. Lyder, D. L., Peter, S. R., Tinto, W. F., Bissada, S. M., McLean, S. and Reynolds, W. F. Minor cassane diterpenoids of *Caesalpinia bonduc*. *J. Nat. Prod.*, **1998**, *61*, 1462-1465.

11. Peter, S., Tinto, W. F., McLean, S., Reynolds, W. F. and Yu, M. Cassane diterpenes from *Caesalpinia bonducella*. *Phytochemistry*, **1998**, *47*, 1153-1155.

12. Kinoshita, T., Kaneko, M., Noguchi, H. and Kitagawa, I. New cassane diterpenes from *Caesalpinia bonduc* (Fabaceae). *Heterocycles*, **1996**, *43*, 409-414.

13. Lyder, D. L., Tinto, W. F., Bissada, S. M., McLean, S. and Reynolds, W. F. Caesalpinin B, a rearranged cassane furanoditerpene of *Caesalpinia bonduc*. *Heterocycles*, **1998**, *48*, 1465-1469.

14. Ragasa, C. Y., Ganzon, J., Hofilena, J., Tamboong, B. and Rideout, J. A. A new furanoid diterpene from *Caesalpinia pulcherrima*. *Chem. Pharm. Bull.*, **2003**, *51*, 1208-1210.

15. Roach, J. S., McLean, S., Reynolds, W. F. and Tinto, W. F. Cassane diterpenoids of *Caesalpinia pulcherrima*. *J. Nat. Prod.*, **2003**, *66*, 1378-1381.

16. Jiang, R-. W., Ma, S-. C., He, Z-. D., Huang, X-. S., But, P. P-. H., Wang, H., Chan, S-. P., Ooi, E-. C., Xu, H-. X. and Mak, T. C. W. Molecular structure and antiviral activities of naturally occurring and modified cassane furanoditerpenoids and frieldelane triterpenoids from *Caesalpinia minax*. *Bioorg. Med. Chem.*, **2002**, *10*, 2161-2170.

17. Kalauni, S. K., Awale, S., Tezuka, Y., Banskota, A. H., Linn, T. Z. and Kadota, S. Methyl migrated cassane-type furanoditerpenes of *Caesalpinia crista*. *Chem. Pharm. Bull.*, **2005**, *53*, 1300-1304.

18. Kinoshita, T., Haga, Y., Narimatsu, S., Shimada, M. and Goda, Y. The isolation and structure elucidation of new cassane diterpene-acids from *Caesalpinia crista* L. (Fabaceae), and review on the nomenclature of some *Caesalpinia* species. *Chem. Pharm. Bull.*, **2005**, *53*, 717-720.

19. Kalauni, S. K., Awale, S., Tezuka, Y., Banskota, A. H., Linn, T. Z. and Kadota, S. New cassane-type diterpenes of *Caesalpinia crista* from Myanmar. *Chem. Pharm. Bull.*, **2005**, *53*, 214-218.

20. Cheenpracha, S., Karalai, C., Ponglimanont, C., Chantrapromma, K. and Laphookhieo, S. Cassane-type diterpenes from the seeds of *Caesalpinia crista*. *Helv. Chim. Acta*, **2006**, *89*, 1062-1066.

21. Kido, T., Taniguchi, M. and Baba, K. Diterpenoids from Amazonian crude drug of Fabaceae. *Chem. Pharm. Bull.*, **2003**, *51*, 207-208.

22. Linn, T. Z., Awale, S., Tezuka, Y., Banskota, A. H., Kalauni, S. K., Attamimi, F., Ueda, J., Asih, P. B. S., Syafruddin, D., Tanaka, K. and Kadota, S. Cassane- and norcassane-type diterpenes from *Caesalpinia crista* of Indonesia and their

antimalarial activity against the growth of *Plasmodium falciparum*. *J. Nat. Prod.*, **2005**, *68*, 706-710.

23. Omar, S., Zhang, J., MacKinnon, S., Leaman, D., Durst, T., Philogene, B. J. R., Arnason, J. T., Sanchez-Vindas, P. E., Poveda, L., Tamez, P. A. and Pezzuto, J. M. Traditionally-used antimalarials from the Meliaceae. *Curr. Top. Med. Chem.*, **2003**, *3*, 133-139.

24. Ahmad, V. U. and Usmanghani, K. Bondenolide, a new diterpenoid from the seeds of *Caesalpinia bonduc*. *Z. Naturforsch.*, **1997**, *52b*, 410-412.

25. Jiang, R-. W., But, P. P-. H., Ma, S-. C., Ye, W-. C., Chan, S-. P. and Mak, T. C. W. Structure and antiviral properties of macrocaesalmin, a novel cassane furanoditerpenoid lactone from the seeds of *Caesalpinia minax*. *Tetrahedron Lett.*, **2002**, *43*, 2415-2418.

26. Kitagawa, I., Simanjuntak, P., Watano, T., Shibuya, H., Fujii, S., Yamagata, Y. and Kobayashi, M. Indonesian medicinal plants. XI. Chemical cstructures of caesaldekarins a and b, two new cassane-type furanoditerpenes from the roots of Caesalpinia major (Fabaceae). *Chem. Pharm. Bull.*, **1994**, *42*, 1798-1802.

27. Rao, Y. K., Fang, S-. H. and Tzeng, Y-. M. Anti-inflammatory activities of flavonoids isolated from *Caesalpinia pulcherrima*. *J. Ethnopharmacol.*, **2005**, *100*, 249-253.

28. Pavia, D. L., Lampman, G. M. and Kriz, G. S. Introduction to Spectroscopy, *3rd ed.*, Brooks/Cole Thomson Learning, USA, **2001**.

29. Seto, H., Fujioka, S., Takatsuto, S., Koshino, H., Shimizu, T. and Yoshida, S. Synthesis and 6-oxy functionalized campest-4-en-3-ones: efficient hydroperoxidation at C-6 of campest-5-en-3-one with molecular oxygen and silica gel. *Steroids*, **2000**, *65*, 443-449.

30. Mulheirn, L. J. Identification of C-24 alkylated stereanes by PMP spectroscopy. *Tetrahedron Lett.*, **1973**, *14*, 3175-3178.

31. Christophoridou, S., Dais, P., Tseng, L-. H and Spraul, M. Separation and identification of phenolic compounds in olive oil by coupling high-performance liquid chromatography with postcolumn solid-phase extraction to nuclear magnetic resonance spectroscopy (LC-SPE-NMR). *J Agric. Food Chem.*, **2005**, *53*, 4667-4679.

32. Van Loo, P., De Bruyn, A. and Budesinsky, M. Reinvestigation of the structural assignment of signals in the proton and carbon-13 NMR spectra of the flavone apigenin. *Magn. Reson. Chem.*, **1986**, *24*, 879-882.

33. Atal, C. K., Dhar, K. L. and Pelter, A. Structure of pipataline, an extractive from *Piper peepuloides*. *Chem. Ind.*, **1967**, *52*, 2173-2174.

34. Peng, C., Bodenhausen, G., Qiu, S., Fong, H. H. S., Farnsworth, N. R., Yuan, S. and Zheng, C. Computer-assisted structure elucidation: application of CISOC-SES to the resonance assignment and structure generation of betulinic acid. *Magn. Reson. Chem.*, **1998**, *36*, 267-278.

35. Bhandari, P., Kumar, N., Singh, B. and Kaul, V. K. Bacosterol glycoside, a new 13,14-*seco*-steroid from *Bacopa monnieri*. *Chem. Pharm. Bull.*, **2006** *54*, 240-241.

36. Ahmad, B. and Alam, T. Components from whole plant of *Phyllanthus amarus* Linn. *Ind. J. Chem.*, **2003**, *42B*, 1786-1790.

37. Sharma, S. K., Ali, M. and Singh, R. New 9β-lanostane-type triterpenic acid and 13,14-*seco*-steroidal esters from the roots of *Artemisia scoparia*. *J. Nat. Prod.*, **1996**, *59*, 181-184.

38. Habig, W. H., Pabst, M. J. and Jakoby, W. B. Glutathione *S*-transferases. First enzymic step in mercapturic acid formation. *J. Biol. Chem.*, **1974**, *249*, 7130-7139.

CHAPTER 3

Chemical Studies on *Nauclea latifolia*

3.1 Introduction

Nauclea latifolia Sm. (Rubiaceae) is a medicinally important plant predominantly distributed in the tropical regions of sub-Sahara Africa. It is locally known as Uburu-Ilu (Uvuru-Ilu) in Igbo land, and its roots and stem have been medicinally used as chewing stick in the Eastern and Northern parts of Nigeria.[1] The aqueous and alcoholic extracts of various parts of this plant are used in the treatment and alleviation of various disease conditions in ethno-medicine. For example, the ethanolic extracts of its roots and stem have been reported to possess *in vitro* anti-plasmodial activity against chloroquine-sensitive and chloroquine-resistant Nigerian and FCB1-Colombia strains of *Plasmodium falciparum* (IC_{50} = 0.6-7.5 μg/mL).[2,3] This extract has also shown *in vivo* anti-helminthic activity against a mixture of nematode species,[4] as well as antibacterial and antifungal activities against pathogenic bacteria and fungi.[1,5] Consequently, the aqueous root extract of this plant has been applied in the treatment of infectious diseases, for example, malaria caused by *P. falciparum*.[6] In a neuropharmoclogical study using rat model, the aqueous extract of this plant has been reported to contain some psychoactive compounds.[7] In addition, the polyphenolic extract showed anti-amoebic and spasmolytic activities against the growth of *Entamoeba histolytica* with minimum inhibitory concentration (MIC) < 10 μg/mL.[8]

Previous phytochemical investigations on the crude extracts of *N. latifolia* and other members of the family Rubiaceae have resulted in the isolation of predominantly monoterpene indole alkaloids and glycosides of pentacyclic oleanane- and ursane-type

triterpenes.[9-11] Amongst the first indole quinolizine alkaloids to be isolated from *N. latifolia* are naufoline (**62**), descarbomethoxynauclechine (**63**), nauclechine (**64**),[12] augustine (**65**) and its derivatives (**66-68**).[13] Later, a glyco-monoterpene indole alkaloid, strictosidine lactam (**70**), was also isolated from the methanolic extract of *N. latifolia* heartwood.[14]

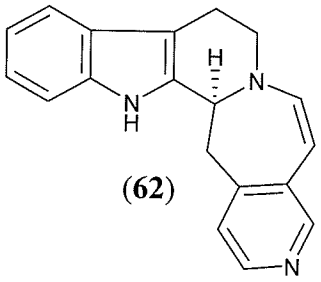

(**62**)

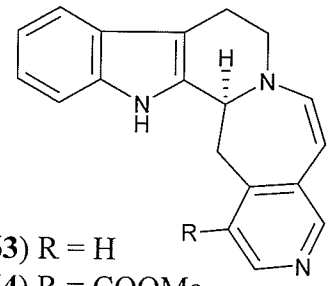

(**63**) R = H
(**64**) R = COOMe

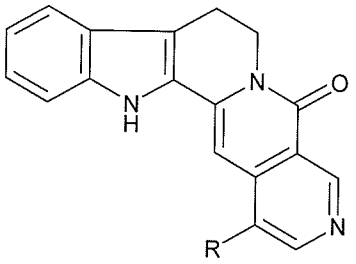

(**65**) R = CH=CH$_2$
(**66**) R = CHOH.Me
(**67**) R = H
(**68**) R = Ac
(**69**) R = Et

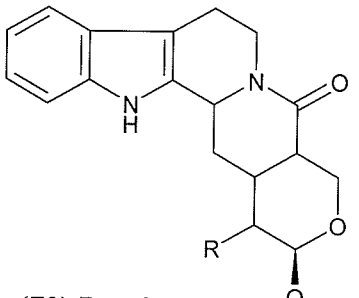

(**70**) R = CH=CH$_2$
(**71**) R = Et

Compound **70** has been reported to exhibit anti-plasmodial activity with IC_{50} values 0.45 and 0.37 μg/mL against *P. falciparum* strains K1 and NF54, respectively.[10] An earlier reported proposal of the easy conversion of strictosidine lactam (**71**) into dihydroaugustine (**69**) in the presence of ammonia[15] elicited an argument that the previously reported compounds (**62-68**) were in fact artifacts produced from the different derivatives of strictosidine lactam (**70**) since isolation work was carried out in the

presence of ammonia.[14,16] A structurally-related compound, naulafine (**72**) alongside other glyco-monoterpene indole alkaloids, cadambine (**73**), 3α-dihydrocadambine (**74**) and naucleidinal (**75**)[17] were also isolated by the same authors from *N. latifolia*.

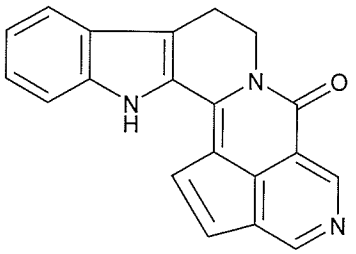

(**72**)

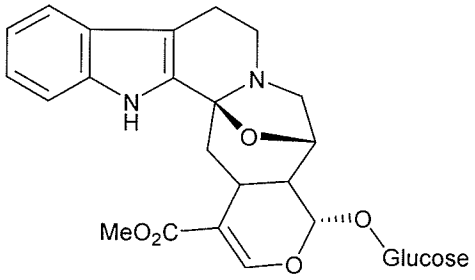

(**73**)

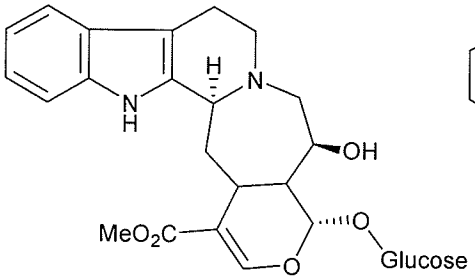

(**74**)

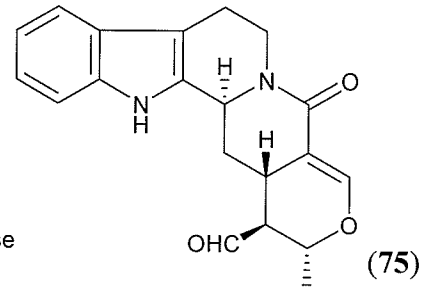

(**75**)

The pathway for the transformation of glyco-monoterpene indole alkaloids into pyridinium ring-containing indole alkaloids has recently been proposed.[18] This involves a chemoenzymatic transformation of the alkaloid (**76**) in the presence of β-glucosidase and 10% aqueous NH_4OAc at 37°C leading to incorporation of the ammonium nitrogen into the structure (scheme 3.1).[18] This pathway could be an evidence to support the natural biosynthesis and occurrence of the pyridinium indole alkaloids in *N. latifolia*.

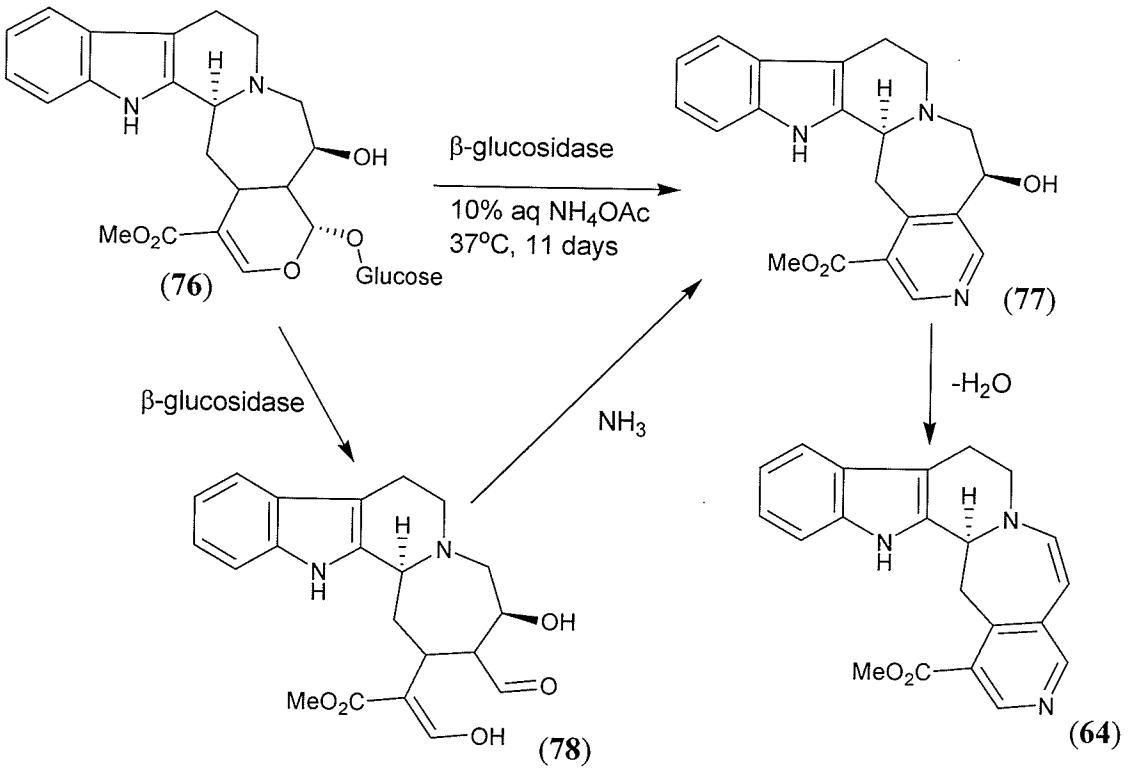

Scheme 3.1 Pathway for the chemoenzymatic transformation of **76** into pyridinium indole alkaloids[18]

In addition to these compounds, bioassay-guided fractionations of the bioactive chloroform and butanol fractions of another member of the *Nauclea* genus, *N. orientalis*, using the assay for inhibition of the secreted aspartic protease (SAP) resulted in the isolation of indole and glyco-indole alkaloids, nauclealines A (**79**) and B (**80**), naucleosides A (**81**) and B (**82**) as well as a B/C rings rearranged alkaloid, pumiloside (**83**).[19]

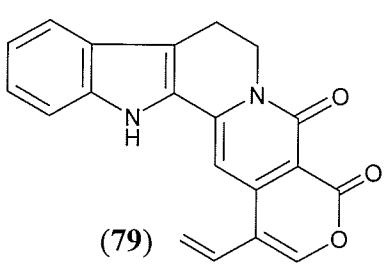

(79)

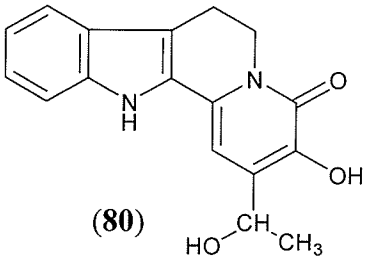

(80)

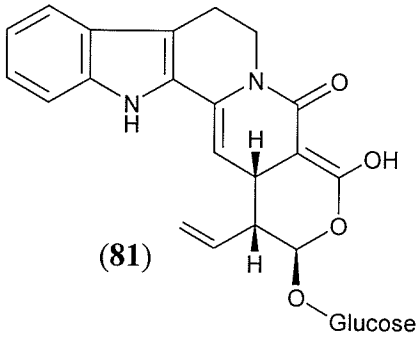

(81)

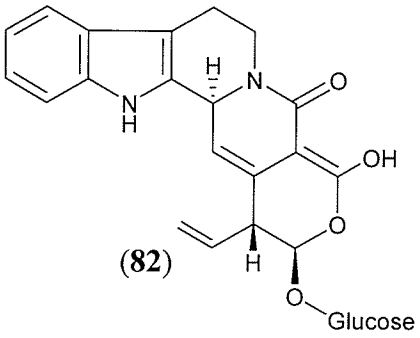

(82)

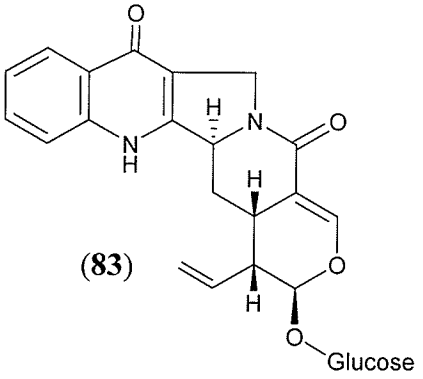

(83)

These compounds were inactive in their pure forms in the inhibition of *Candida* SAP suggesting that there could possibly be synergism of the various constituents of the bioactive fractions in the activity previously observed in these fractions.[19] Other recent phytochemical analyses conducted on the crude extracts of the bark and wood of *N. latifolia* resulted in the isolation of other indole alkaloids, naucleamides A (**84**), B (**85**), C (**86**) and D (**87**).[9] In addition to these, a structurally unique indole alkaloid possessing a pentacyclic ring system with an amino acetal bridge, naucleamide E (**88**), was also isolated.[9] In a latter report, a C-5 carboxylated strictosidine lactam, 3α,5α-

tetrahydrodeoxycordifoline lactam and cadambine acid were also isolated from another species of *Nauclea, N. diderrichii*.[20]

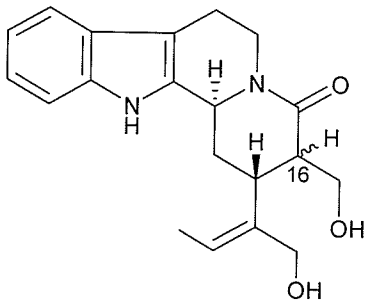

(**84**) R = H_α-16
(**85**) R = H_α-16

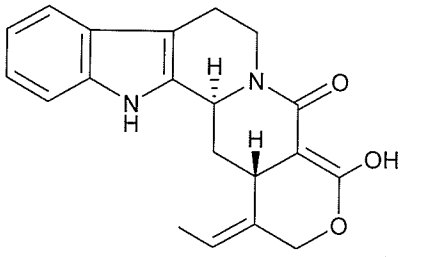

(**86**)

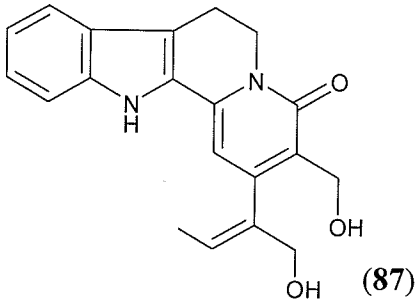

(**87**)

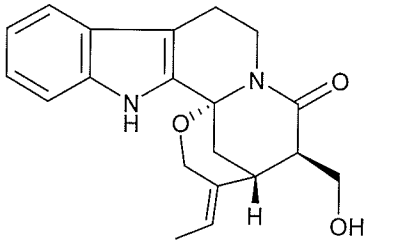

(**88**)

Prior to these reports, fractionations of the organic extract of *N. orientalis* obtained at basic pH using ammonia resulted in the isolation of angustine-type indole alkaloids, which exhibited *in vitro* antiproliferative activity against human bladder carcinoma T-24 cell lines and EGF-dependent mouse epidermal keratinocytes.[21]

Biosynthesis of Indole Alkaloids

Biosynthetically, these monoterpene indole alkaloids can be produced from an amino acid (tryptophan) decarboxylation derivative, tryptamine (**89**) and a product of the mevalonate pathway, geraniol, in a pathway of several reaction steps.[22] Geraniol is converted to *seco*-loganin (**90**) in a number of steps that also involves glycosylation

reaction. Subsequently, conjugation of tryptamine (**89**) and *seco*-loganin (**90**) produces strictosidine (**93**). This reaction occurs via a Mannich-type reaction catalyzed by strictosidine synthetase (Scheme 3.2). Strictosidine is believed to be the key intermediate in the biosynthesis of other glyco-monoterpene indole and indole alkaloids.[22,23]

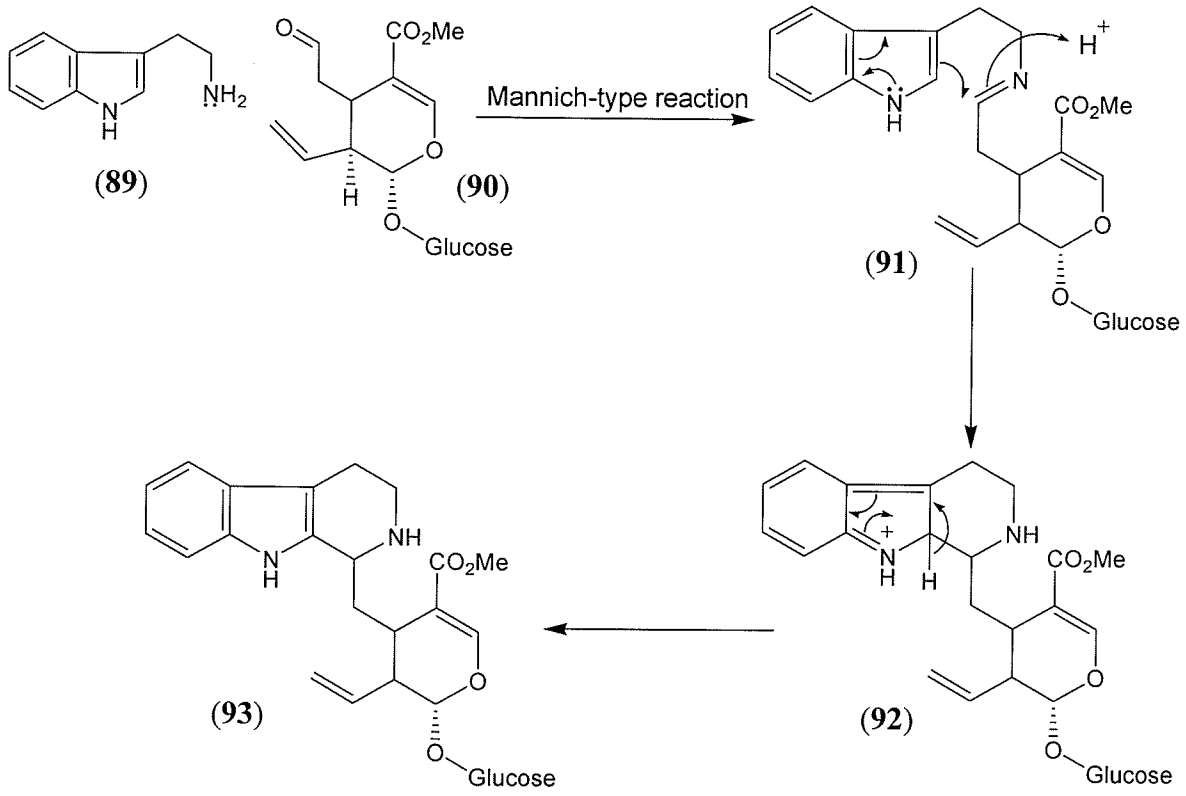

Scheme 3.2 Biosynthesis of strictosidine (**93**) from *seco*-loganin (**90**) and tryptamine (**89**)[22]

In addition to indole alkaloids, oleanane-, ursane-type tripertenoidal and *seco*-iridoids have also been isolated from *N. latifolia*, *N. diderrichii* and other members of the family Rubiaceae. These triterpenes include chincolic acid, quinovic acid, 3-oxoquinovic acid, quinovic acid and chincolic acid glycosides as well as *seco*-iridoids and their glycosides, for example dideroside (**94**).[24-26] Previously, following a bioassay-directed

fractionations, isolated quinovic acid glycosides from a member of the same family, *Uncaria tomemtosa* (Rubiaceae), showed *in vivo* anti-inflammatory activity in male Wister rats[27] as well as moderate *in vitro* antiviral activity.[28,29]

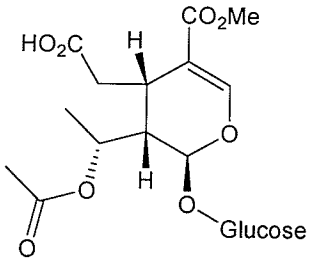

(**94**)

Recently, the ethanolic extracts of *N. latifolia* was reported to exhibit concentration-dependent inhibitory activity against parasitic helminths GSTs with IC_{50} values of 15 and 28 μg/mL for *Ascaris suum* and *Onchocerca volvulus* GSTs, respectively.[30] No report on isolation of the GST-inhibiting principles was found in the literature. In our assays, the crude extract of *N. latifolia* showed a concentration-dependent *in vitro* inhibition of GST with IC_{50} value of 10.5μg/mL. Phytochemical studies on this extract resulted in the isolation of five known compounds. These compounds include a glyco-monoterpene indole alkaloid, strictosamide (**70**) as well as four pentacyclic ursane-type triterpenoidal glycosides, quinovic acid-3-O-α-quinovosylpyranoside (**95**), quinovic acid-3-O-β-rhamnosylpyranoside (**96**), quinovic acid-3-O-α-rhamnosylpyranoside (**97**) and quinovic acid-3-O-β-fucosylpyranoside (**98**). This chapter describes the isolation and structure elucidation of these compounds (**70, 95-98**) as well as their bioactivity in the inhibition of GST.

3.2 RESULTS AND DISCUSSION

The roots of *N. latifolia* (2 kg) collected from Anambra, Nigeria were air-dried and pulverized into small particles. The pulverized plant material was extracted with 75% aqueous ethanol at room temperature for 48 h to afford a yellow colored gummy material (12.43 g). This extract was assayed for GST inhibition, and it showed *in vitro* inhibition of GST with IC_{50} 10.5μg/mL. This extract was subsequently subjected to various chromatographic techniques including column chromatography, TLC and High Performance Liquid Chromatography (HPLC) to isolate five compounds (**70, 95-98**).

3.2.1 Strictosamide (70)

The first compound (**70**) was isolated as a yellow solid from an EtOAc-MeOH column chromatographic fraction of the extract by reverse-phase HPLC on C_{18} (ODS) column. Its UV spectrum showed a maximum absorption at 280 nm characteristic of an indole chromophore.[9] The EI MS of **70** showed the molecular ion peak (M^+) at *m/z* 498. Another ion peak observed at *m/z* 336 was due to the loss of a sugar moiety from the molecular ion.

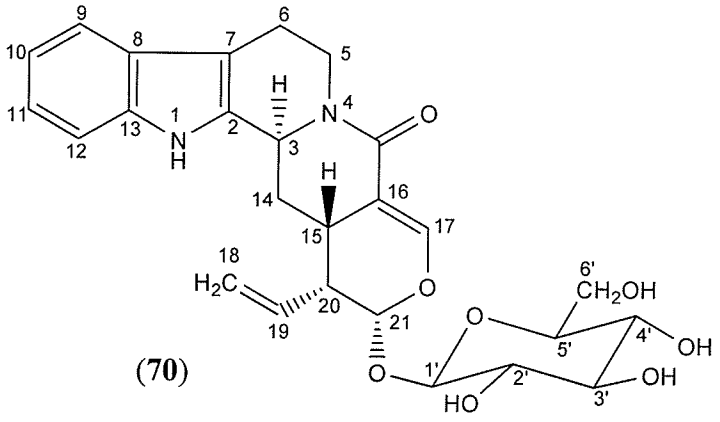

(70)

The ^{1}H NMR (acetone-d_6, 300 MHz) spectrum of **70** showed aromatic signals at δ 7.45 (H-9), 7.32 (H-12), 7.04 (H-11) and 7.01 (H-10), due to the aromatic protons of the indole unit in the structure. The doublet that resonated at δ 7.25 (J = 1.6 Hz) was assigned to the C-17 olefinic proton. The splitting and small coupling constant observed for H-17 was due to allylic coupling with the C-15 proton. Other doublets observed at δ 5.35 (J = 11 Hz) and 5.25 (J = 10.8 Hz) represent the C-18 methylene protons while the one-proton multiplet at δ 5.72 represents the C-19 olefinic proton. Signals were also observed between δ 2.95 and 4.60 due to the protons of the sugar unit; their δ values indicated proximity to electron-rich environments. The ^{13}C NMR (acetone-d_6, 50 MHz) spectrum of **70** showed the resonances of all the 26 carbons present in this compound. Their multiplicities were deduced on the basis of information derived from the Attached Proton Test (APT) spectrum and this showed the presence of 5 CH_2, 15 CH and 6 quaternary carbon atoms in this compound. These spectroscopic data were compared with literature data[14,19,31] and were discovered to be same as those reported for a major indole alkaloid of the *Nauclea* species, strictosamide (**70**). In order to avoid ambiguity in the identification of the compound and in assigning the δ values of the proton and carbon signals, 2D NMR (COSY, HSQC, HMBC) spectra of **70** were obtained in d_6-acetone, and these were used to confirm the structure of this compound. A combination of ^{1}H, ^{13}C NMR and mass spectral data (Experimental section) helped to identify compound **70** as strictosamide, as the ^{1}H and ^{13}C NMR chemical shift values of **70** were identical to those of strictosamide reported in the literature.[14,19,31] Based on these spectral data, compound **70** was characterized as strictosamide. The TLC and HPLC analysis of the column chromatographic fractions revealed that this compound is a major secondary metabolite

of *N. latifolia*. Compound **70** could be biosynthesized from strictosidine (**93**), a glyco-monoterpene indole alkaloid from whence most indole alkaloids are derived in plants.[22] Strictosamide (**70**) had been previously isolated as a minor constituent from the leaves of *Uncaria rhynchophylla*[11] and also from *N. latifolia*.[14]

3.2.2 Quinovic acid-3-O-α-6-deoxyglucopyranoside (95)

The second compound (**95**, yellow solid) was isolated as a precipitate from a column chromatographic fraction (FJ) of *N. latifolia* (see Experimental). Its IR spectrum displayed intense absorption bands at 3424 (OH), 2927 (CH), 1697 (C=O), 1457 (C=C) and 1071 (C-O) cm^{-1}. EI MS of **95** showed the molecular ion peak at *m/z* 632. The UV spectrum displayed a terminal absorption showing the absence of a conjugation π system in the compound.

The ^1H NMR spectrum (CD_3OD, 300 MHz) of compound **95** showed four three-proton singlets at δ 0.85, 0.90, 0.99 and 1.03 due to the C-24, C-26, C-25 and C-23 methyl protons, respectively. A doublet at δ 0.92 (J = 5.1 Hz), integrating for six protons, was assigned to the C-29 and C-30 methyl protons, whereas another downfield doublet at δ 1.26 (J = 6.2 Hz) was assigned to the C-6′ methyl protons. The sp^2 hybridized H-12 appeared as a broad singlet at δ 5.62, and the doublet at δ 4.25 (J = 6.2 Hz) was assigned to the anomeric proton (H-1′) of the sugar unit. The signals between δ 3.45 and 4.25 represent a pattern typical of the oxymethine protons of a sugar unit.[32] This suggested that compound **95** contains a sugar moiety in its structure, and this supported a previous observation of a characteristic black spot on TLC for compound **95** on charring after spraying with 10% H_2SO_4. ^1H-^1H correlation spectroscopy of **95** revealed an interaction

between the signal at δ 3.45 (H′-5) and the doublet at δ 1.26 (H-6′). This observation and the absence of the oxymethylene signal in the ^{1}H NMR spetrum of **95** confirmed that the sugar unit is a 6-deoxy sugar. The coupling constant of the anomeric proton (J = 6.2 Hz) aided the tentative identification of the sugar unit as quinovose. This J value represents an axial-equatorial relationship between H-2′ and H-1′ as observed for α-glucose.[32] In the COSY-45° spectrum, cross peaks were also observed between H-12 (δ 5.62) and H-11 (δ 1.95) alongside several other interactions. The ^{13}C NMR spectrum (CD_3OD, 75 MHz) of **95** showed that the compound contains 36 carbon atoms in its structure. Distortionless Enhancement by Polarization Transfer (DEPT) 135° experiment was used to establish the multiplicities of these carbon atoms, and this showed the presence of 7 CH_3, 9 CH_2 and 12 CH. Subtraction of DEPT from the broadband ^{13}C NMR signals showed the presence of 8 quaternary carbon atoms in the compound. The HSQC and HMBC spectra were also obtained in the complete elucidation of the structure of **95**. The HSQC spectrum aided the assignment of the protons to their respective carbon atoms, and the HMBC spectrum was used in connecting the COSY-derived partial structures of **95**. The ^{1}H, ^{13}C NMR and the HSQC interactions of **95** are shown in Experimental. In addition to these data, the relative configurations of the stereogenic centers were assigned using NOESY. Relative to the C-25 methyl group which assumes a β-orientation due to biogenetic reasons, the configurations of other chiral centers were assigned, and these include α-orientation for H-3, H-5 and H-9, and β-orientation for H_3-26. Based on these spectroscopic data, a literature search resulted in the identification of compound **95** as quinovic acid-3-O-α-quinovosylpyranoside. The ^{1}H and ^{13}C NMR data of the aglycone of **95** were similar to those reported by Miana and Al-Hazim[33] for quinovic acid isolated from *Fagnonia*

cretica. The entire spectroscopic and spectrometric data of **95** were the same as those reported by Hao and co-workers[34] for a quinovic acid glycoside isolated from *Neonauclea sessifolia*.

3.2.3 Quinovic acid-3-O-β-rhamnosylpyranoside (96)

The column chromatographic fraction (FI-10) of *N. latifolia* that resulted from the column chromatography of fraction FI, on preparative TLC using EtOAc-methanol (95:5) as the mobile phase (see Experimental), yielded compound **96** as a yellow solid.

The ^{1}H NMR (CD_3OD, 200 MHz) spectrum for compounds **96** was similar to that of compound **95**. The anomeric proton (H-1′) of compound **96** which resonated at δ 4.22 also showed a *J* value of 6.2 Hz. This indicated that the H-1′ and H-2′ of the sugar moiety are in axial-equitorial orientation relative to each other as observed for compound **95**. However, compounds **95** and **96** had different R_f values (0.34 and 0.27, respectively) in ethylacetate-methanol (9.5:0.5) solvent system. This observation indicated that the sugar moieties in the two compounds are different. The ^{13}C NMR spectrum (CD_3OD, 50 MHz) of compound **96** showed the resonances for all 36 carbon atoms. The resonances for the C-27 and C-28 carbonyl carbons were observed at δ 179.6 and 183.2, respectively whereas signals for the olefinic carbon atoms C-12 and C-13 were observed at δ 129.9 and 134.6, respectively. The oxymethine carbon (C-3) resonated at δ 90.8 in the ^{13}C NMR spectrum of **96** indicating the highly electronegative environment of the carbon atom due to the attachment of the sugar moiety. The ^{13}C signals of the sugar unit were also observed in the ^{13}C NMR spectrum of **96** at δ 107.2, 75.4, 73.2, 73.0, 71.7 and 17.2 due to C-1′, C-4′, C-2′, C-3′, C-5′ and C-6′, respectively. The δ values of the carbon

signals were very similar to that of compound **95**. The complete ^{13}C NMR δ assignments of the carbon atoms in **96** are shown in Experimental. Based on the *J* value of the anomeric proton in the ^{1}H NMR spectrum and the ^{13}C NMR δ shift values of the carbon atoms of the glycone[32], the sugar unit was tentatively identified as β-rhamnose. These data, alongside information derived from the literature,[32-36] supported the identification of this compound as quinovic acid-3-O-β-rhamnosylpyranoside (**96**).

3.2.4 Quinovic acid-3-O-α-rhamnosylpyranoside (97)

Compounds **97** was isolated as a yellow solid by preparative TLC from a secondary column chromatographic fraction that eluted with 70%EtOAC-30%MeOH (see Experimental). The ^{1}H NMR (CD_3OD, 200 MHz) spectrum for compounds **97** was similar to those of compounds **95** and **96** except for the *J* value of the anomeric proton (H-1′). Unlike the ^{1}H NMR spectra of compounds **95** and **96**, which had resonances for H-1′ with $J_{H\text{-}1',H\text{-}2'}$ = 6.2 Hz depicting axial-equatorial orientation between these protons, the ^{1}H NMR of compound **97** showed a similar resonance at δ 4.20 with a coupling constant $J_{H\text{-}1',H\text{-}2'}$ = 1.6 Hz. The small coupling constant observed for this proton represents equitorial-equitorial orientation of the H-1′ and H-2′ protons relative to each other. The ^{13}C NMR spectrum (CD_3OD, 50 MHz) of compound **97** showed the resonances for all 36 carbon atoms. These resonances were similar to those observed in the ^{13}C NMR spectra of compounds **95** and **96**. The signals for the olefinic carbon atoms C-12 and C-13 were observed at δ 129.2 and 135.3, respectively whereas the oxymethine carbon (C-3) resonated at δ 90.9 in the ^{13}C NMR spectrum of **97**. The ^{13}C signals of the sugar unit were also observed in the ^{13}C NMR spectrum of **97** at δ 106.8, 78.4, 77.8, 75.8,

71.7 and 18.6 due to C-1′, C-4′, C-2′, C-3′, C-5′ and C-6′, respectively. The complete ^{13}C NMR δ assignments of the carbon atoms in **97** are shown in Experimental. The *J* value of the anomeric proton in the ^{1}H NMR spectrum and the ^{13}C NMR δ shift values of the carbon atoms of the glycone[32] enabled the tentative identification of the sugar unit as α-rhamnose. These data, alongside information derived from the literature,[32-36] suggested that the identity of this compound is quinovic acid-3-O-α-rhamnosylpyranoside (**97**).

3.2.5 Quinovic acid-3-O-β-fucosylpyranoside (98)

Compounds **98** was isolated as a yellow solid by preparative TLC from the same *N. latifolia* fraction where compounds **96** and **97** were isolated (see Experimental). Its IR spectrum showed absorption bands at 3220 (OH), 1686 (C=O) and 1456 (C=C) cm^{-1}. The ^{1}H NMR (CD_3OD, 200 MHz) spectrum for compound **98** was similar to that of compound **95-97** except for the *J* value of the anomeric proton (H-1′). In contrast, the coupling constant observed for the anomeric proton in ^{1}H NMR spectrum of compound **98** gave the highest *J* value, $J_{H\text{-}1',H\text{-}2'}$ = 7.4 Hz, representing an axial-axial relationship between H-1′ and H-2′ as observed in β-glucose.[32] However, the absence of the oxymethylene signals in both the ^{1}H and ^{13}C NMR spectra of **98** invalidates any assumption of the presence of glucose in the structure of this compound. The ^{13}C NMR spectrum (CD_3OD, 50 MHz) of compound **98** showed the resonances for all 36 carbon atoms. The complete ^{13}C NMR δ assignments of the carbon atoms in **97** are shown in Experimental. The *J* value of the anomeric proton in the ^{1}H NMR spectrum and the ^{13}C NMR δ shift values of the carbon atoms of the glycone[32] enabled the tentative identification of the sugar unit as β-fucose. These data together with information from the

literature[32-36] supported the identification of this compound as quinovic acid-3-O-β-fucosylpyranoside (**98**).

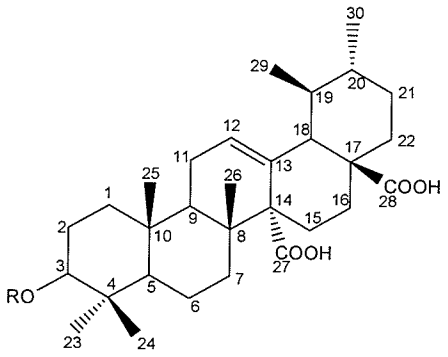

(**95**) R = 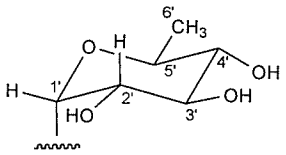

(**96**) R = 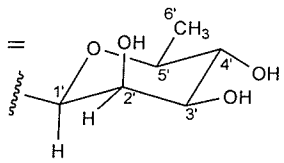

(**97**) R = 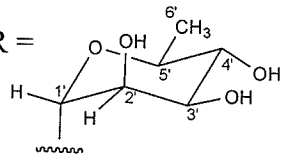

(**98**) R = 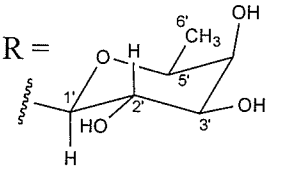

These spectroscopic data suggest that these compounds (**95-98**) have the same aglycone skeleton but differ only in their glycone moieties. Compounds **96-98** have been previously isolated from *N. latifolia*[26] as well as some other plants of the genus *Nauclea*[24,25] and of the family Rubiaceae[34,35]. Based on HPLC analyses, these compounds (**95-98**) alongside other quinovic acid gycosides have been reported to be ubiquitous in *Nauclea diderrichii*.[25] Previously, quinovic acid-3-O-6-deoxy-D-glucopyranoside was reported as the chemical component of *Mitragyna inermis* responsible for its cytotoxic activity in Hela (human carcinoma of the cervix) cell lines.[37] These compounds (**95-98**) alongside strictosamide (**70**) were assayed for *in vitro* inhibition against the activity of equine liver GST.

3.2.6 Enzyme Inhibition

Figure 3.1 shows the varying extents of *in vitro* inhibitory activity against GST for compounds **70**, **95-98** with IC_{50} values of 20.5 to 143.8 μM.

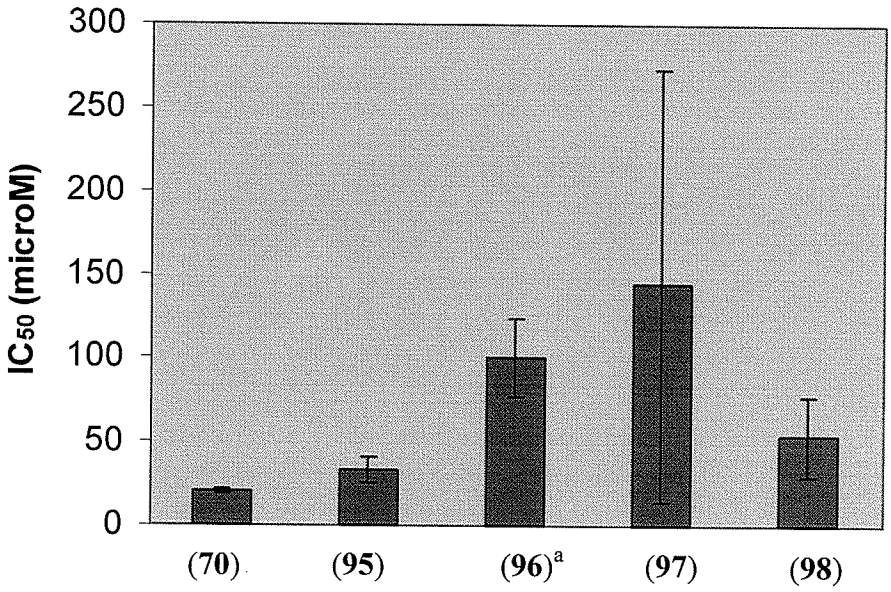

Fig. 3.1 GST inhibitory activity data represented as IC_{50} (μM) for compounds **70**, **95-98**. Results are expressed as means (±SDEV) of triplicate experiments; [a)]results are means (±SDEV) of duplicate experiments.

The indole alkaloid, strictosamide (**70**), showed the best GST inhibitory activity with IC_{50} value of 20.5±1.16 μM. This compound displayed a concentration-dependent activity with an inhibition of up to 77.7±1.9% of the enzyme activity at a maximum concentration of 133 μM. This activity is comparable to the GST inhibitory activity of a previously applied chemosensitizer, ethacrynic acid (**22**; IC_{50} = 16.0 μM).[38] Previously, tryptophandehydrobutyrine diketopiperazine (TDD) was reported as a GST inhibitor with an IC_{50} value of 26.5 μM.[38] TDD is an indole-containing compound, isolated from *Streptomyces* sp., belonging to a class of natural products called diketopiperazines.[38] Based on literature search, strictosamide is the second indole-containing natural product

to be reported to exhibit GST inhibition after TDD. Nevertheless, it was not established whether the GST inhibitory activity observed for TDD was due to the indole moiety or the parent diketopiperazine structure. This dearth of evidence would invalidate any comparison of the observed activity of strictosamide and the reported activity of TDD in GST inhibition.

Compounds **95-98** showed varying degrees of activity in the inhibition of GST (Fig. 3.1). Their IC_{50} values ranged from 33.6 to 143.8 μM. Quinovic acid-3-O-α-quinovosylpyranoside (**95**) displayed the best activity of all the quinovic acid glycosides with an IC_{50} value of 33.6±7.76 μM. Due to the presence of the same aglycone (quinovic acid) in all the four compounds (**95-98**), the variation in their activity would be ascribed to the different sugar moieties attached to the algycone. Nevertheless, comparison of the IC_{50} data of these compounds would be inefficient in the study of structure-activity relationships of **95-98** as the IC_{50} value for compound **96** was based on duplicate experiments as opposed to triplicate, and there was a highly significant error in the IC_{50} value of compound **97** (Fig. 3.1). That notwithstanding, a trend was observed in the above chart and that resulted in the following inferences. The large difference observed between the GST-inhibitory activities of **95** (IC_{50} 33.6 μM) and **97** (IC_{50} 143.8 μM) indicated that there is no effect of the C-1′ configuration of the sugars on the activity of the enzyme as these two compounds contain two different sugars oriented in the α-configuration at the anomeric carbon. This was supported by the differences in the activities of compounds **96** (IC_{50} 100.42 μM) and **98** (IC_{50} 53.49 μM), both of which contained sugars oriented in the β-configuration at the anomeric carbon.

Conversely, the trend in activity of these compounds in GST inhibition changed when analyzed based on the parent sugar structures. Irrespective of the sugar configuration at the anomeric carbon, the quinovic acid rhamnosylpyranosides (**96**, **97**) showed high IC_{50} values as compared to the quinovosylpyranoside (**95**) and fucosylpyranoside (**98**). This suggests that the configuration at C-2′ of the sugar moieties may have an effect on the activity of these compounds in the inhibition of the enzyme. When considered from a different perspective, these compounds (**95-98**) displayed activity with inhibition of up to 69.3±7.4%, 50.1±3.0, 55.5±5.2 and 78.8±10.4% of the enzyme activity for compounds **95**, **96**, **97** and **98**, respetively at a concentration of 105.5 μM. This shows that at higher concentration, compound **98** exhibited a slightly higher GST inhibitory activity than compound **95** even though **95** had a significantly lower IC_{50} value. As the latter experiments were all carried out in triplicate, this latter analysis would be ideal in the comparison of the activities of the compounds in GST inhibition. This shows that compounds **96** and **97** inhibited about half of GST activity at 105 μM with minimum errors. The overall trend supported the earlier inference with the activity of the rhamnosylpyranosides lower than those of the quinovosylpyranoside and fucosylpyranoside. By and large, to the best of my knowledge, this is the first report of the inhibition of GST by quinovic acid glycosides.

3.3 EXPERIMENTAL

3.3.1 General

The general experimental procedures of chromatography and spectroscopy utilized in this experimental work were the same as discussed in chapter 2 (section 2.3.1). In addition to these methods, High Performance Liquid Chromatography (HPLC) was carried out on a *Waters* HPLC system equipped with a binary pump (*Waters* 1525) and a Photodiode Array (PDA) detector (*Waters* 2996) using a 4 μm C_{18} *Waters* Nova Pak column (3.9 × 150 mm) and a 5 μm *Zobrax* ODS column (9.4 × 250 mm). IR spectra of compounds **70**, **96-98** were recorded on a *Nicolet Nexus 870 FT-IR* spectrometer.

3.3.2 Plant Material

The root of *N. latifolia* (2 kg) was collected in March 2005 from Anambra, Nigeria by Dr. Pete Uzoegwu of the University of Nigeria, and identified by a plant taxonomist, Alfred Ozioko. A voucher specimen (BDCP037) was deposited in the herbarium of Biotechnology Development and Conservation Programme (BDCP) Research Centre, Nsukka, Nigeria.

3.3.3 Extraction and Isolation

The root of *N. latifolia* (2 kg) was extracted with 75% ethanol at room temperature for 48 h, and evaporated under reduced pressure to give yellow-colored gum. The crude extract (12.43 g) was loaded unto a silica gel column (SiO_2 gel size in column, 10 × 145 mm) and fractionated using 0-100% hexane-EtOAc, 0-100% EtOAc-MeOH and 0-50% MeOH-CH_3CN in a gradient fashion to afford 215 fractions. These fractions were

analyzed by TLC, and fractions of similar R_f values were pooled together. The resulting 19 fractions (FA to FS) were screened for activity against GST to afford the fractions that eluted with 15%hexane/85%EtOAc – 85%EtOAc/5%MeOH (FI, 45.5 % inhibition at 20 μg/mL) and 80%EtOAc/20%MeOH (FJ, IC_{50} = 25.4 μg/mL) as the most active fractions. Compound **95** (87.4 mg, 0.7 % yield, R_f 0.34 in 95%EtOAc – 5%MeOH) precipitated from FJ as a yellow solid. This was subsequently isolated from the fraction by gravity filtration, and washed with hexanes and EtOAc. Fraction I was subjected to gradient elution column chromatography (cc) using the Hex-EtOAc-MeOH solvent system to afford several fractions (FI-1 to FI-15). Preparative TLC on the secondary chromatographic fraction that was obtained on elution with 70%EtOAC-30%MeOH (FI-10) using 95%EtOAc–5%MeOH yielded three compounds, **96** (2.2 mg, R_f 0.27), **97** (3.9 mg, R_f 0.27) and **98** (2.7 mg, R_f 0.17) as well as **95** (5.2 mg). A fraction obtained from the 2° column with 60%EtOAC-40%MeOH (FI-11) was subjected to reverse-phase HPLC using C-18 Waters analytical column using 0-100% 0.1%AcOH/H_2O→MeOH as mobile phase to purify compound **70** (17.9 mg, R_t 8.84 min) as a yellow solid. Compound **70** was also isolated from another fraction (FI-12, eluted from the 2° cc with 50%EtOAC-50%MeOH) by gradient elution reverse-phase HPLC on a 5 μm *Zobrax* ODS column using 80%H_2O/MeOH→MeOH (0-100%) at a flow rate 1.0 mL/min with 10 μL injection per run for 30 min total run time. The peaks in the HPLC analyses were monitored at 245 nm using the PDA detector.

Strictosamide (**70**); Yellow solid; IR ν_{max} (KBr) = 3339 (N-H, O-H), 2926 (C-H), 1653 (C=O), 1576 (C=C), 1466 (C=C), 1074 (C-O) cm^{-1}; ^1H NMR (acetone-d_6, 300 MHz) δ = 10.22 (1H, *s*, H-1), 7.45 (1H, *d*, *J* = 7.6 Hz, H-9), 7.32 (1H, *d*, *J* = 7.6 Hz, H-12), 7.25 (1H, *d*, *J* = 1.4 Hz, H-17), 7.04 (1H, *t*, *J* = 7.5 Hz, H-11), 7.01 (1H, *t*, *J* = 7.5 Hz, H-10), 5.72 (1H, *m*, H-19), 5.35 (1H, *d*, *J* = 11.0 Hz, H_a-18), 5.30 (1H, *d*, *J* = 1.8 Hz, H-21), 5.25 (1H, *d*, *J* = 10.8 Hz, H_b-18), 5.02 (1H, *br s*, H-3), 4.92 (1H. *dd*, *J* = 13.8, 9.6 Hz, H-5), 4.60 (1H, *d*, *J* = 7.4 Hz, H-1′), 4.05 (1H, *br s*, H-3′), 3.70 (1H, *br s*, H-6′), 3.62 (1H, *br s*, H-6′), 3.32 (1H, *br s*, H-5′), 3.25 (1H, *br s*, H-4′), 2.95 (1H, *br s*, H-2′), 2.92 (1H, *m*, H-6), 2.80 (1H, *m*, H-15), 2.66 (1H, *m*, H-20), 2.62 (1H, *dd*, *J* = 13.8, 9.6 Hz, H-6), 2.45 (1H, *m*, H-14), 2.05 (1H, *m*, H-14); ^{13}C NMR (acetone-d_6, 50 MHz) δ: = 167.2 (C-22), 149.3 (C-17), 137.9 (C-13), 134.9 (C-2), 134.5 (C-19), 128.8 (C-8), 122.6 (C-11), 120.7 (C-18), 120.3 (C-10), 118.8 (C-9), 112.4 (C-12), 110.4 (C-7), 109.3 (C-16), 100.6 (C-1′), 98.2 (C-21), 78.3 (C-3′), 78.1 (C-5′), 74.4 (C-2′), 71.4 (C-4′), 62.7 (C-6′), 55.2 (C-3), 44.9 (C-20), 27.4 (C-14), 25.0 (C-15), 22.2 (C-6); CIMS *m/z*: = 343 (M^++1); EIMS *m/z*: = 342 (M^+), 324, 265, 249, 209, 198, 185, 169, 146, 142, 115, 69, 55, 41.

Quinovic acid-3-O-α-6-deoxyglucopyranoside (**95**); Yellow solid, R_f 0.34 in 9.5:0.5 EtOAc-MeOH; IR ν_{max} (KBr): = 3424 (O-H), 2927 (C-H), 1697 (C=O), 1457 (C=C), 1071 (C-O) cm^{-1}; ^1H NMR (CD_3OD, 300 MHz) δ: = 5.62 (1H, *br s*, H-12), 4.25 (1H, *d*, *J* = 6.2 Hz, H-1′), 3.63 (1H, H-3′), 3.62 (1H, H-2′), 3.45 (2H, H-4′ and H-5′), 3.12 (1H, *dd*, *J* = 11.5, 4.4 Hz, H-3), 2.28 (2H, *m*, H-9 and H-18), 1.26 (3H, *d*, *J* = 6.2 Hz, H_3-6′), 1.03 (3H, *s*, H_3-23), 0.99 (3H, *s*, H_3-25), 0.92 (6H, *d*, *J* = 5.1 Hz, H_3-29 and H_3-30), 0.90 (3H, s, H_3-26), 0.85 (3H, *s*, H_3-24), 0.78 (1H, *br d*, *J* = 11.4 Hz, H-5); ^{13}C NMR (CD_3OD, 75 MHz) δ: = 181.6 (C-28), 179.0 (C-27), 133.8 (C-13), 130.4 (C-12), 107.0 (C-1′), 90.6 (C-3), 75.3 (C-4′), 73.1 (C-2′), 72.9 (C-3′), 71.6 (C-5′), 57.3 (C-14), 56.9 (C-5), 55.6 (C-18), 49.5 (C-9), 48.0 (C-17), 40.7 (C-8), 40.3 (C-1), 40.1 (C-4), 40.0 (C-10), 38.3 (C-20), 38.0 (C-19), 37.8 (C-7), 37.6 (C-22), 31.2 (C-21), 28.6 (C-15), 27.1 (C-23), 26.5 (C-2), 25.8 (C-16), 23.9 (C-11), 21.5 (C-30), 19.3 (C-6), 19.1 (C-29), 18.2 (C-26), 17.1 (C-6′), 16.9 (C-25), 16.9 (C-24).

Quinovic acid-3-O-β-6-deoxymannopyranoside (**96**); Yellow solid, R_f 0.27 in 9.5:0.5 EtOAc-MeOH; IR ν_{max} (KBr): = 3461 (O-H), 2926 (C-H), 1691 (C=O), 1455 (C=C), 1074 (C-O) cm^{-1}; ^1H NMR (CD_3OD, 200 MHz) δ: = 4.22 (1H, *d*, *J* = 6.2 Hz, H-1′); ^{13}C NMR (CD_3OD, 50 MHz) δ: = 183.2 (C-28), 179.6 (C-27), 134.6 (C-13), 129.9 (C-12), 107.2 (C-1′), 90.8 (C-3), 75.4 (C-4′), 73.2 (C-2′), 73.0 (C-3′), 71.7 (C-5′), 57.7 (C-14), 57.0 (C-5), 55.9 (C-18), 49.1 (C-9), 48.1 (C-17), 40.7 (C-8), 40.6 (C-1), 40.2 (C-4), 40.0 (C-10), 38.5 (C-20), 38.0 (C-19), 38.0 (C-7), 31.6 (C-21), 28.6 (C-15), 27.2 (C-23), 26.9 (C-2), 26.1 (C-16), 24.0 (C-11), 21.7 (C-30), 19.4 (C-6), 19.3 (C-29), 18.4 (C-26), 17.2 (C-6′), 17.0 (C-25), 17.0 (C-24).

Quinovic acid-3-O-α-6-deoxymannopyranoside (**97**); Yellow solid, R_f 0.27 in 9.5:0.5 EtOAc-MeOH; IR ν_{max} (KBr): = 3244 (O-H), 2927 (C-H), 1699 (C=O), 1456 (C=C), 1076 (C-O) cm^{-1}; ^1H NMR (CD_3OD, 200 MHz) δ: = 4.20 (1H, *d*, *J* = 1.6 Hz, H-1′); ^{13}C NMR (CD_3OD, 50 MHz) δ: = 182.2 (C-28), 179.8 (C-27), 135.3 (C-13), 129.2 (C-12), 106.8 (C-1′), 90.9 (C-3), 78.4 (C-4′), 77.8 (C-2′), 75.8 (C-3′), 71.7 (C-5′), 58.0 (C-14), 56.9 (C-5), 56.3 (C-18), 49.1 (C-9), 48.1 (C-17), 40.7 (C-8), 40.7 (C-1), 40.2 (C-4), 40.0 (C-10), 38.5 (C-20), 38.2 (C-19), 38.0 (C-7), 30.9 (C-21), 30.9 (C-15), 28.6 (C-23), 28.6 (C-2), 26.3 (C-16), 23.9 (C-11), 21.8 (C-30), 19.5 (C-6), 19.5 (C-29), 19.4 (C-26), 18.6 (C-6′), 17.2 (C-25), 17.1 (C-24).

Quinovic acid-3-O-β-6-deoxygalactopyranoside (**98**); Yellow solid, R_f 0.17 in 9.5:0.5 EtOAc-MeOH; IR ν_{max} (KBr): = 3220 (O-H), 2924 (C-H), 1686 (C=O), 1456 (C=C), 1102 (C-O) cm^{-1}; ^1H NMR (CD_3OD, 200 MHz) δ: = 4.22 (1H, *d*, *J* = 7.4 Hz, H-1′); ^{13}C NMR (CD_3OD, 50 MHz) δ: = 183.2 (C-28), 179.7 (C-27), 134.6 (C-13), 130.0 (C-12), 107.3 (C-1′), 90.8 (C-3), 75.4 (C-4′), 73.3 (C-2′), 73.0 (C-3′), 71.7 (C-5′), 57.7 (C-14), 57.1 (C-5), 56.0 (C-18), 49.4 (C-9), 48.1 (C-17), 40.8 (C-8), 40.6 (C-1), 40.3 (C-4), 40.1 (C-10), 38.6 (C-20), 38.3 (C-19), 38.0 (C-7), 38.0 (C-22), 31.6 (C-21), 28.7 (C-15), 27.3 (C-23), 26.9 (C-2), 26.1 (C-16), 24.0 (C-11), 21.8 (C-30), 19.5 (C-6), 19.4 (C-29), 18.5 (C-26), 17.2 (C-6′), 17.1(C-25), 17.1 (C-24).

3.3.4 Assay for Glutathione *S*-Transferase Inhibition.

The activity of the isolated compounds in the inhibition of GST was assayed as previously outlined in section 2.3.4.

3.4 REFERENCES

1. Deeni, Y. Y. and Hussain, H. S. N. Screening for antimicrobial activity for alkaloids of *Nauclea latifolia*. *J. Ethnopharmacol.*, **1991**, *35*, 91-96.
2. Zirihi, G. N., Mambu, L., Guédé-Guina, F., Bodo, B. and Grellier, P. In vitro antiplasmodial activity and cytotoxicity of 33 West African plants for treatment of malaria. *J. Ethnopharmacol.*, **2005**, *98*, 281-285.
3. Benoit-Vical, F., Valentin, A., Cournac, V., Pélissier, Y., Mallié, M. and Bastide, J-. M. In vitro antiplasmodial activity of stem and root extracts of *Nauclea latifolia* S.M. (Rubiaceae). *J. Ethnopharmacol.*, **1998**, *61*, 173-178.
4. Onyeyili, P. A., Nwosu, C. O., Amin, J. D. and Jibike, J. I. Antihelmintic activity of crude aqueous extract of *Nauclea latifolia* stem bark against ovine nematodes. *Fitoterapia*, **2001**, *72*, 12-21.
5. Okoli, A. S. and Iroegbu, C. U. Evaluation of extracts of *Anthocleista djalonensis*, *Nauclea latifolia* and *Uvaria afzalii* for activity against bacterial isolates from cases of non-gonococcal urethritis. *J. Ethnopharmocol.*, **2004**, *92*, 135-144.
6. Arkhurst, F. S. and Arkhurst, J. C. Method and composition for treating malaria. United States patent application 20030068393, **2003**.
7. Amos, S., Abbah, J., Chindo, B., Edmond, I., Binda, L., Adzu, B., Buhari, S., Odutola, A. A., Wambebe, C. and Gamaniel, K. Neuropharmocological effects of the aqueous extract of *Nauclea latifolia* root bark in rats and mice. *J. Ethnopharmacol.*, **2005**, *97*, 53-57.

8. Tona, L., Kambu, K., Ngimbi, N., Mesia, K., Penge, O., Lusakibanza, M., Cimanga, K., De Bruyne, T., Apers, S., Totte, J., Peters, L. and Vlietinck, A. J. Antiamoebic and spasmolytic activities of extracts from some antidiarreal traditional preparations used in Kinshasa, Congo. *Phytomedicine*, **2000**, *7*, 31-38.

9. Shigemori, H., Kagata, T., Ishiyama, H., Morah, F., Ohsaki, A. and Kobayashi, J. Naucleamides A-E, new monoterpene indole alkaloids from *Nauclea latifolia*. *Chem. Pharm. Bull.*, **2003**, *51*, 58-61.

10. Abreu, P. and Pereira, A. New indole alkaloids from *Sarcocephalus latifolius*. *Nat. Prod. Lett.*, **2001**, *15*, 43-48.

11. Takayama, H. and Kogure, N. Chemistry of indole alkaloids related to the corynanthe-type from *Uncaria*, *Nauclea* and *Mitragyna* plants. *Curr. Org. Chem.*, **2005**, *9*, 1445-1464.

12. Hotellier, F., Delaveau, P., Besselievre, R. and Pousset, J-.L. Naufoline et descarbométhoxy-naucléchine deux nouveaux alcaloides isolés du *Nauclea latifolia* Sm. (Rubiacées). *C. R. Acad. Sc. Paris*, **1976**, *282*, 595-597.

13. Hotellier, F., Delaveau, P. and Pousset, J-.L. Nauclefine and naucletine, two new indoloquinolizidine alkaloids from *Nauclea latifolia*. *Phytochemistry*, **1975**, *14*, 1407-1409.

14. Brown, R. T., Chapple, C. L. and Lashford, A. G. Isolation of strictosidine (isovincoside) lactam from *Nauclea latifolia*. *Phytochemistry*, **1977**, *16*, 1619-1620.

15. Brown, R. T., Charalambides, A. A. and Cheung, H. T. Synthesis of dihydroangustine. *Tetrahedron Lett.*, **1973**, *49*, 4837-4838.

16. Phillipson, D. J. and Heminway, S. R. Angustine and related alkaloids from species of *Mitragyna*, *Nauclea*, *Uncaria* and *Strychnos*. *Phytochemistry*, **1974**, *13*, 973-978.

17. Hotellier, F., Delaveau, P. and Pousset, J-.L. Naucléidinal et epinaucléidinal, alcaloides du *Nauclea latifolia*. *Phytochemistry*, **1980**, *19*, 1884-1885.

18. Takayama, H., Tsutsumi, S., Kitajima, M., Santiarworn, D., Liawruangrath, B. and Aimi, N. Gluco-indole alkaloids in Thailand and transformation of 3α-dihydrocadambine into indolopyridine alkaloid, 16-carbomethoxynaufoline. *Chem. Pharm. Bull.*, **2003**, *51*, 232-233.

19. Zhang, Z., ElSohly, H. N., Jacob, M. R., Pasco, D. S., Walker, L. A. and Clark, A. M. New indole alkaloids from the bark of *Nauclea orientalis*. *J. Nat. Prod.*, **2001**, *64*, 1001-1005.

20. Lamidi, M., Ollivier, E., Mahiou, V., Faure, R., Debrawer, L., Nze Ekekang, L. and Balansard, G. Gluco-indole alkaloids from the bark of *Nauclea diderrichi*. ^{1}H and ^{13}C NMR assignments of 3α-5α-tetrahydrodeoxycordifoline lactam and acdambine acid. *Magn. Reson. Chem.*, **2005**, *43*, 427-429.

21. Erdelmeier, C. A. J., Regenass, U., Rali, T. and Sticher, O. Indole alkaloids with in vitro antiproliferative activity from the ammoniacal extract of *Nauclea orientalis*. *Planta Med.*, **1994**, *58*, 43-48.

22. Dewick, P. M. "Medicinal Natural Products: A biosynthetic approach", *2nd ed.*, John Wiley & Sons, **2001**.

23. Stockigt, J. and Zenk, M. H. Strictosidine (isovincoside): the key intermediate in the biosynthesis of monoterpene indole alkaloids. *J. Chem. Soc. Chem. Commun.*, **1977**, 646-648.

24. Adeoye, A. O. and Waigh, R. D. Secoiridoid and triterpenic acids from the stems of *Nauclea diderrichii*. *Phytochemistry*, **1983**, *22*, 975-978.

25. Lamidi, M., Martin-Lopez, T., Ollivier, E., Crespin-Maillard, F., Nze Ekekang, L. and Balansard, G. Separation of saponins and determination of quinovic acid 3-O-a-L-rhamnopyranoside from *Nauclea diderrichii* (de Wild) Merr. bark by high performance liquid chromatography. *Chromatographia*, **1995**, *41*, 581-584.

26. Ngnokam, D., Ayafor, J. F., Connolly, J. D. and Nuzillard, J. M. Nauclefolinine: a new alkaloid from the roots of *Nauclea latifolia*. *Bull. Chem. Soc. Ethiopia*, **2003**, *17*, 173-176.

27. Aquino, R., de Feo, V., De Simone, F., Pizza, C. and Cirino, G. Plant metabolites. New compounds and anti-inflammatory activity of *Uncaria tomentosa*. *J. Nat. Prod.*, **1991**, *54*, 453-459.

28. Cerri, R., Aquino, R., de Simone, F. and Pizza, C. New quinovic acid glycoside from *Uncaria tomentosa*. *J. Nat. Prod.*, **1988**, *51*, 257-261.

29. Aquino, R., de Simone, F., Pizza, C., Conti, C. and Stein, M. L. Plant metabolites. Structure and in vitro antiviral activity of quinovic acid qlycosides from *Uncaria tomentosa* and *Guettarda platyipoda*. *J. Nat. Prod.*, **1989**, *52*, 679-685.

30. Fakae, B. B., Campbell, A. M., Barret, J., Scott, I. M., Teesdale-Spittle, P. H., Liebau, E. and Brophy, P. M. Inhibition of glutathione S-transferases (GSTs)

from parasitic nematodes by extracts from traditional Nigerian medicinal plants. *Phytother. Res.*, **2000**, *14*, 630-634.

31. Erdelmeier, C. A. J., Wright, A. D., Orjala, J., Baumgartner, B., Rali, T. and Sticher, O. New indole alkaloid glycosides from *Nauclea orientalis*. *Planta Med.*, **1991**, *57*, 149-152.

32. Kasai, R., Okihara, M., Mizutani, K. And Tanaka, O. ^{13}C NMR study of α- and β-anomeric pairs of D-mannopyranosides and L-rhamnopyranosides. *Tetrahedron*, **1979**, *35*, 1427-1432.

33. Maina, G. A. and Al-Hazimi, H. M. G. Assignment of the ^{13}C NMR spectrum of quinovic acid. *Phytochemistry*, **1987**, *26*, 225-227.

34. Kang, W-. Y., Du, Z-. Z. and Hao, X-. J. Triterpenoid saponins from *Neonauclea sessilifolia* Merr. *J. Asian Nat. Prod. Res.*, **2004**, *6*, 1-6.

35. Itoh, A., Tanahashi, T., Nagakura, N. and Nishi, T. Two triterpenoid saponin from *Neonauclea sessilifolia*. *Chem. Pharm. Bull.*, **2003**, *51*, 1335-1337.

36. Mostafa, M., Nahar, N., Mosihuzzaman, M., Sokeng, S. D., Fatima, N., Rahman, A. U., Choudhary, M. I. Phosphodiesterase-I inhibitor quinovic acid glycosides from *Bridelia ndellensis*. *Nat. Prod. Res.*, **2006**, *20*, 686-692.

37. Cheng, Z-. H., Yu, B-. Y. and Yang, X-. W. 27-Nor-triterpenoid glycosides from *Mitragyna inermis*. *Phytochemistry*, **2002**, *61*, 379-382.

38. Komagata, D., Sawa, R., Kinoshita, N., Imada, C., Sawa, T., Naganawa, H., Hamada, M., Okami, Y. and Takeuchi, T. Isolation of glutathione *S*-transferase inhibitors. *J. Antibiot.*, **1992**, *45*, 1681-1683.

CHAPTER 4

Chemical Studies on *Ambrosia psilostachya*

4.1 INTRODUCTON

Secondary metabolites can be used as chemotaxonomic markers. The variations in the distribution of the secondary metabolites of some plant species have been encountered across various localities in the world. For instance, the genus *Ambrosia* has over 5 species amongst which is *Ambrosia psilostachya*,[1] which vary in its natural product constituents across different populations. *A. psilostachya* is a weed, commonly known as Perennial ragweed, that is 3-105 cm high with horizontal running roots.[2] It is abundantly distributed in Winnipeg, Manitoba, Canada and in the rest of the midland and prairie regions of North America especially the U.S.A.[2] It is well known for the presence of several sesquiterpene lactones as major secondary metabolites.[1]

Sesquiterpenes are a group of C_{15} terpenoids derived from three C-5 isoprenoid units of the mevalonate biosynthetic pathway, the same pathway that produces steroids and other terpenes.[3] *A. psilostachya* has been reported to contain the pseudoguanolide type sesquiterpene skeleton, and a total of over 25 compounds of this series have been isolated from this plant.[1,4] These compounds are distributed in groups of about 1-5 major sesquiterpene lactones in every single populations of the plant.[1,4-8] Amongst the major sesquiterpene lactones isolated from *Ambrosia* species are parthenin (**99**),[4] coronopilin (**100**),[5] cumanin (**101**), cumanin-3-acetate (**102**),[4] ambrosiol (**103**)[6] and a rearranged dilactone, psilostachyin C (**104**).[7] In addition to these natural products, minor sesquiterpene lactones have also been isolated from this plant, and these include a germacranolide dilactone, isabelin (**105**),[8] psilostachyins A (**106**) and B (**107**),[7] 3-

hydroxydamsin (**108**),[9] cumambrin B (**109**) and sesquiterpene lactone dimmers, arrivacins A (**110**) and B (**111**).[10] Previous studies of about 40 years ago indicated that these sesquiterpene lactones are unevenly distributed amongst the various populations of *A. psilostachya* across North America (Table 4.1).[1,4] From a report derived from one of the studies, *A. psilostachya* population in the prairie region of Canada, represented by Saskatchewan, was shown to constitute of a large amount of coronopilin (**100**, 80%) and ambrosiol (**103**, 20%) as the major sesquiterpene lactones, but not the other major sesquiterpene lactones.[1] It was further reported from similar studies carried out in different locations of Texas, U.S.A., that there could be variations in the constituent of this plant in different populations that are proximate to each other (Table 4.1).

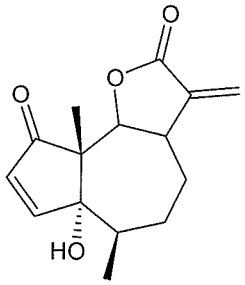

(**99**)

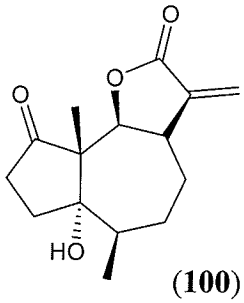

(**100**)

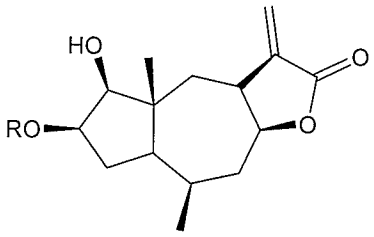

(**101**) R = H
(**102**) R = OAc

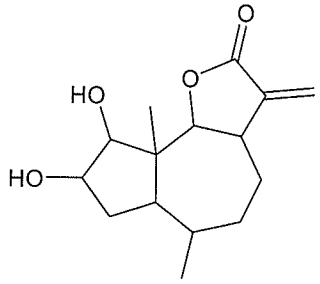

(**103**)

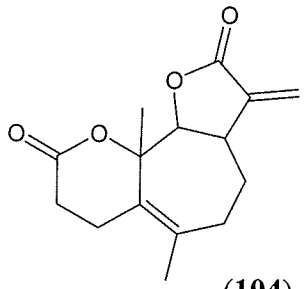

(**104**)

This latter observation invalidates any possible generalization, without proper and thorough investigations, of the relatedness of the sesquiterpene lactones compositions of *A. psilostachya* in the various populations distributed across the Prairie region of Canada.

Table 4.1 Distribution of major sesquiterpene lactones within some of the different *A. psilostachya* populations in North America[1,4]

Location	Major sesquiterpene lactone(s)
Los Angeles, U.S.A.	Coronopilin (**100**), parthenin (**99**)[4]
San Diego, U.S.A.	Coronopilin (**100**), cumanin (**101**), cumanin-3-acetate (**102**), parthenin (**99**)[4]
Santa Barbara, U.S.A.	Cumanin (**101**), cumanin-3-acetate (**102**), cumanin diacetate[4]
Houston, Texas, U.S.A.	Coronopilin (**100**), parthenin (**99**)[1]
Austin, Texas, U.S.A.	Ambrosiol (**103**)[1]
Carapan, Mexico	Ambrosiol (**103**)[1]
Saskatchewan, Canada	Coronopilin (**100**), ambrosial (**103**)[1]

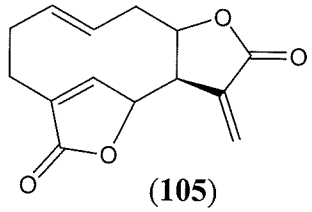

(**105**)

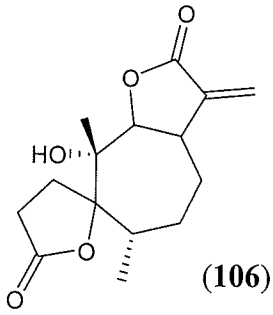

(**106**)

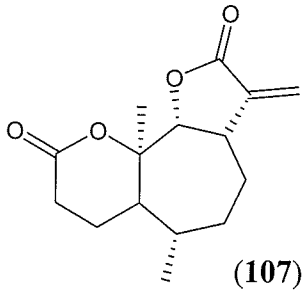

(**107**)

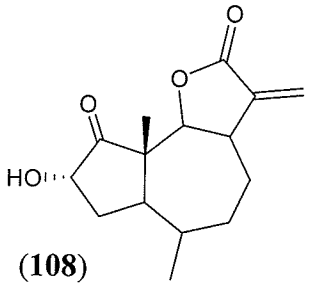

(**108**)

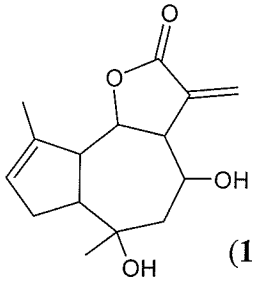

(**109**)

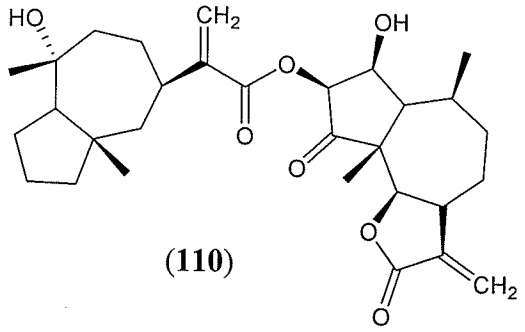

(**110**)

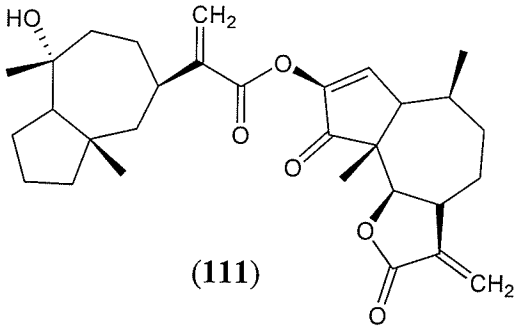

(**111**)

Even though no significant biological activity has been reported for extracts from *A. psilostachya*, some of the isolated compounds and structurally related sesquiterpene lactones from other terrestrial plant sources have shown interesting pharmacological activity. For example, certain peptidic allergens have been associated with some members of the genus *Ambrosia*, *A. psilostachya*, *A. artemisiifolia* and *A. trifida*. These allergens (for instance, the *Amb* V homologues) have been reported to elicit immunological (Ig E and Ig G) responses in human T-cells.[11] In addition to the bioactive peptides, cumanin isolated from the Autónoma, Mexico population of *A. psilostachya*, has been reported to exhibit inhibitory activity (IC_{50} = 9.38 μM) against LPS-induced nitric oxide (NO) production at low concentrations in peritoneal macrophages with a 95% inhibition at 20 μM.[12] This bioactivity may have applications in anti-inflammatory chemotherapy.

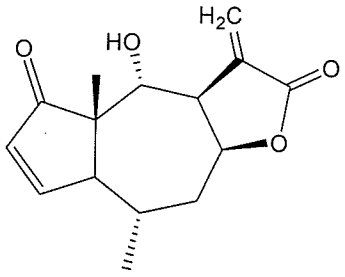

(112)

The structural feature responsible for activity was identified using helenalin (**112**) in the same assay, and this resulted in inhibition of NO production (IC_{50} < 0.1 μM) with a complete inhibition at 2 μM.[12] The authors concluded that inhibition of NO production, via inhibition of necrosis factor-κB (NF-κB) in their assay, occurred by the binding of the α,β-unsaturated carbonyl functionality of the sesquiterpene lactone to the sulfhydryl group of the protein via Michael addition. This explains the high activity observed for

helenalin, whose pharmacological activity and cytotoxicity has been associated with the two α,β-unsaturated carbonyl systems in its structure leading to double alkylation of the thiols of the target proteins in the cells under investigation.[13,14] Prior to these reports, sesquiterpene lactone dimers, arrivacins A (**110**) and B (**111**), formed by esterification of sesquiterpene acid to free hydroxyl groups of sesquiterpene lactones, were isolated from the Arrivaca-Cienega, Arizona, U.S.A population of *A. psilostachya*.[10] These compounds have shown anti-bacterial activity as well as angiotensin II receptors-binding activity.[10] The latter activity might be applied in the regulation of the renin-angiotensin system (RAS) in the management of high blood pressure.

By and large, the sulfhydryl binding activity of sesquiterpene lactones due to their α-methylene-γ-lactone functionality have enabled their application as generic inhibitors of thiol-containing enzymes and other biological targets; this principle has been applied in anti-inflammatory, antimicrobial and anti-neoplastic chemotherapy.[15] For example, based on inhibition of thiol-containing enzymes and other protein targets, several naturally-occurring and synthetic sesquiterpene lactones have been shown to exhibit diverse biological activities which include 1) aromatase inhibition in breast cancer chemotherapy,[16] 2) inhibition of the expression of inducible cyclooxygenase and pro-inflammatory cytokines in lipopolysaccharide (LPS)-stimulated macrophages which might be applied towards the treatment of inflammation,[17] 3) multiple effects in anticancer chemotherapy, which include prevention of metastasis, inhibition of inflammation and induction of apoptosis (due primarily to deleterious effects on NF-κB and mitogen-activated protein kinase (MAPK) signal transduction pathway)[17-19] and 4) inhibition of Ca^{2+}-ATPase from sarcoplasmic reticulum[20]. Based on these bioactivities, it

is suggestive that these sesquiterpene lactones could be applied in diverse ways in the modern day chemotherapy.

There is no report in the literature on isolation of sesquiterpene lactones from *A. psilostachya* of Manitoba origin. This part of the thesis describes the isolation and structure elucidation of the major sesquiterpene lactone of *A. psilostachya* collected from Winnipeg. With reference to the widely accepted claim of the bioactivity of sesquiterpene lactones in the inhibition of enzymes,[15] the isolated sesquiterpene lactone was assayed for *in vitro* activity in GST inhibition, taking into consideration the free thiol-containing cys-47 residue near the active site of the enzyme. Antifungal activity of the compound was also assayed against two strains of *Candida albicans* (14053 and 98028) using the Mueller-Hinton disk agar diffusion method.

4.2 RESULTS AND DISCUSSION

The weed (*A. psilostachya*, 1 kg) was air-dried, macerated and extracted with methanol. The solvent was evaporated under pressure to yield 100 g of a gummy extract. The gum was re-dissolved in 80% aqueous methanol and its lipid content was later removed by solvent-solvent partitioning using hexanes. The resulting extract was concentrated to yield 96 g of a gummy material that was subjected to column chromatography and TLC to isolate compound **100**.

4.2.1 Coronopilin (100)

Compound **100** was isolated as a white crystalline solid. The TLC and HPLC analysis showed that **100** was a major compound present in the column chromatography fractions of the plant under investigation. The MS spectrum of compound **100** showed a molecular ion peak at *m/z* 264. The ion at *m/z* 246 was due to the loss of water molecule from the M^+ and this suggested the presence of a hydroxyl group in **100**. The IR spectrum confirmed this functionality by displaying an absorption band at 3245 cm^{-1} (OH) together with absorption bands for other functional groups at 1780 (C=O), 1720 (C=O), 1542 (C=C) and 1160 (C-O) cm^{-1}.

The ^{1}H-NMR (CD_3OD, 300 MHz) spectrum of **100** showed the presence of a singlet at δ 1.08 and a doublet at δ 1.17, each integrating for three protons assigned to the C-15 and C-14 methyl protons, respectively. Other signals observed in the spectrum include a one-proton multiplet at δ 3.40 and a downfield doublet at δ 4.85 (J = 7.8 Hz), which were assigned to C-7 and C-6 methine protons, respectively. The downfield δ values of H-7 and H-6 indicated the deshielded effects induced by the environment of

these protons. Two other doublets were observed at δ 5.66 (J = 2.8 Hz) and 6.15 (J = 2.8 Hz), integrating for one proton each; the J value indicated that these protons are proximate to each other. The COSY-45° spectrum of **100** revealed the presence of two isolated spin systems (**100a** and **100b**) in the entire structure of this compound. The first spin system was traced from the H_3-17 (*d*) at δ 1.17, which showed connectivity with the signal at δ 2.10 (H-10). The latter ^{1}H-NMR signal displayed ^{1}H-^{1}H spin correlations with signals at δ 2.30 (H_α-9) and 1.62 (H_β-9). This system was linked to the olefinic signals by cross peaks observed between H-7 (δ 3.40) and the diastereotopic signals for CH_2-8 at δ 2.03 (*m*) and 1.75 (*m*). The H-7 signals also showed interaction with the deshielded methine signal at δ 4.85 (*d*).

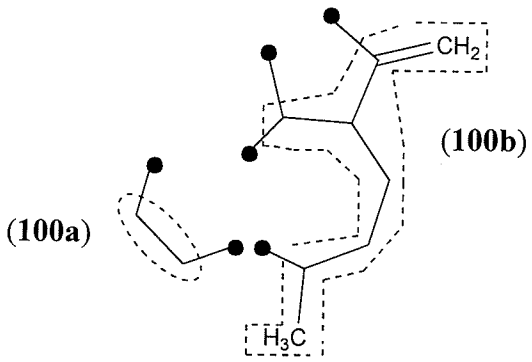

The ^{13}C-NMR (CD_3OD, 50 MHz) spectrum of compound **100** showed resonances for all 15 carbon atoms in this compound. The APT spectrum was recorded to determine the multiplicities of these carbon atoms, and it was found to contain 2 CH_3, 5 CH_2, 3 CH and 5 quaternary carbon atoms. The HSQC spectrum of **100** was utilized in assigning the protons to their respective carbon atoms. The complete ^{1}H, ^{13}C-NMR, APT and HSQC data of compound **100** are represented in the Experimental (section 3.3.3). The two spin systems observed in the COSY spectrum were connected by HMBC interactions. Complete ^{1}H/^{13}C long-range interactions of **100** as observed in the HMBC spectrum are

shown in structure **100c**. A combination of ^{1}H-, ^{13}C-NMR and MS data provided a molecular formula $C_{15}H_{20}O_4$ corresponding to a compound with six degrees of unsaturation. These spectroscopic and spectrometric data collected for this compound were similar to those observed for a widely distributed STL, coronopilin.[21,22] The slight variations in the ^{1}H- and ^{13}C-NMR δ values when compared to literature values[21,22] were due to the fact that these spectra were obtained in different deuterated solvents. To ensure accuracy in data interpretation, the ^{13}C-NMR of compound **100** was also recorded in d_6-acetone and $CDCl_3$ (Table 4.2). This provided nearly the exact δ values of the ^{13}C in compound **100** as reported in the literature.[21,22] That notwithstanding, the carbonyl carbon observed in the ^{13}C-NMR (broadband and APT) spectra at δ 221.6 did not show any heteronuclear interaction with any proton in the HMBC spectrum. This observation aroused a doubt about the existence and position of this group in the structure of the compound.

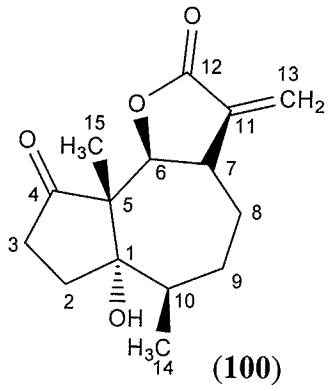

(100)

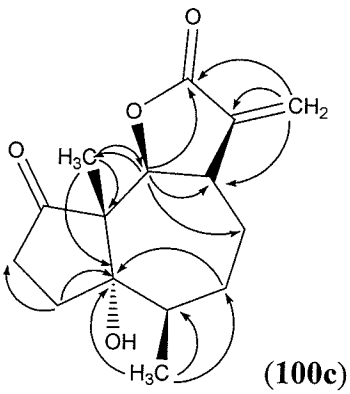

(100c)

The 2D-NOESY experiment was conducted for the determination of the relative configurations of the stereogenic centers. Relative to the β-orientation assumed for the C-15 methyl group due to biogenetic considerations, the orientations of the other stereogenic centers as assigned using the NOESY spectrum are illustrated in structure **100**. Nevertheless, the orientation of the C-1 OH group could not be established using

NOESY. X-ray crystallographic experiment was later conducted on the compound to confirm the existence and position of the carbonyl carbon (^{13}C-NMR signal at δ 221.6) in the structure. The single crystal X-ray data of compound was obtained and deciphered to provide **100** as the structure of the compound. The X-ray crystal structure data has been deposited at the Cambridge Crystallographic Data Centre (CCDC) with the reference number CDCC 634102. The crystal structure **100d** provides the structure with all the protons attached to their respective carbon atoms whereas **100e** has all the protons removed for clarity. This structure shows that the C-15 and C-14 methyl group are oriented in the β configuration whereas C-6 and C-7 methine protons are α oriented. These data confirmed that compound **100** is coronopilin. Moreover, we have reported the X-ray crystal structure of coronopilin for the first time.[23] The configuration of the C-1 OH group was assigned the α configuration due to 1) biogenetic consideration based on reported data[21] and 2) the best inference that could be derived from X-ray crystallography data. The handedness of the compound could not be determined from X-ray crystallography. Previously, coronopilin has been isolated from *A. psilostachya*[5] and some other members of the genus[4], and also from *Parthenium hysterophorus*[21] and *Hymenoclea salsola.*[22] Despite its occurrence in such a large amount in these plants, no significant biological activity has been associated with it. In this project, the activity of this compound was assayed in the *in vitro* inhibition of GST as well as in the inhibition of the growth of two strains of pathogenic fungi, *C. albicans*.

Table 4.2 ^{13}C-NMR (50 MHz) of coronopilin (**100**) in CD_3OD, $CDCl_3$ and acetone-d_6

^{13}C-NMR (50 MHz) δ (ppm) of coronopilin (100)			
Carbon atom	**CD_3OD**	**$CDCl_3$**	**acetone-d_6**
C-1	85.2	85.0	84.9
C-2	33.0	33.1	32.6
C-3	32.7	31.9	32.4
C-4	221.6	217.4	218.0
C-5	60.6	58.7	59.6
C-6	81.9	85.0	80.2
C-7	45.9	44.6	45.6
C-8	28.5	27.5	28.3
C-9	31.2	30.2	31.1
C-10	43.2	42.9	42.9
C-11	142.9	140.8	142.9
C-12	172.9	184.2	**X**
C-13	122.4	121.5	120.7
C-14	17.6	17.3	17.4
C-15	14.9	14.7	14.7

X – peak was not observed in the ^{13}C-NMR spectrum

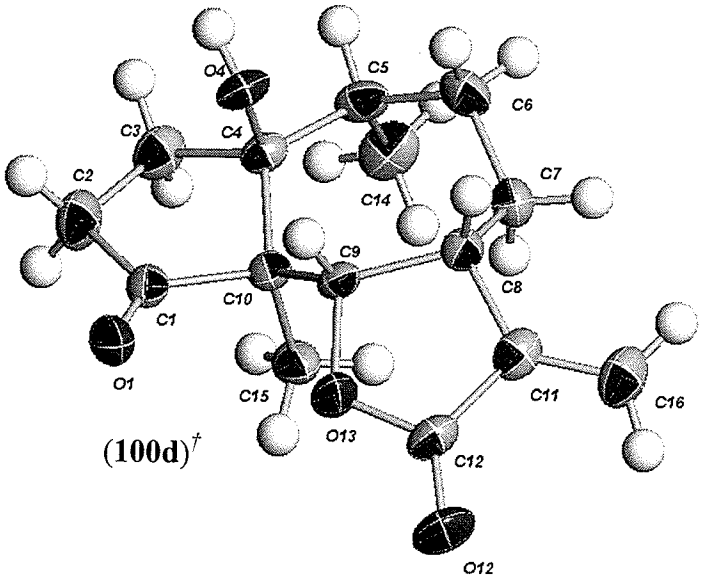

(100d)†

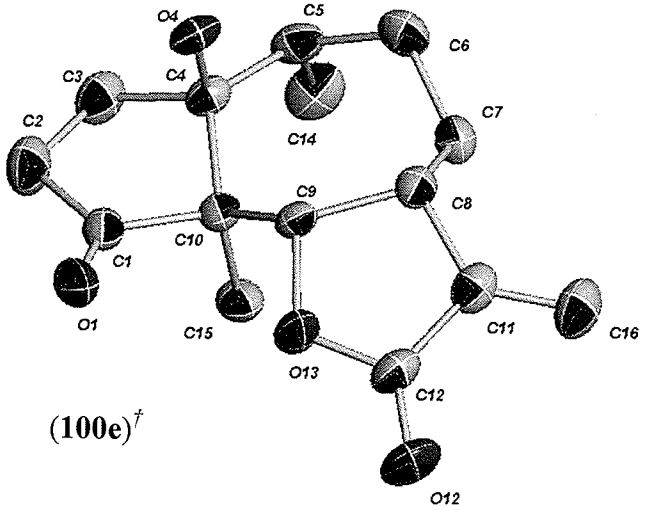

(100e)†

†*Arbitrary atom numbering; for the correct atom numbering, see structure* ***100****.*

4.2.2 Results of Enzyme Inhibition and Antifungal assays

Coronopilin (**100**) showed a moderate concentration-dependent inhibition of the activity of GST with an IC_{50} value of 120.3 ± 7.57 μmol. It has been previously reported that helenalin (**112**), a structurally-related sesquiterpene lactone did not exhibit GST inhibition except in the form of a glutathione conjugate.[24] The activity observed for compound **100** could possibly be due to the orientation of the α-methylene-γ-lactone ring at the C-6/C-7 position compared to helenalin (**112**), which possesses the same ring oriented in the C-7/C-8 position. Moreover, the possibility of Michael addition reaction on the exocyclic methylene group in the formation of glutathione adduct of coronopilin during the assay period, which could also inhibit GST, would not be ignored. A previous report, using helenalin and its derivative, has shown that the glutathione adducts of inactive STLs could inhibit GST.[24]

In the antifungal assay against the growth of pathogenic fungi, coronopilin (**100**) showed no activity against the two strains of *C. albicans* (14053 and 98028) at a 50 μg/mL maximum concentration after 48 h of assay.

4.3 EXPERIMENTAL

4.3.1 General

The general experimental procedures of chromatography and spectroscopy utilized in this experiment were the same as shown in sections 2.3.1 and 3.3.1. In addition to these methods, the X-ray crystallography data were obtained on a *Bruker AXS P4/SMART 1000* diffractometer.

4.3.2 Plant Material

The plant was collected from the surroundings of Winnipeg, Manitoba in August 2004, and identified as *A. psilostachya* (perennial ragweed) by Dr. Richard Staniforth of the Department of Biology, University of Winnipeg, Manitoba.

4.3.3 Isolation of coronopilin from *Ambrosia psilostachya*

A. psilostachya (1 kg) was air-dried, pulverized and extracted with methanol (1 L). The solvent was later removed under pressure, using a rotary evaporator, to yield 100 g of a gummy extract. The gum was re-dissolved in 1:4 H_2O-MeOH, and later subjected to solvent-solvent partitioning using hexanes to remove lipids. The de-fatted extract was concentrated to yield a gum (96.02 g) which was later subjected to silica gel (60 Å mesh size) column chromatography by gradient elution using 0-100% hexane-EtOAc and 0-100% EtOAc-MeOH to afford several fractions. Analytical TLC was carried out on the fractions using hexane-EtOAc (3:7) and spots were visualized under UV at 254 nm and by spraying with 10% H_2SO_4. Thereafter, fractions of similar R_f values were pooled together. The fractions of high concentrations were used in this study, and these showed

the presence of a major spot on analytical TLC. Preparative TLC was later carried out on the major pooled fractions that eluted with 40%hexane-60%EtOAc, and this resulted in the isolation of coronopilin (**100**, 32 mg) as a white crystalline solid. Compound **100** was re-crystallized in methanol by evaporation method. This was carried out by dissolving 10 mg of the compound in 20 mL of methanol and allowing the solution to air-dry after 48 h, to produce needle-shaped colorless crystals. Purity of the compound was confirmed by observation of a homogenous spot on TLC and a single peak on reverse phase HPLC on ODS (C-18) Waters Nova Pak column using various solvent systems.

Coronopilin (**100**) White crystalline solid, R_f 0.46 in 100% Et_2O; $[\alpha]^{24}_D$ (MeOH) = 29.4 (c = 0.17); IR ν_{max} (KBr): = 3225 (OH), 2933 (CH), 1621 (C=C), 1728 (C=O), 1702 (lactone C=O) cm^{-1}; ^1H NMR (CD_3OD, 300 MHz) δ: = 6.15 (1H, *d*, *J* = 2.8 Hz, H_a-13), 5.66 (1H, *d*, *J* = 2.8 Hz, H_b-13), 4.85 (1H, *d*, *J* = 7.8 Hz, H-6), 3.40 (1H, *m*, H-7), 2.65 (1H, *ddd*, *J* = 1.4, 4.4, 9.6 Hz, H_β-3), 2.41 (2H, *ddd*, *J* = 1.9, 4.4, 9.6 Hz, H-2), 2.30 (1H, *dt*, *J* = 4.3, 12.6 Hz, H_α-9), 2.10 (1H, *m*, H-10), 2.03 (1H, *ddd*, *J* = 2.2, 4.3, 12.6 Hz, H_β-8), 1.75 (1H, *m*, H_α-8), 1.68 (1H, *m*, H_α-3), 1.62 (1H, *m*, H_β-9), 1.17 (1H, *d*, *J* = 7.7 Hz, H-14), 1.08 (1H, *s*, H-15); ^{13}C NMR (CD_3OD, 75 MHz) δ: = 221.6 (C-4), 172.9 (C-12), 142.9 (C-11), 122.4 (C-13), 85.2 (C-1), 81.9 (C-6), 60.6 (C-5), 45.9 (C-7), 43.2 (C-10), 33.0 (C-2), 32.7 (C-3), 31.2 (C-9), 28.5 (C-8), 17.6 (C-14), 14.9 (C-15); CIMS *m/z*: = 265 (M^++1); EIMS *m/z*: = 264 (M^+), 246, 231, 218, 204, 191, 163, 141, 123, 95, 55, 43.

4.3.4 X-ray Crystallography

Crystals of coronopilin (**100**) were grown by solvent evaporation at 25 °C. Single crystal X-ray diffraction experiment on compound **100** was carried out by Dr. Andreas Decken of the Department of Chemistry, University of New Brunswick, Fredericton, Canada. Single crystals were coated with Paratone-N oil, mounted using a 20 micron cryo-loop and frozen in the cold nitrogen stream of the goniometer. A hemisphere of data was collected on a Bruker AXS P4/SMART 1000 diffractometer using ω and θ scans with a scan width of 0.3 ° and 30 s exposure times. The detector distance was 5 cm. The data were reduced and corrected for absorption. The structure was solved by direct methods and refined by full-matrix least squares on F^2. All non-hydrogen atoms were refined using anisotropic displacement parameters. Hydrogen atoms were found in Fourier difference maps and refined using isotropic displacement parameters. A complete X-ray crystallographic data, which include the bond lengths and angles as well as the atomic coordinates, anisotropic displacement parameters, hydrogen coordinates and isotropic displacement parameters can be found on the Cambridge Crystallographic Data Centre (CCDC) with reference number CCDC 634102.

4.3.5 Assay for Glutathione *S*-Transferase Inhibition

The *in vitro* activity of the coronopilin in the inhibition of GST was assayed as previously outlined in section 2.3.4.

Table 4.3 X-ray crystal data and structure refinement for coronopilin (**100**)

Empirical formula	C15 H20 O4	
Formula weight	264.31	
Temperature	173(1) K	
Wavelength	0.71073 Å	
Monochromator used	Graphite	
Crystal size	0.40 x 0.30 x 0.05 mm^3	
Color and habit	Colorless, plate	
Crystal system	Monoclinic	
Space group	P2(1)	
Unit cell dimensions	a = 6.512(3) Å	$\alpha = 90°$
	b = 12.106(5) Å	$\beta = 103.539(6)°$
	c = 8.933(4) Å	$\gamma = 90°$
Volume	684.7(5) $Å^3$	
Z	2	
Density (calculated)	1.282 Mg/m^3	
Absorption coefficient	0.092 mm^{-1}	
F(000)	284	
Theta range for data collection	2.34 to 27.49°	
Completeness to theta = 25.00°	99.9 %	
Scan type	ω and ϕ	
Scan range	0.3°	
Exposure time	30s	
Index ranges	$-8 \le h \le 8, -15 \le k \le 14, -11 \le l \le 11$	
Standard reflections collection	50 frames at beginning and end of data	
Crystal stability	no decay	
Reflections collected	4603	
Independent reflections	2346 [R(int) = 0.0237]	
System used	SHELXL 5.1	
Solution	Direct methods	
Hydrogen atoms	Found, refined isotropically	
Absorption correction	SADABS	
Max. and min. transmission	0.9954 and 0.9641	
Refinement method	Full-matrix least-squares on F^2	
Data/restraints/parameters	2346 / 1 / 253	
Goodness-of-fit on F^2	1.044	
Final R indices [I>2sigma(I)]	R1 = 0.0288, wR2 = 0.0684	
R indices (all data)	R1 = 0.0334, wR2 = 0.0719	
Largest/mean shift/esd	0.000/0.000	
Absolute structure parameter	-0.5(9)	
Largest diff. peak and hole	0.192 and -0.114 $e.Å^{-3}$	

CONCLUSIONS

In summary, phytochemical studies on the extracts of *Caesalpinia bonduc* resulted in the isolation of neocaesalpin (**40**), 17-hydroxy-campesta-4,6-dien-3-one (**41**), caesaldekarin J (**42**), apigenin (**43**), pipataline (**44**), betulinic acid (**45**), 13,14-*seco*-stigmasta-5,14-dien-3α-ol (**46**) and 13,14-*seco*-stigmasta-9(11),14-dien-3α-ol (**47**). The structures of these compounds were elucidated using spectroscopy. Neocaesalpin (**40**), 17-hydroxy-campesta-4,6-dien-3-one (**41**) were identified as new natural products. These compounds showed weak to moderate or no inhibitory activity against GST, an enzyme that has been implicated in resistances of cancer cells and parasitic organisms towards chemotherapeutic agents. An attempt to study the structure-activity relationships (SAR) of some of the compounds resulted in the semi-synthesis of compounds **57-61** by acetylation, oxidation and epoxidation. These compounds were also either weakly active or inactive in GST inhibition but some were discovered to display enhanced activity by meager degrees.

Similarly, the chemical constituents of the ethanolic extract of *Nauclea latifolia* were also investigated. This resulted in the isolation of strictosamide (**70**), quinovic acid-3-O-α-quinovosylpyranoside (**95**), quinovic acid-3-O-β-rhamnosylpyranoside (**96**), quinovic acid-3-O-α-rhamnosylpyranoside (**97**) and quinovic acid-3-O-β-fucosylpyranoside (**98**). The structures of these compounds were also deciphered by spectroscopic studies. Strictosamide (**70**) was isolated as a major secondary metabolite of *N. latifolia* based on HPLC analysis. These compounds also showed varying extents of GST inhibitory activities with strictosamide (**70**) showing the best activity (IC_{50} = 20.5 μM). This activity is comparable to the activity of ethacynic acid, a GST inhibitor

previously applied as a chemosensitizer. Assay results for the other compounds (**95-98**) indicated that the nature of the sugar molecules attached to the quinovic acid aglycone could affect their GST-inhibiting potentials. These results showed that the configuration of the sugars at C-1′ does not have any effect of their activity, but the position of the C-2′ hydroxyl group affected the activity of the enzyme.

Lastly, phytochemical studies on *Ambrosia psilostachya* have resulted in the isolation of coronopilin (**100**), a pseudoguaianolide sesquiterpene lactone. The sesquiterpene lactone contents of *A. psilostachya* have been used as chemotaxomonic markers in the identification of different populations of the plant. This study is the first investigation of the sesquiterpene lactone contents of the Winnipeg, Manitoba population of *A. psilostachya*. High Performance Liquid Chromatography analysis of the fractions of this plant showed that coronopilin (**100**) is one of the major sesquiterpene lactone present in this population. The structure of **100** was also elucidated using spectroscopic techniques. In addition, the X-ray crystal structure was also established using single crystal X-ray crystallography. Coronopilin showed a concentration-dependent inhibition of the activity of GST. The activity of the compound could be due to the orientation of the lactone ring of coronopilin (**100**) or due to the formation of a glutathione adduct during the assay or both. Coronopilin showed no activity in the inhibition of growth of two pathogenic strains of *Candida albicans*.

FUTURE WORK

Future work on this project includes:

1. Isolation of other equine liver GST-inhibiting natural products from the bioactive fractions of *C. bonduc*, *N. latifolia* and *A. psilostachya* extracts;
2. Preparation of a library of naturally-occuring compounds that could inhibit equine liver GST;
3. Study of their mode of action and determination of their kinetic parameters in the *in vitro* inhibition of equine liver GST;
4. Study of the specificity of these natural products as inhibitors of other GST isoenzymes, e.g. GST-P, GST-M, pfGST, OvGST2, that have been shown to interfere with the activity of anti-cancer and anti-parasitic drugs;
5. Assay for anti-parasitic activity of these GST inhibiting natural products to investigate if GST inhibition could be linked to the activity of anti-parasitic agents.

REFERENCES

1. Miller, H. E., Mabry, T. J. and Turner, B. L. Infraspecific variation of sesquiterpene lactones in *Ambrosia psilostachya* (compositae). *Amer. J. Bot.*, **1968**, *55*, 316-324.
2. Basset, I. J. and Crompton, C. W. The biology of Canadian weeds II. *Ambrosia artemisiifolia* L and *A. psilostachya* DC. *Can. J. Plant Sci.*, **1975**, *55*, 463-476.
3. Dewick, P. M. "Medicinal Natural Products: A biosynthetic approach", *2nd ed.*, John Wiley & Sons, **2001**.
4. Geissman, T. A., Griffin, S., Waddell, T. G. and Chen, H. H. Sesquiterpene lactones. Some new constituents of *Ambrosia* species: *A. psilostachya* and *A. acanthicarpa*. *Phytochemistry*, **1969**, *8*, 145-150.
5. Herz, W. and Högenauer, G. Isolation and structure of coronopilin, a new sesquiterpene lactone. *J. Org. Chem.*, **1961**, *26*, 5011-5013.
6. Mabry, T. J., Renold, W., Miller, H. E. and Kagan, H. B. The structure of ambrosial, a new sesquiterpene lactone from *Ambrosia psilostachya*. *J. Org. Chem.*, **1966**, *31*, 681-684.
7. Miller, H. E., Kagan, H. B., Renold, W. and Mabry, T. J. Psilostachyin, a new type of sesquiterpene lactone. *Tetrahedron Lett.*, **1965**, *38*, 3397-3403.
8. Yoshioka, H., Mabry, T. J. and Miller, H. E. Isabelin, a novel germacranolide dilactone from *Ambrosia psilostachya* DC. *Chem. Commun.*, **1968**, *24*, 1679-1681.
9. Miller, H. E. and Mabry, T. J. 3-Hydroxydamsin, a new pseudoguaianolide from *Ambrosia psilostachya* DC (compositae). *J. Org. Chem.*, **1967**, *32*, 2929-2931.

10. Chen, Y., Bean, M. F., Chambers, C., Francis, T., Huddleston, M. J., Offen, P., Westley, J. W. and Carte, B. K. Arrivacins, novel pseudoguaianolide esters with potent angiotensin II binding activity from *Ambrosia psilostachya*. *Tetrahedron*, **1991**, *47*, 4869-78.

11. Huang, S.-K. and Marsh, D. G. Human T-cells responses to ragweed allergens: *Amb* V homologues. *Immunology*, **1991**, *73*, 363-365.

12. Lastra, A. L., Ramírez, T. O., Salazar, M. M. and Trujillo-Ferrara, J. The ambrosanolide cumanin inhibits macrophage nitric oxide synthesis: some structural considerations. *J. Ethnopharmacol.*, **2004**, *95*, 221-227.

13. Hall, H., Starnes, C. O., Lee, K. H. and Wadell, G. Mode of action of sesquiterpene lactones as anti-inflammatory agents. *J. Pharm. Sci.*, **1980**, *69*, 537-543.

14. Hall, H. I., Grippo, A. A., Holbrook, D. J., Roberts, G., Lin, H. C., Kim, H. L. and Lee, K. H. Role of thiol agents in protecting against the toxicity of helenalin in tumor-bearing mice. *Planta Med.*, **1989**, *55*, 513-517.

15. Konaklieva, M. I. and Plotkin, B. J. Lactones: generic inhibitors of enzymes? *Mini-Rev. Med. Chem.*, **2005**, *5*, 73-95.

16. Blanco, J. G., Gil, R. R., Bocco, J. L., Meragelman, T. L., Genti-Raimondi, S. and Flury, A. J. Aromatase inhibition by an 11,13-dihydro derivative of a sesquiterpene lactone. *Pharmocol. Exp. Ther.* **2001**, *297*, 1099-1105.

17. Hwang, D., Fischer, N. H., Jang, B. C., Tak, H., Kim, J. K. and Lee, W. Inhibition of the expression of inducible cyclooxygenase and proinflammatory cytokines by

sesquiterpene lactones in macrophages correlates with the inhibition of MAP kinases. *Biochem. Biophys. Res. Commun.*, **1996**, *226*, 810-818.

18. Zhang, S., Won, Y.-K., Ong, C.-O. and Shen, H.-M. Anti-cancer potential of sesquiterpene lactones: bioactivity and molecular mechanisms. *Curr. Med. Chem.*, **2005**, *5*, 239-249.
19. Hehner, S. P., Hofmann, T. G., Dröge, W. and Schmitz, M. L. The anti-inflammatory sesquiterpene lactone parthenolide inhibits NF-κB by targeting the IκB kinase complex. *J. Immunol.* **1999**, *163*, 5617-5623.
20. Wictome, M., Khan, Y. M., East, J. M. and Lee, A. G. Binding of sesquiterpene lactone inhibitors to the Ca^{2+}-ATPase. *Biochem. J.* **1995**, *310*, 859-868.
21. Picman, A. K., Towers, G. H. N. and Subra Rao, P. V. Coronopilin, another major sesquiterpene lactone in *Parthenium hysterophorus*. *Phytochemistry*, **1980**, *19*, 2206-2207.
22. Balza, F. and Towers, G. H. N. Structural analysis of sesquiterpene lactones from *Hymenoclea salsola*. *Phytochemistry*, **1988**, *27*, 1421-1424.
23. Ata, A., Diduck, C., Udenigwe, C. C., Zahid, S. and Decken, A. New chemical constituents of *Ambrosia psilostachya*, *ARKIVOC*, **2007**, *xiii*, 195-203.
24. Schmidt, T. J. Glutathione adducts of helenalin and 11α,13-dihyrohelenalin acetate inhibit glutathione *S*-transferase from horse liver. *Planta Med.*, **2000**, *66*, 106-109.
25. Schmidt, T. J. Helenanolide-type sesquiterpene lactones-III. Rates and stereochemistry in the reaction of helenalin and related helenanolides with sulfhydryl containing biomolecules. *Bioorg. Med. Chem.*, **1997**, *5*, 645-653.

APPENDIX

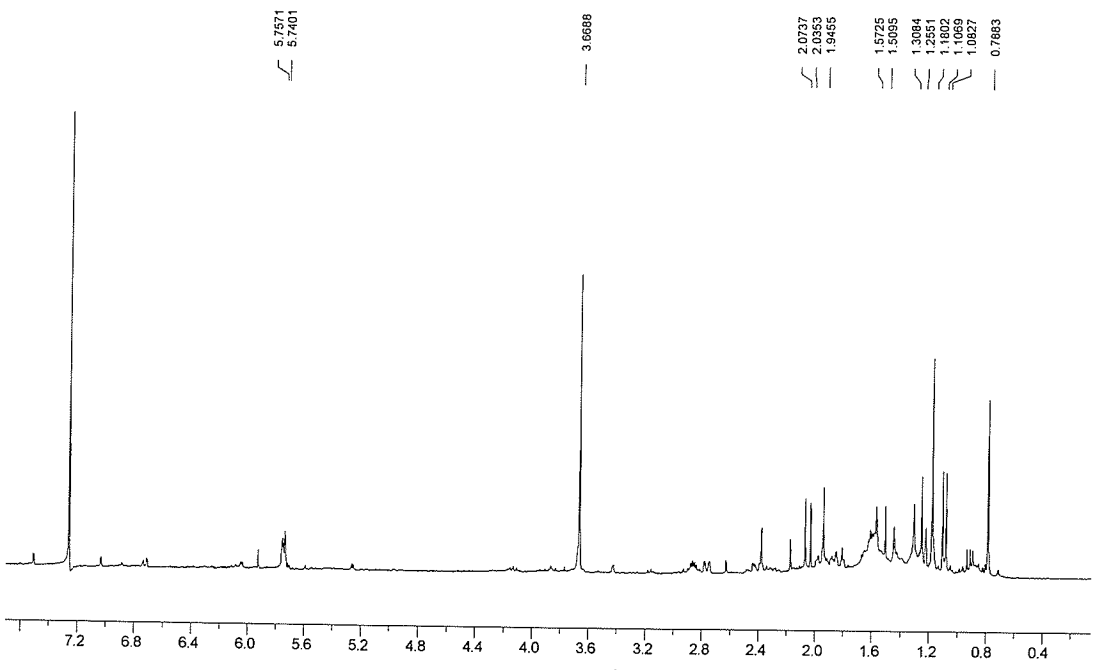

A1. ^{1}H NMR spectrum of compound **40** in $CDCl_3$

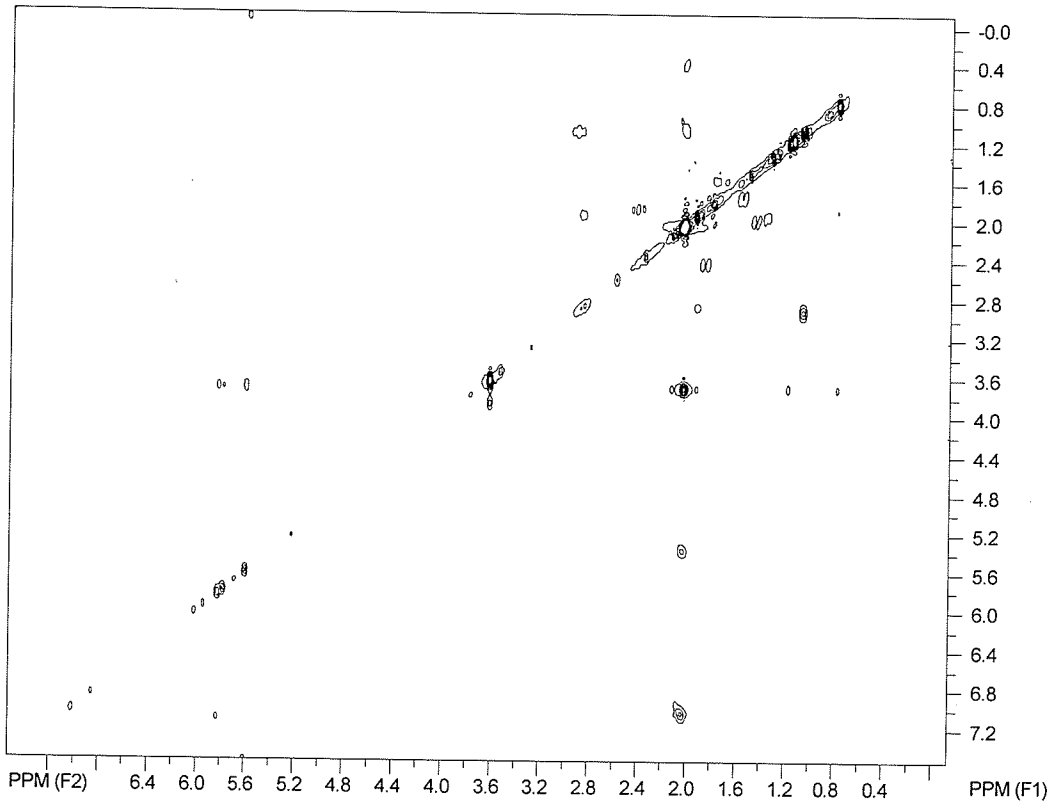

A2. ^{1}H-^{1}H COSY spectrum of compound **40** in $CDCl_3$

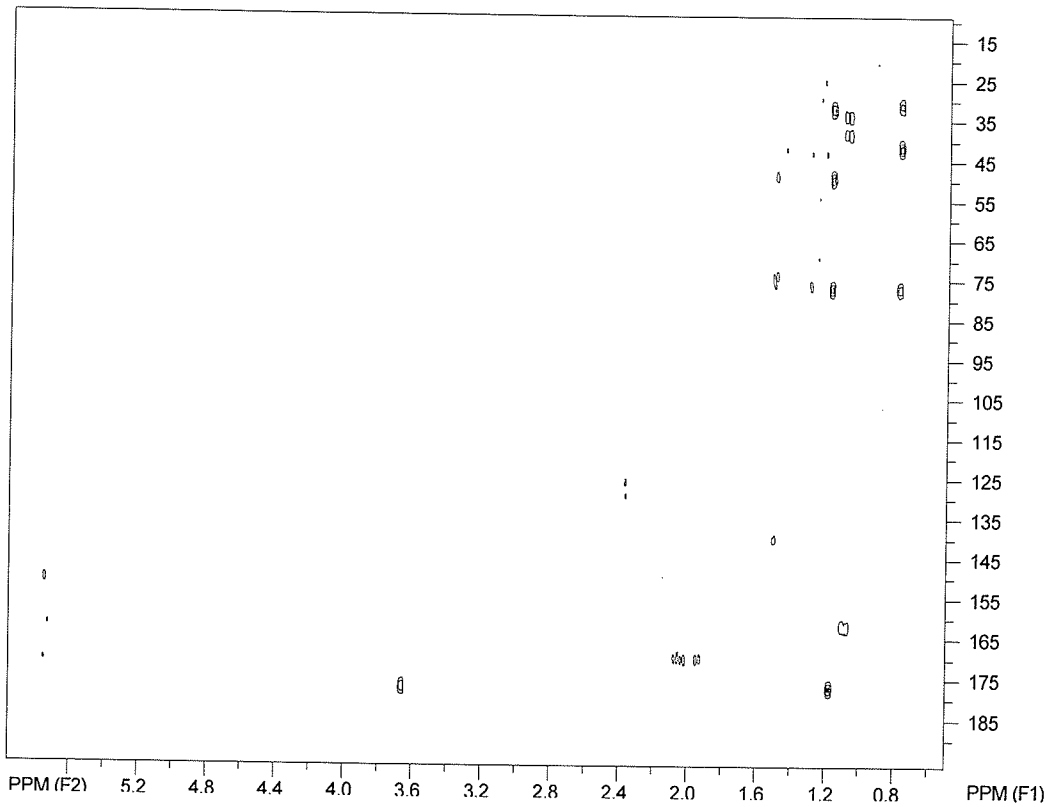

A3. $^{1}H/^{13}C$ HMBC spectrum of compound **40** in $CDCl_3$

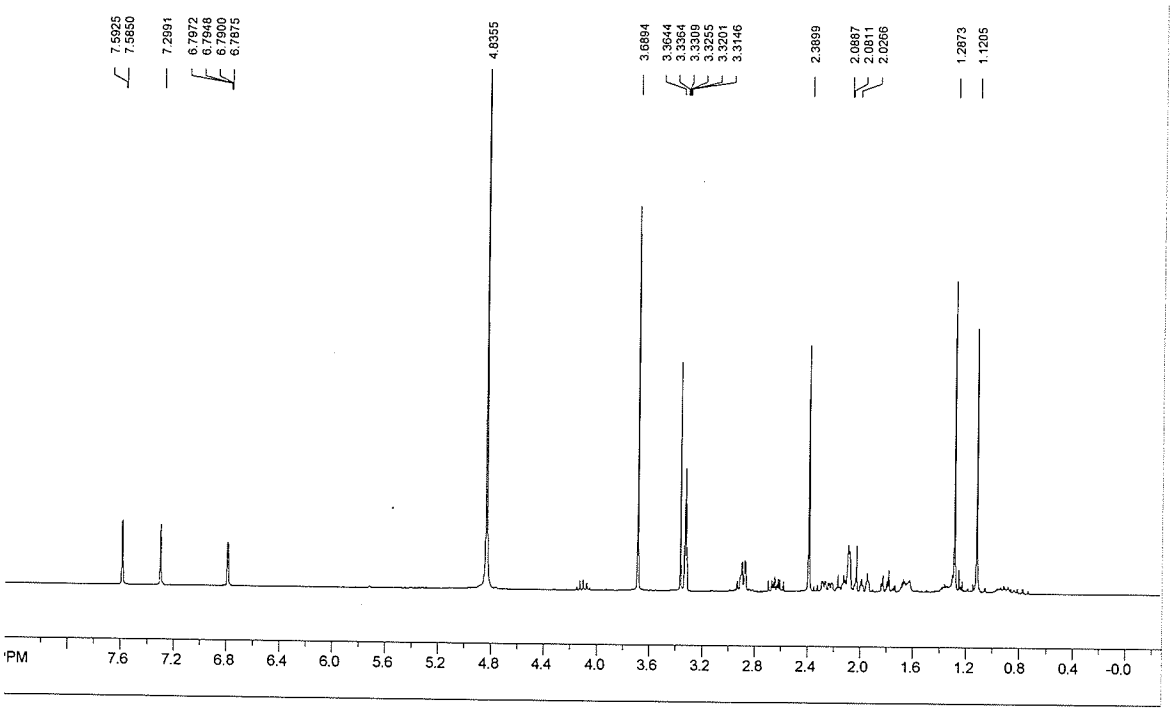

A4. ^{1}H NMR spectrum of compound **42** in $CDCl_3$

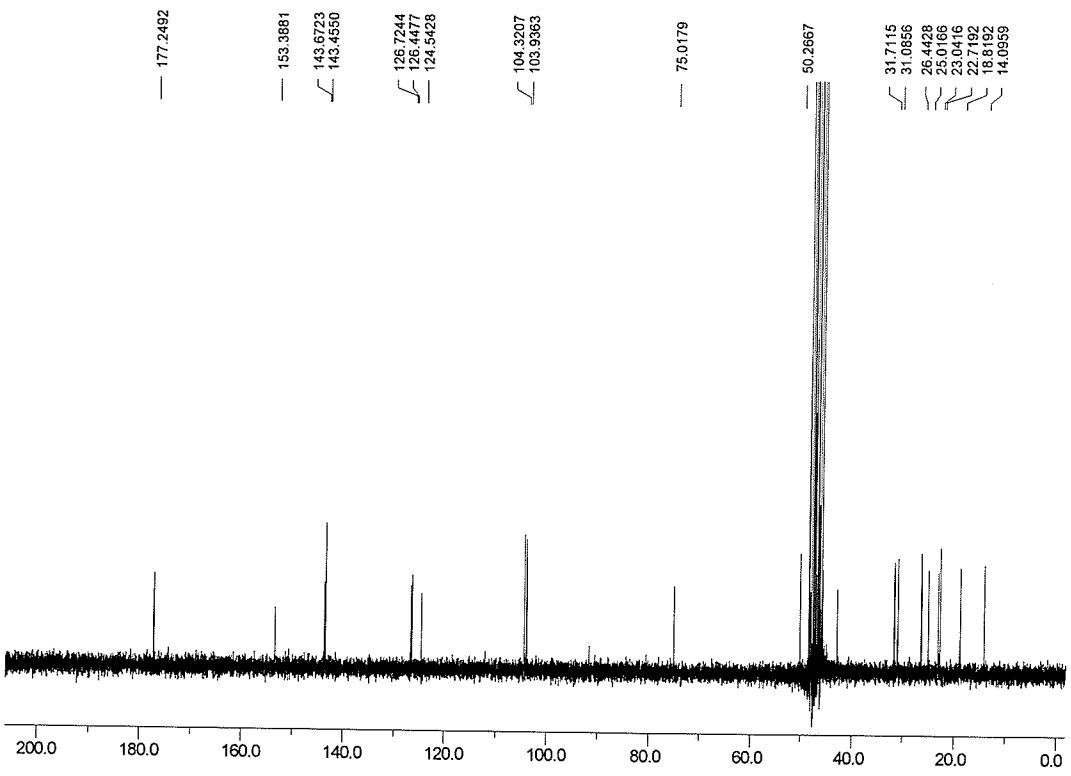

A5. ^{13}C NMR spectrum of compound **42** in $CDCl_3$

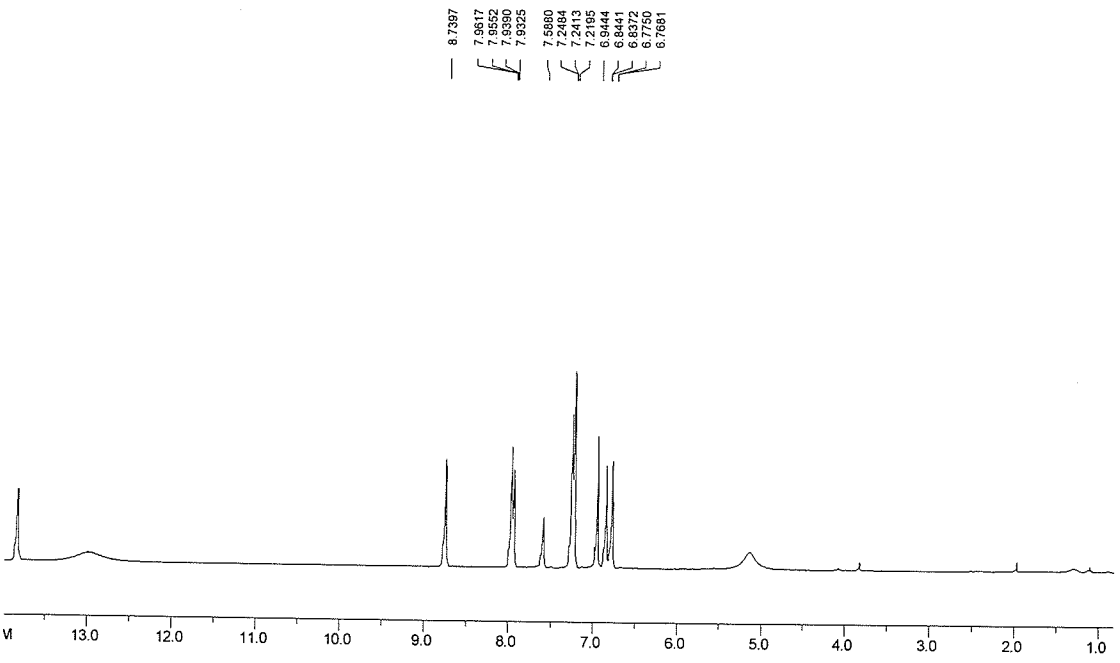

A6. ^{1}H NMR spectrum of compound **43** in C_5D_5N

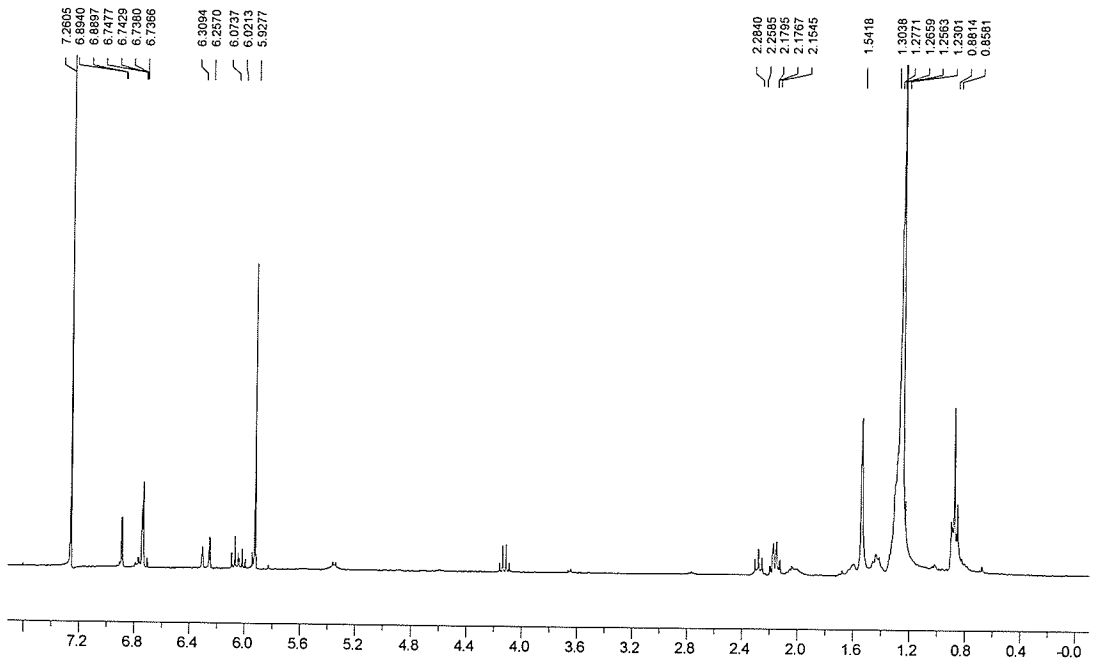

A7. ^{1}H NMR spectrum of compound **44** in $CDCl_3$

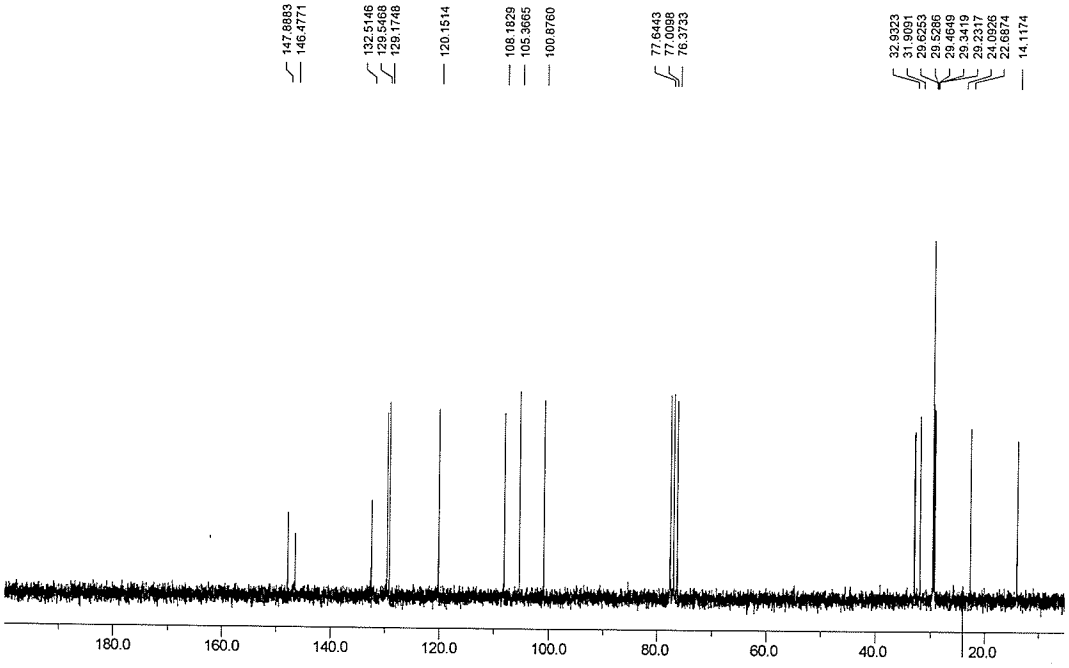

A8. ^{13}C NMR spectrum of compound **44** in $CDCl_3$

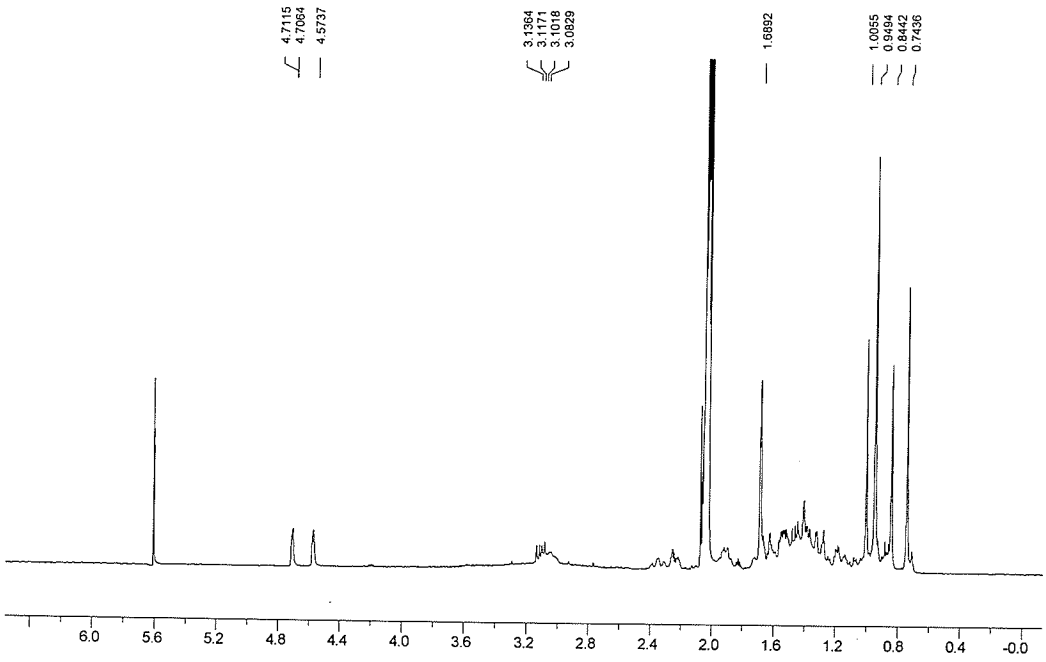

A9. ^{1}H NMR spectrum of compound **45** in $(CD_3)_2CO$

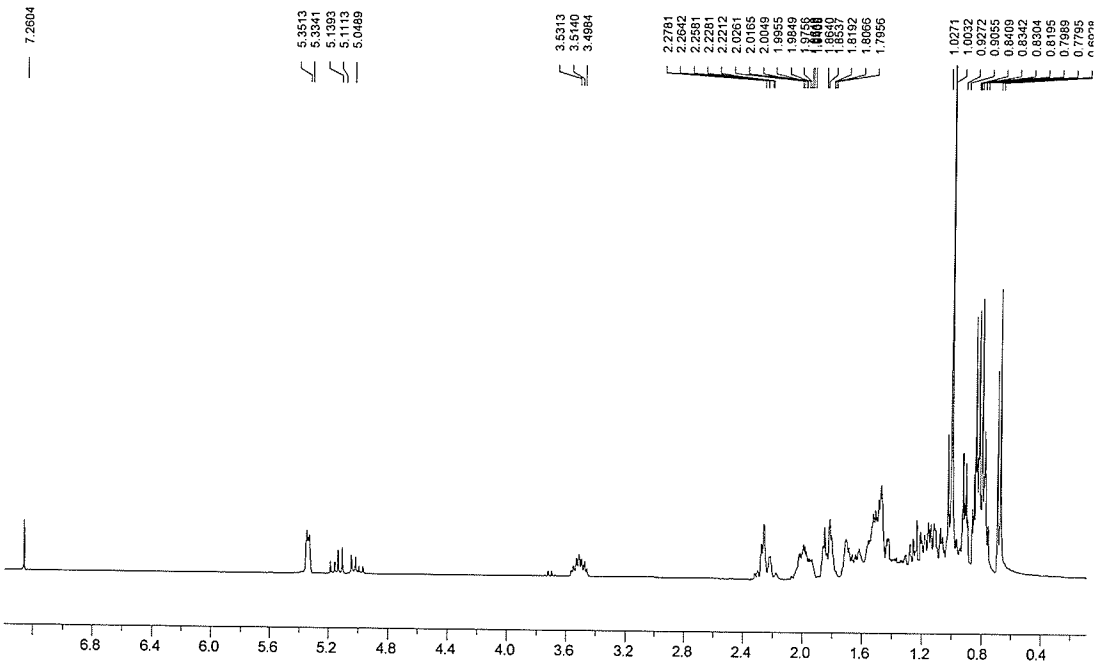

A10. ^{1}H NMR spectrum of compound **46** in $CDCl_3$

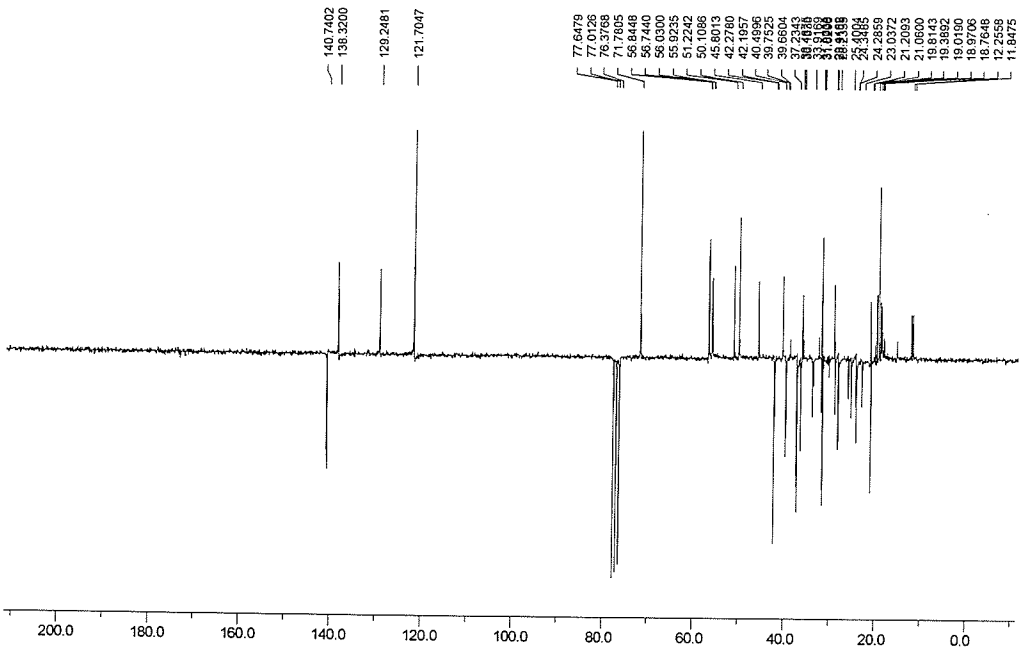

A11. ^{13}C NMR (APT) spectrum of compound **46** in $CDCl_3$

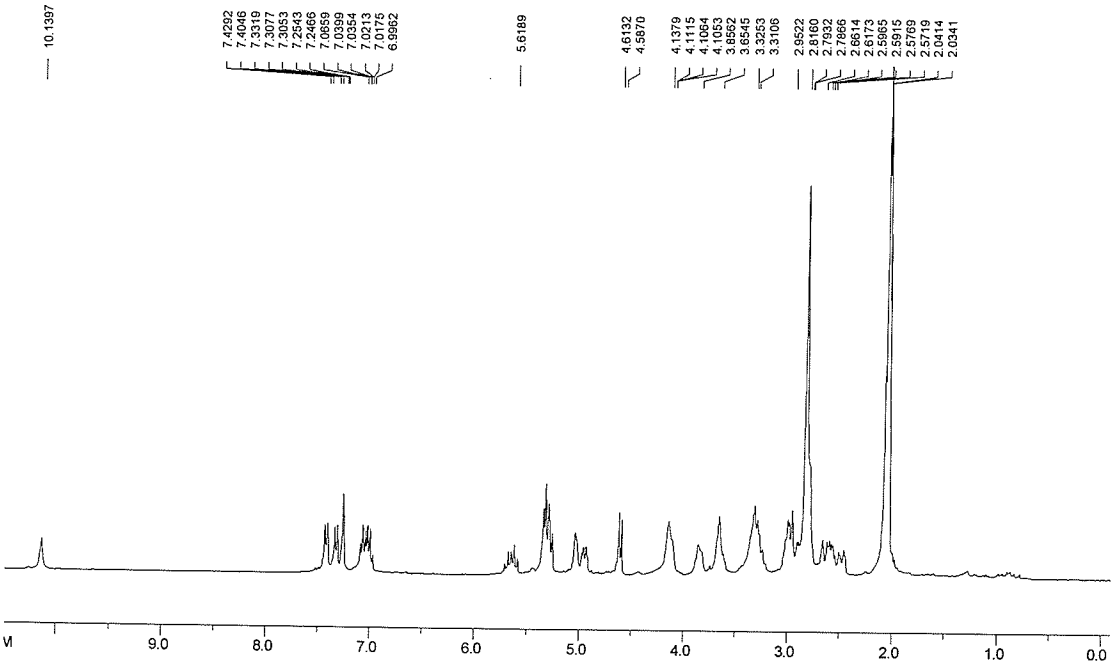

A12. ^{1}H NMR spectrum of compound **70** in CD_3OD

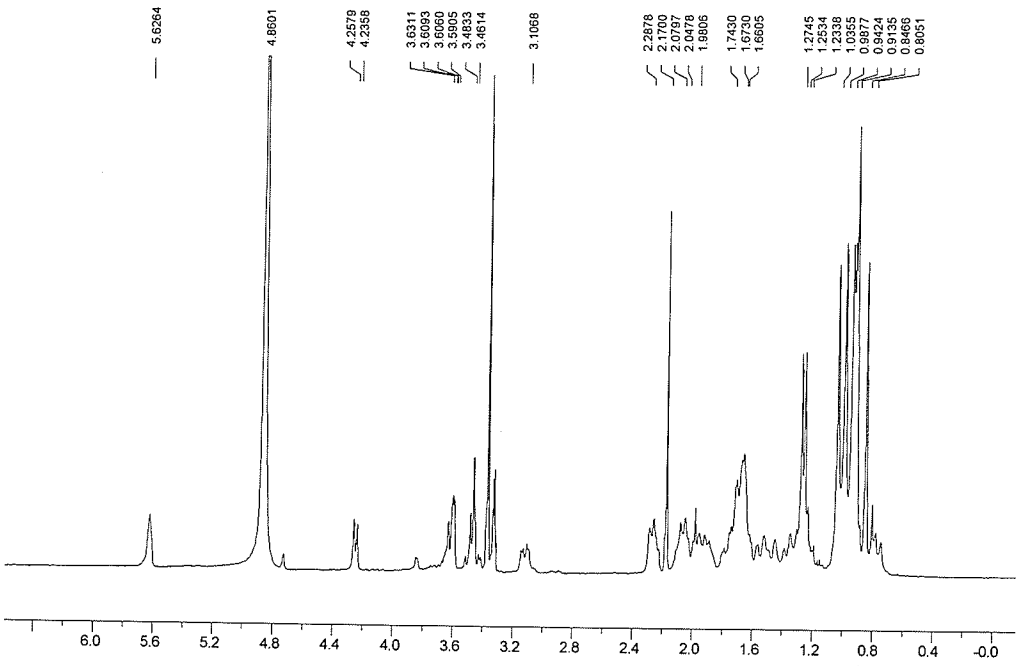

A13. ^{1}H NMR spectrum of compound **95** in CD_3OD

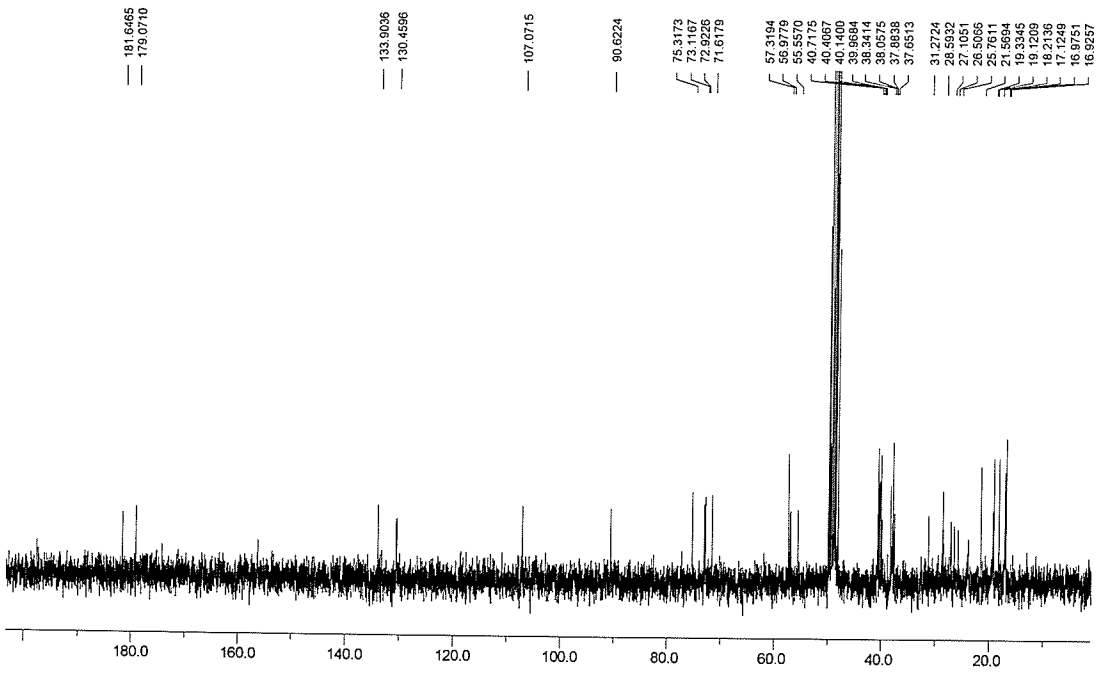

A14. ^{13}C NMR spectrum of compound **95** in CD_3OD

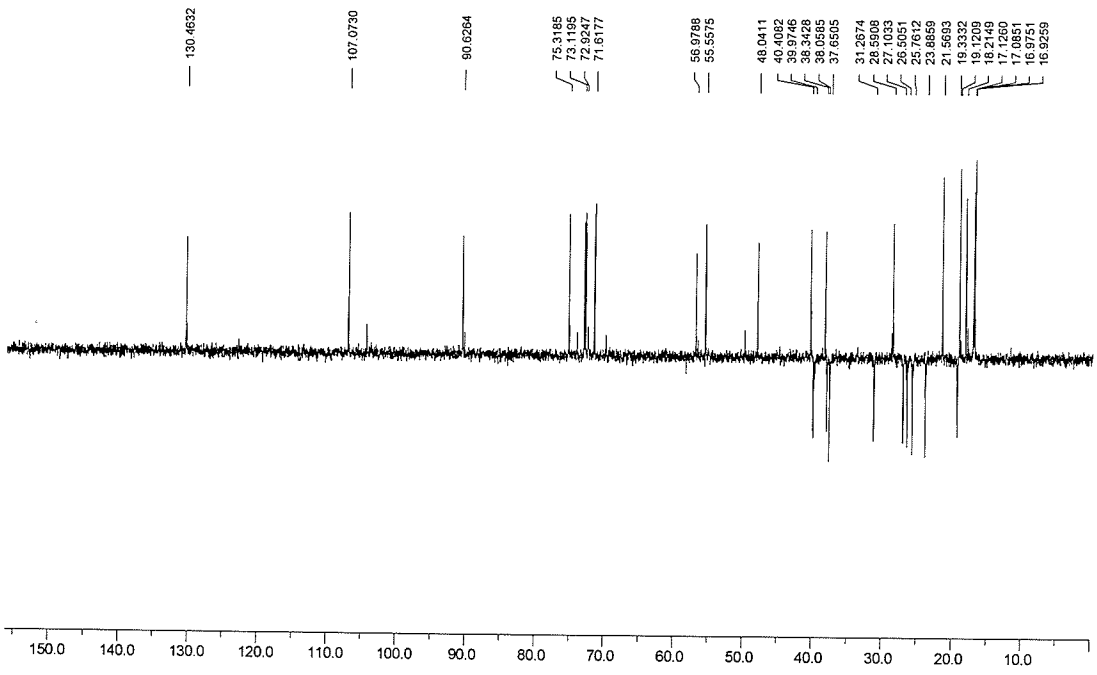

A15. DEPT spectrum of compound **95** in CD_3OD

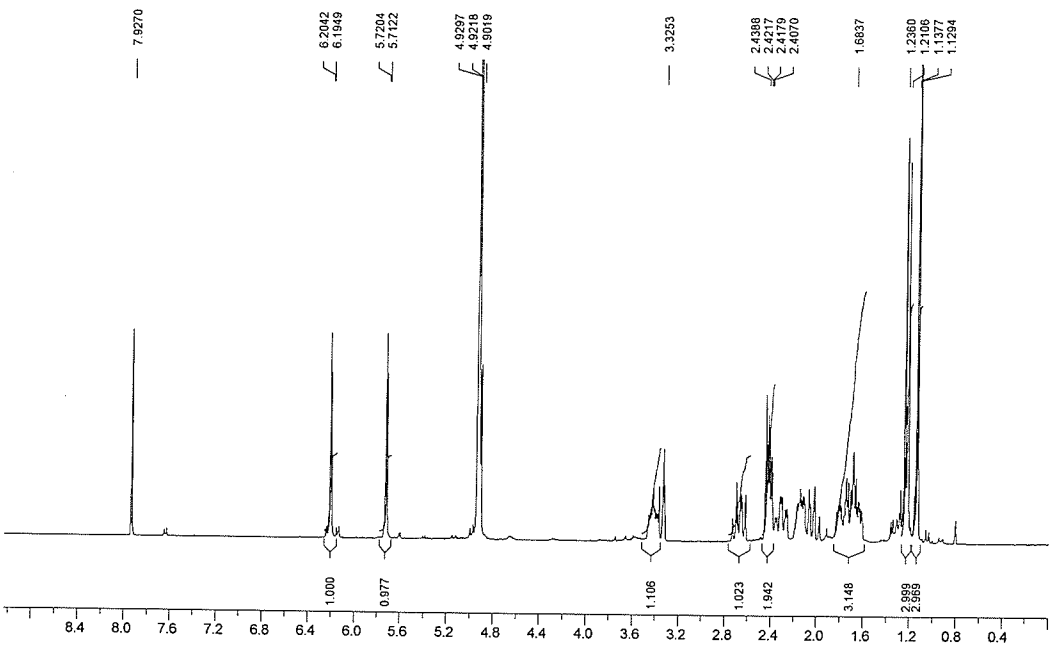

A16. ^{1}H NMR spectrum of compound **100** in CD_3OD

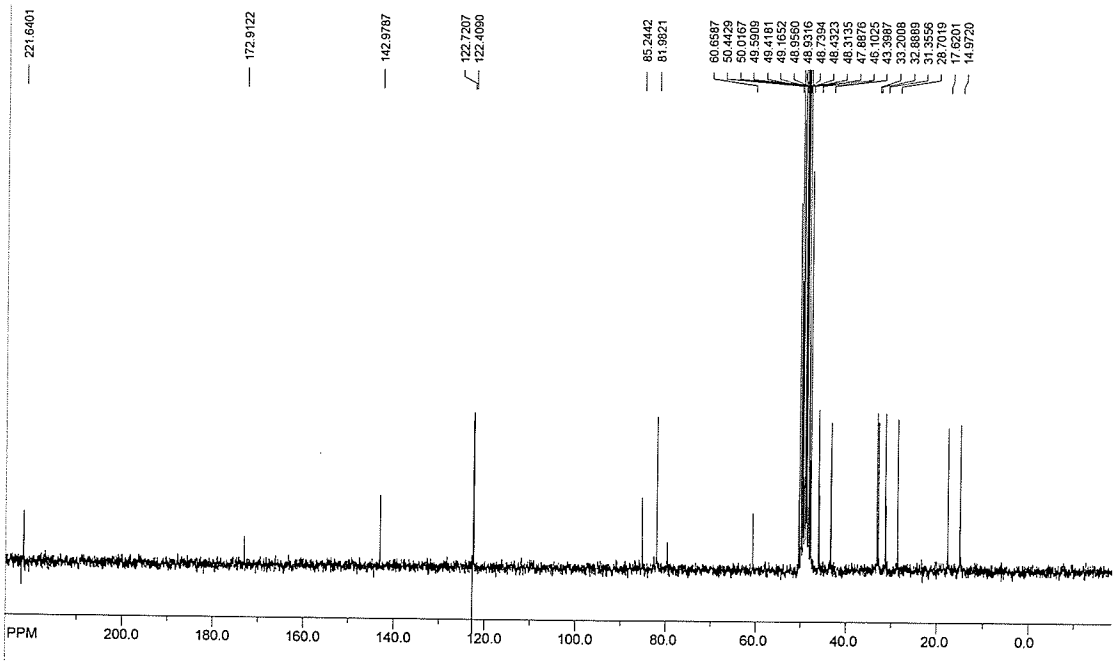

A17. ^{13}C NMR spectrum of compound **100** in CD_3OD